2733

APPLICATIONS OF ELECTRICAL RESISTIVITY METHOD IN SEA-WATER INTRUSION PROBLEM IN AYN ZAYANAH AREA NEAR BENGHAZI, LIBYA

by

Mohamed B.A. Abdelmalik

1983

T-2733

A thesis submitted to the Faculty and the Board of Trustees of the Colorado School of Mines in partial fulfillment of the requirements for the degree of Master of Science (Geophysics).

Golden, Colorado

Date: May 6, 1983

Signed: M. B. Abdelmalik
Mohamed B.A. Abdelmalik

Golden, Colorado

Date: May 6, 1983

Approved: George V. Keller
George V. Keller
Thesis Advisor and Head,
Department of Geophysics

ABSTRACT

Sea-water intrusion into fresh water is a common problem facing most coastal aquifer regions in the world. The problem arises as a result of lowering the groundwater level by excessive usage of the fresh water.

The combination of DC resistivity soundings and bore hole logs was used to delineate sea-water fronts and the salinity problem in the Ayn Zayanah area near Benghazi, Libya.

Sixteen electrical resistivity soundings and three resistivity profilings using the Schlumberger array were performed by Condrill AB Company. Another eight core wells were run by different bore hole logs in the area. Long normal resistivity and neutron logs were used to determine water salinity using a cross-plot technique. The electrical resistivity sounding data has been interpreted using a computer-assisted inversion program with support from the resistivity logs. Additional information from core analysis and permeability tests has also been used.

The area generally represents a coastal, unconfined Middle-Miocene limestone aquifer lying on a sea-water wedge. The aquifer is characterized by karst, fractures, and fissures through which the groundwater movement takes place

towards a drainage area close to the sea at Blue Lagoon and Ayn Zayanah spring.

The sea-water intrusion problem can be prevented and controlled basically by raising the groundwater level or by injecting fresh water near the coast in order to increase the hydraulic gradient towards the sea. The groundwater level can be raised by decreasing the amount of water being drained to the sea through the Blue Lagoon. This can be successfully controlled by construction of a dam on the Blue Lagoon. The injection of fresh water, along a line of wells adjacent and parallel to the sea, provides a pressure ridge against the sea-water wedge to prevent it from further inlandward transgression.

TABLE OF CONTENTS

LIST OF FIGURES

LIST OF TABLES

LIST OF MAPS

ACKNOWLEDGEMENTS

I would like to express my sincere gratitude to my Thesis Advisor, Dr. G.V. Keller, for his continued guidance and encouragement throughout the writing of this thesis.

Equally, I would like to extend my sincere thanks to Dr. A.A. Kaufman and Dr. C.H. Stoyer for serving as my graduate committee members and for their valuable advice.

I would also like to express my appreciation and thanks to Dr. A. Zohdy from the U.S. Geological Survey, and R. DeLaboulaye, President of Geoconsult, for sharing their experience and useful comments about the subject of this thesis.

Special thanks are reserved for Dr. A. El-Arnauti, head of the Geology Department at Garyounis University, M. Sayid, engineer from SDWR, Benghazi Branch, and my brothers for their great understanding and assistance in sending me all the information and data needed to complete this study.

The author also wishes to acknowledge the scholarship granted by Garyounis University, Benghazi, Libya, during his graduate studies at the Colorado School of Mines.

INTRODUCTION

Water is very important for human consumption, agriculture, and industry. Vitality exists wherever water exists, and adequate good quality water is necessary for such purposes. In arid and semiarid environments, the surface waters in terms of rivers or streams are limited or do not exist at all. It has become very important for other sources, like groundwater, to be discovered. Geophysical methods have been used successfully for groundwater exploration worldwide. Electric resistivity, seismic refraction, bore hole logging, induced polarization, self potential, gravity, and electromagnetism are the geophysical methods used for groundwater exploration. The DC electricity method has been widely used for groundwater exploration, where water quality can be defined directly from the resistivity value as a function of water salinity, and porosity of the aquifer.

The DC electrical resistivity method has been used for more than half a century in measuring the earth's resistivity. However, during the past three decades, the design of field equipment and interpretation manner have changed a little compared with the change of using different electrode configurations in field survey, and evaluating resistivity measurements with regard to a geological study (Keller, 1967).

The applications of the resistivity method in groundwater exploration have greatly increased over the past decade. Also, a combination of different geophysical methods is most likely used to solve various difficult cases in groundwater prospecting. However, there is no unique, effective approach to be followed in using the geophysical methods in groundwater exploration (Worthington, 1975). In recent years, more attention has been given to the application of the geoelectric methods for groundwater prospecting (Krulc, 1969). Delineating fresh water bodies from saline water bodies and minimizing drilling costs are good advantages of these methods (Breusse, 1963).

Groundwater salinity is a very common phenomenon in arid, semiarid, and coastal environments. In deserts, fresh groundwater is usually accumulated in the form of floating lenses over a saline water. In coastal areas the groundwater is susceptible to direct intrusion from the sea water. The sea-water intrusion may reach several thousand feet inland, contaminating confined or unconfined potable water aquifers in the area. Salt and fresh water are theoretically separated and controlled by what is called a salt-fresh water interface, which is dipping landward from the coast. This interface is actually a transition zone with a gradual increase in salinity with depth. The application of the DC electrical

resistivity method in sea-water intrusion into unconfined coastal aquifer is the basic topic of this research.

The proposal of this study is to delineate any sea-water intrusion through a karstic limestone unconfined aquifer and study the salinity problem caused by the sea-water intrusion in the area using DC resistivity sounding and bore hole logging. In addition to this, core analysis, water quality, and permeability test data have also been used.

THE AREA OF STUDY

Ayn Zayanah is located on the coast of Libya, at about fourteen kilometers northeast of Benghazi City (Figure 1). The area of study is approximately 20 square kilometers (Figure 2). The area is generally flat, with an unnoticeable, very gentle slope of about 2°-4° towards the Mediterranean Sea. The highest elevation is approximately 25 meters above the mean sea level in the Coeffiah Caves area, while the average elevation near the coast is about four meters above sea level in the Blue Lagoon vicinity close to the highway (Figure 2). The area represents a suburb of Benghazi City, where there are small villages, building projects taking place beside a major powerline, pipelines for water supply, a highway, and other subways are passing through the area. All of these aspects are possible sources of noise which, as well as geologic noise, may affect the field measurements.

The area is suffering from a salinity problem due to the movement of sea water into the fresh water aquifers in the coastal zone. Many other areas along the coast are having the same problem, where brine swamps similar to the Sebkha area represent evidences for sea-water intrusion.

Particularly, the Ayn Zayanah area is characterized by an active discharge spring through which the groundwater is

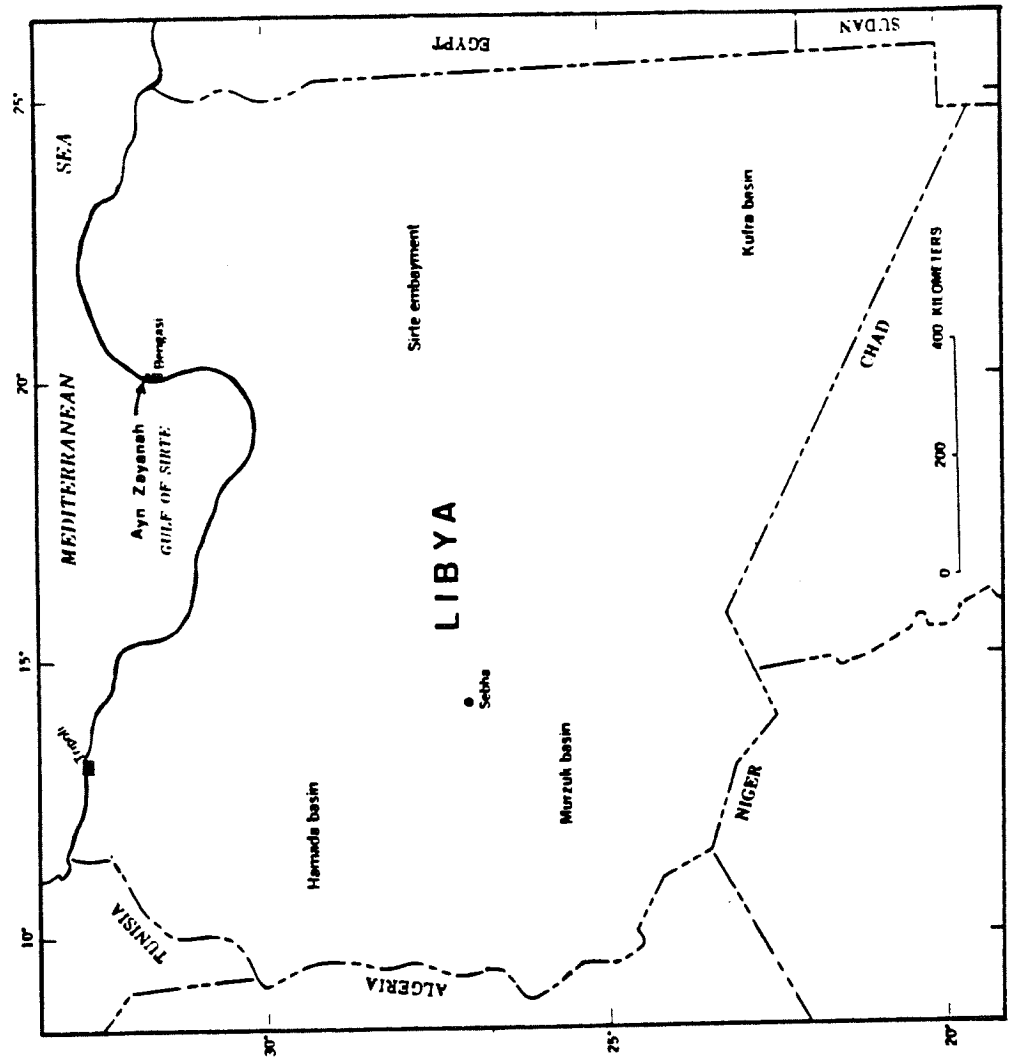

Figure 1. Area of study location map.

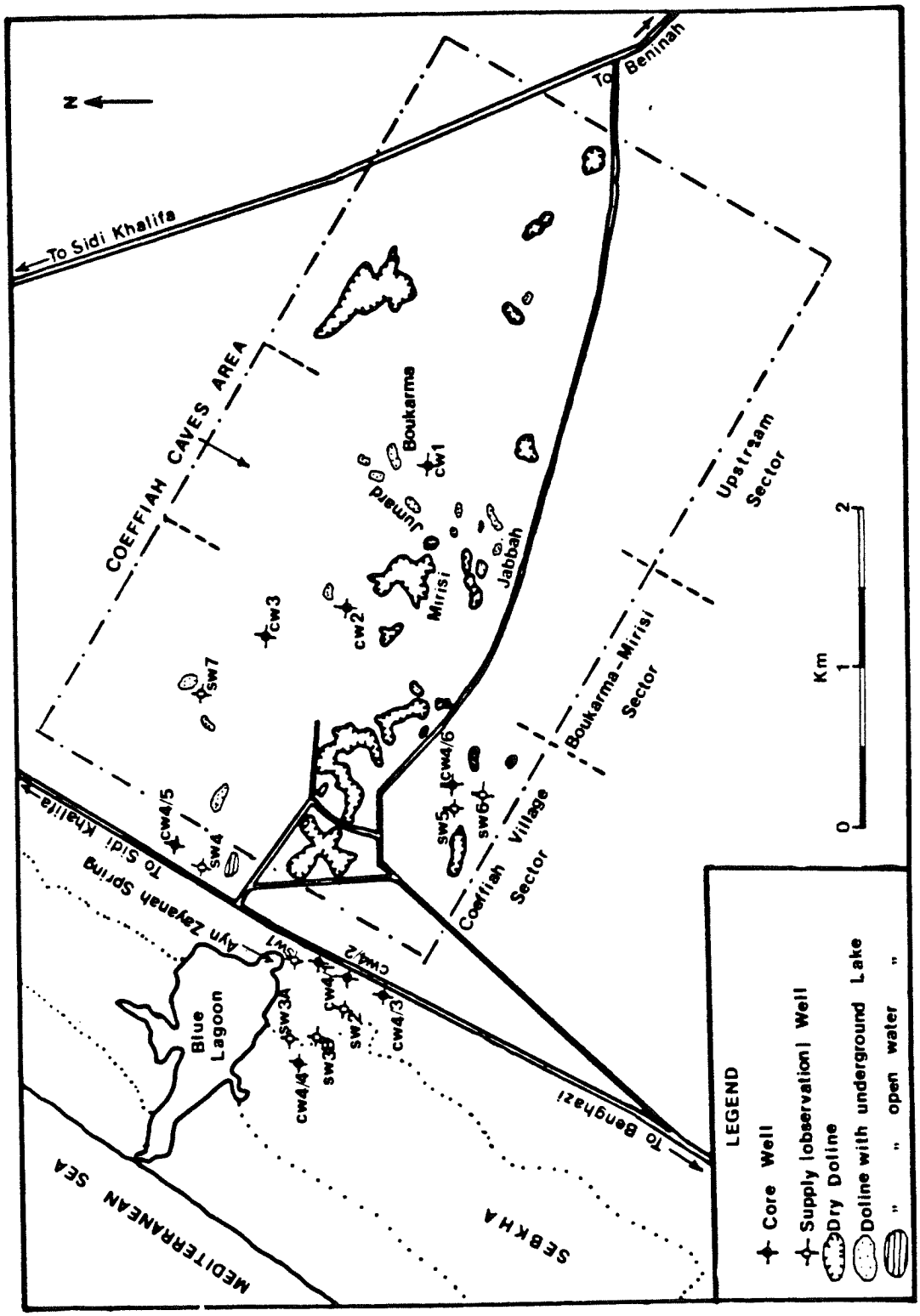

Figure 2. Ayn Zayanah and Coeffiah area map.

driven to the Blue Lagoon, which is open to the sea. The groundwater unconfined aquifer is of karstic limestone. The circulation of the groundwater is mainly controlled through the karst, cavity, and fissures of the aquifer. Unfortunately, the occurrence of the karst and cavities introduce a complex salinity pattern, particularly where a deep vertical karst exists.

According to all of these facts, a decision was made by the Secretariat of Dams and Water Resouces Technical Committee to assign a study project using geophysical methods for groundwater investigation in the area. The geophysical methods which were applied in the area will be mentioned later.

The author has chosen such a study because it is one of the most important problems facing the groundwater exploration in many areas along the coast of Libya. Groundwater is the only source available in the country, depending on the annual rainfall precipitation, and no other surface water in terms of rivers or streams exists.

SEA-WATER INTRUSION IN COASTAL AQUIFERS

Coastal aquifers are usually susceptible to salinity problems due to their direct contact with salt water from seas or oceans. This direct contact is under natural hydrostatic equilibrium control between salt and fresh water bodies. Under normal conditions, the fresh water moves into the sea-water region. Excessive use of fresh water in coastal aquifers lowers the fresh-water level, thus inland water movement does occur, giving the sea water a chance to move into the fresh-water region. This is known as sea-water intrusion in coastal aquifers. The sea-water intrusion may reach several thousand feet inland, contaminating all potable water wells in the area (Davis, 1966). Under normal conditions, an interface sloping landward from the coast is developed, separating the low-density floating fresh water from the sea water. This is known as salt-fresh water interface (Figure 3). However, the salt-fresh water interface position is controlled by the hydrostatic equilibrium between the two phases. Therefore, under normal conditions, the hydraulic gradient is always positive towards the sea and the opposite is true. The relation between the hydrostatic equilibrium and salt-fresh water interface was established mathematically by Ghyben and Herzberg (Davis, 1966) as the

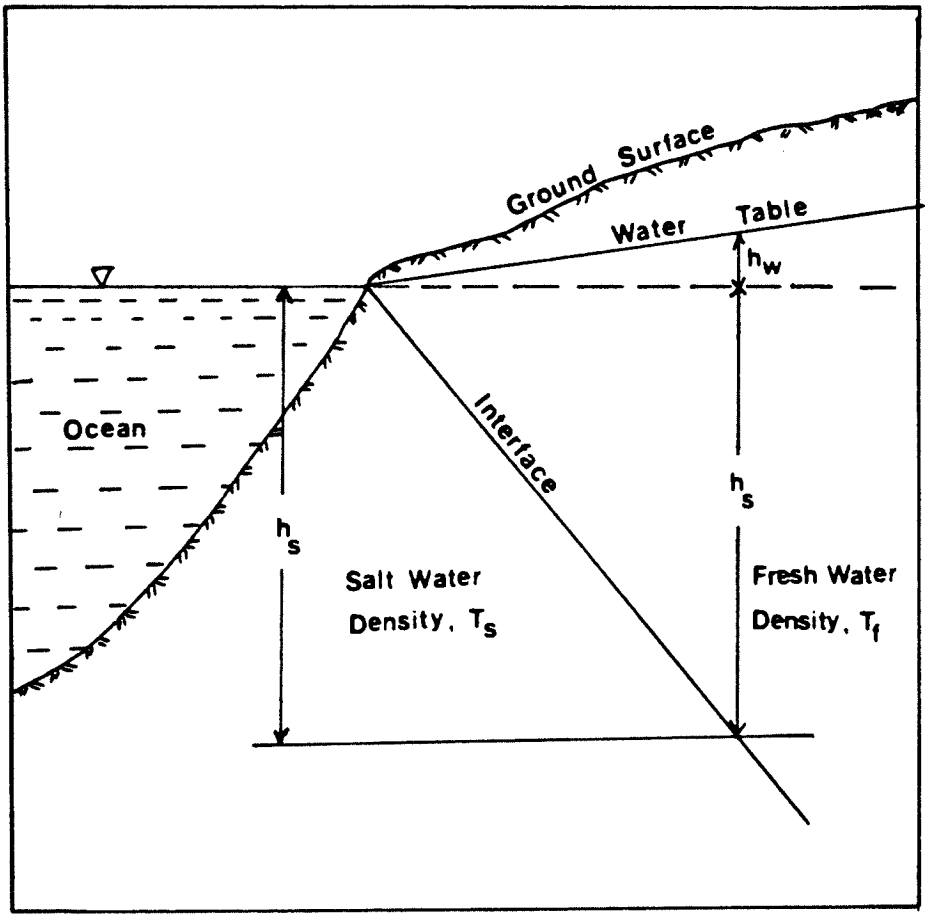

Figure 3. Salt-fresh water interface relation.

following:

$$hs = - \frac{T_f}{T_s - T_f} h_w \qquad (1)$$

where T_f is the density of fresh water, T_s is the density of the sea water, and h_w is the elevation of the groundwater table above mean sea level. Assuming that $T_s = 1.026$ g/cm^3 and $T_f = 1.0$ g/cm^3, then the following equation is obtained:

$$h_s \doteq -38\ h_w \qquad (2)$$

where the minus sign denotes depth below mean sea level. The above equation is satisfied at certain conditions, where the groundwater table is assumed to be in the horizontal plane and the sea water and fresh water are in static condition. In this nature, the water table could be in a slope plane, and the salt-fresh water interface is most likely a transition zone with a gradual increase in salinity, rather than a static, sharp interface. In this research, such a transition zone has been recognized from resistivity log records. The sea-water intrusion in coastal aquifers is a common problem in many countries of the world.

KARST DEVELOPMENT IN CARBONATE ROCKS

Karst is defined as a distinguished landform of cavities or caverns which developed in highly soluble rocks. Limestones are known as the most soluble rocks, where water is the important solvent factor to produce karst and enlarge rock voids by a simple chemical process. Since limestone is mainly calcium carbonate ($CaCO_3$) in composition, the chemical process is considered as solution and deposition. Calcite is a common mineral in limesone, also soluble in pure water with approximately 15 PPM (Parts Per Million) at 25°C (Frear and Johnston, 1929). The natural chemical process provides much greater concentrations than that. Therefore, the chemical process starts by ionization of $CaCO_3$ in solution as the following:

$$CaCO_3 \rightleftharpoons Ca^{++} + CO_3^{--}. \qquad (A)$$

This represents an ionic equilibrium at this stage, but natural water includes some carbon dioxide dissolved from the air, thus a carbonic acid would be produced and a further chemical process takes place as:

$$CO_2 + H_2O \rightleftharpoons H^+ + HCO_3^{--}. \qquad (B)$$

The result is bicarbonate (HCO_3^{--}) ions in the solution. Now the carbonate ions in (A) react immediately with the hydrogen ions resulting from (B) to produce bicarbonate ions, also; therefore,

$$CO_3^{--} + H^+ \rightleftharpoons HCO_3^{--}. \qquad (C)$$

This reaction causes disequilibrium in (A) and (B), thus more $CaCO_3$ would be ionized in the solution, more CO_2 diffuses from the air to the water, and a chain reaction takes place (Jennings, 1971). Generally speaking, this chemical process is slow due to the diffusion of CO_2 from the air into the water. Temperature is another factor which should be taken into consideration, where a faster process occurs at a higher temperature.

That is basically what may happen in a carbonate aquifer due to groundwater circulation. A karst or cavity is formed from this chemical process in the limestone aquifer. This may provide a high secondary permeability to the aquifer, since limestone generally has a low permeability. Subsurface streams may occur through karstic galleries, if well developed, and interconnected karst in the limestone aquifer is formed. The subsurface karst is usually associated with remarkable geomorphological features known as dolines or sinkholes. Dolines or sinkholes are bowl-shaped depressions resulting from

collapse of surface formation into the karst cavity (Figure 4). The dolines may have different shapes or sizes, depending on the degree of collapsing and formation strength. The collapse is most likely induced by lowering of the groundwater level.

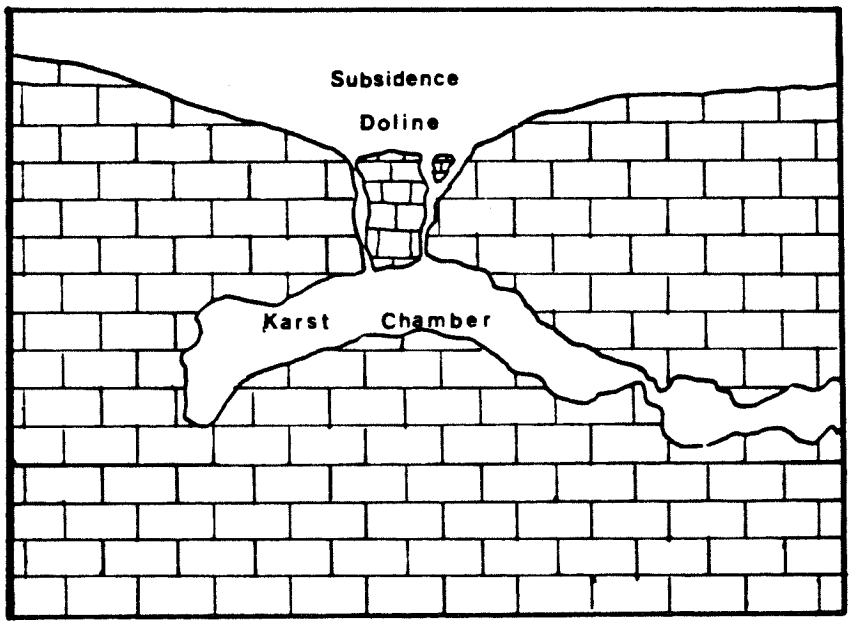

Figure 4. Karst and doline development.

GROUNDWATER IN CARBONATE AQUIFER

The carbonate rocks are generally known by their low permeability, but the rock structure may provide a favorable aquifer. Faults, fractures, fissures, and cavities are such rock structures. All these features in the rock represent a high secondary permeability and control water movements. A great water potential may occupy cavities, karstic channels, or faults in the rock. The carbonate aquifers, or karstic aquifers, are generally susceptible to contamination from other environments. The contaminant could be an industrial waste or a salt water, such as sea-water intrusion into coastal aquifers. This would definitely decrease the water quality and increase salinity problems. However, the depositional environment may control the water quality originally, where continental sedimentary rocks generally have water with lower salinity than marine environment sedimentary rocks (Keller, 1967). Also, coarse-grained rocks are characterized by less water salinity, while fine-grained rocks contain more water salinity. The fine-grained rocks have low surface absorption capacity, because their small surface area cannot prevent salts from diffusing. The water quality of carbonate aquifers is mainly distinguished by its hardness or alkalinity, where a considerable amount of carbonate and bicarbonate ions are dissolved.

GENERAL GEOLOGY OF THE AREA

Geomorphology

The area is generally flat, with an average very gentle slope of about 2° towards the sea. The major geomorphological features in the area are the Blue Lagoon, Sebkha deposits, sand dunes, outcropping limestone, dolines, and caves. The Blue Lagoon represents an intermediate reservoir between Ayn Zayanah spring and the Mediterranean Sea (Map 2). Ayn Zayanah spring is a natural discharge spot of the groundwater circulation in the area, and is influenced by the sea-water intrusion. The Sebkha deposits are generally karstic Middle-Miocene limestone overlayed by brine moisture with silt and clay. This is also known as Terra Rossa. The Sebkha area represents a secondary contaminant to groundwater circulation in the area and extends several kilometers along the coast. The sand dunes occupy the beach strip and are relatively higher in elevation than the Sebkha area. They mainly consist of sand and sand-sized carbonates. These are mainly quaternary deposits. The outcropping Middle-Miocene limestone covers most areas west of the Sebkha deposits. This area is characterized by dolines, caves, and fissures. The dolines or sinkholes are remarkable geomorphological features related to the development and occur-

rence of subsurface karsts or cavities causing a formation collapse. Some of these dolines are filled with open water lakes like the Bujazirah and Abu Zayrah dolines. Other dolines are associated with underground lakes formed by well-developed vertical karsts like the Boukarma and Jumard dolines. Most of the remains are dry dolines. This may depend on water table level relative to ground level, development, orientation, and connections of the karstic system.

Lithology and Structure

The geology of the area was not well-defined before the project of studying the groundwater using geophysical methods and the drilling of some cored wells took place. However, from the core analysis, geomorphology information, and the geologic maps available, it appeared that the area was generally dominated by sequences of limestones and dolomites. These carbonate formations were classified into two major formations, which are Middle-Miocene and Oligo-Miocene formations. The Middle-Miocene formation is known as the Ar-Rajma formation and is considered to be the top sequence of the lithology column, which mainly consists of dolomitic, marly dolomitic, and chalky limestone alternated with fine- to medium-grained biocalcarenites. The Middle-Miocene formation is mainly fossiliferous with various species of lamel-

libranches and gastropods. The bottom of this formation was defined from well CW1 and CW2 core analysis, at depths of 118 m and 136 m, respectively. Therefore, this formation is slightly dipping northwest towards the Blue Lagoon and the Mediterranean Sea, without any major fault in between (Map 1). The Oligo-Miocene formation is known as the Al-Fayadiyah formation, which almost has the same lithology as the Ar-Rajma formation, but is characterized by a layer of dark green plastic calcareous clay with disseminated pyrite crystals at the top of the sequence, followed by marly, dolomitic, and fossiliferous limestone with green clay streaks. The facies of this formation is generally finer than that of the Middle-Miocene due to deposition in relatively deeper water environment. According to correlation of the core analysis of wells CW1 and CW2, the difference in the depth at which the Oligo-Miocene formation has been found to correspond to the slightly normal dipping of the strata, so no major fault structure can be defined. Generally, the formation is slightly dipping by an average of less than 5° towards the northwest. One major karstic system was defined from core analysis and permeability tests within the 30-50 meter depth interval in the vicinity of the cored wells CW1, CW2, and CW3. A similar karstic system was also defined in the cored well CW4/1 within the 10-20 meter depth interval; this karst is apparently an extension of

the previous major karstic system. Unfortunately, a minor karstic feature associated mainly with fossiliferous limestone has been defined within the 10-20 meter depth interval through the cored wells CW4/2, CW4/3, CW4/4, CW4/5, and CW4/6. A deep karstic system was only defined in well CW1 at the 112-116 meter depth interval, where the normal resistivity log shows the 1.0 ohm-meter zone. This deep karstic system is possibly associated with other deep karstic systems in the area.

GEOPHYSICAL METHODS

The author has chosen the DC electrical resistivity sounding and well logging data performed in the area for this study. Spontaneous potential, short and long normal resistivity, neutron, gamma ray, temperature, and caliper log are the well logging tools used for the prospecting program. Core analysis, water quality analysis, and permeability tests are also additional data to this study. Other geophysical methods, seismic refraction, electromagnetic (EM), and gravity, were also applied. The seismic refraction method has been performed basically to trace a limestone bedrock within the Blue Lagoon area as a prestudy for a dam project which was proposed by SDW. The EM method was performed using a grounded long cable (Turam) source with sinusoidal 660 Hz and 220 Hz current. No success has been met with this method, because it is difficult to use this method due to noises from power lines, factories, and lateral change in resistivity (swamps, lakes, dolines, roads). The gravity method was performed in the southwest sector (Coeffiah Caves area), where the major karstic system and cavities occur. This method is sensitive to major karst occurrence rather than minor karst, however connection between karst systems has not been confirmed using this method.

DC Electrical Resistivity Method

The DC electrical resistivity method is one of the most widely used surface methods in measuring earth resistivity. In this method, a direct current from a dry battery is introduced into the ground through two terminal electrodes, while the other two terminal electrodes are used to measure the potential difference caused by the introduced direct current into the earth. Therefore, four terminal electrodes are commonly used to perform a resistivity measurement. There are many electrode configurations which can be used to perform vertical sounding, horizontal profiling, and sectioning surveys (Keller, 1966). Schlumberger, Wenner, and Polar dipoles are the three most commonly used electrode configurations (Figure 5). The vertical sounding survey is carried out by increasing the electrode spacing gradually after each record to study the resistivity variations with depth. The horizontal profiling is performed by moving all four electrodes at a fixed spacing along a profile to trace any lateral variation in resistivity due to change in structure, faults, or dikes. This survey is usually carried out after good understanding of resistivity change in the area from the sounding survey. The sectioning survey is a combination between sounding and profiling where either the current electrodes or the potential electrodes are fixed,

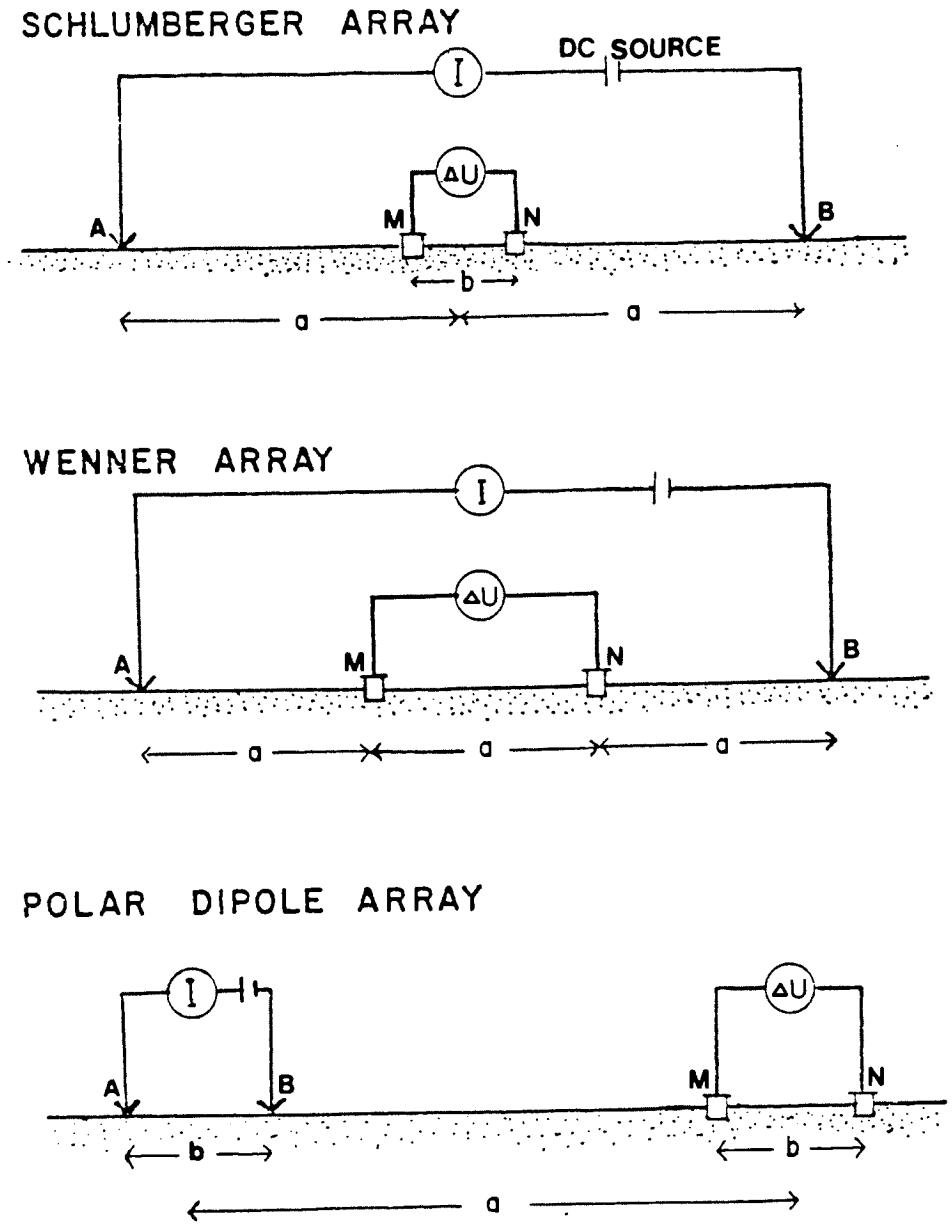

Figure 5. Types of electrode arrays most commonly used in DC resistivity survey.

and the other two electrodes are moved along a profile. This type of survey is useful for making pseudosections to locate buried targets. The sectioning survey is usually performed using polar-dipole array, which is more practical to move the electrodes freely along a profile.

The DC resistivity equipment is made light and simple, so that two persons can handle a resistivity survey. The equipment mainly consists of a dry battery as a direct current source, a potentiometer to measure voltage across the potential electrodes, some copper or steel electrodes, four good, isolated long wire reels, and a measuring tape. Also, a direct current can be provided from a low frequency square wave generator with a commutator to control and reverse the polarity of the potential electrodes at each reverse change of the current through medium (Keller, 1966).

In carrying out resistivity sounding measurements, the following equation is used to calculate the apparent resistivity values:

$$\rho = K \frac{\Delta U}{I} . \qquad (3)$$

This represents the resistivity of the earth as a function of the potential difference and electrode arrangement in a homogeneous isotropic medium where:

ΔU = the potential difference (volts),

I = the input current (Am), and

K = the geometric factor depending on the electrode spacings.

This also represents the apparent resistivity of the earth in anisotropic medium. The geometric factor is usually pre-calculated at different electrode spacing in order to obtain the apparent resistivity field measurements in less time. The following are geometric factors for different common types of electrode arrays:

$$K_S = \pi\left(\frac{a^2}{b} - \frac{b}{4}\right) \qquad \text{(Schlumberger array)} \qquad (4)$$

$$K_W = 2\pi a \qquad \text{(Wenner array)} \qquad (5)$$

$$K_d = \pi\left(\frac{a^3}{b^2} - a\right) \qquad \text{(Polar-dipole array)} \qquad (6)$$

where a and b are distances between potential, and current electrodes are as shown (Figure 5).

Water Salinity Estimation from Bore Hole Logging

The application of electric resistivity logs in ground-water prospecting is similar to the DC resistivity method where electrical properties of water-bearing rocks are used to determine water content, thickness, salinity, and porosity. Combinations of different logging tools are usually used for more detailed study of water-bearing rock characteristics.

Electric resistivity, spontaneous polarization, and porosity logs are the main tools used for quantitative and qualitative evaluation of groundwater. The resistivity of a water is proportional to its mineral content. Therefore, the resistivity of the water indicates its salinity or total dissolved solids at a certain temperature. Also, the resistivity of a water-saturated rock is a function of the water salinity and the porosity of the rock (Jones, 1950). Interconnections and the distribution of the water through the void spaces are other important factors affecting the resistivity value of the water-bearing formation (Keller, 1967). In this study, the occurrence of the karst characteristic in the limestone aquifer may represent the process of the distribution of water through the karstic routes in a relatively large scale, and the resistivity variance upon their interconnections. This may explain, also, that current flows by an electrolytic process through void spaces, and good interconnections allow the current to flow more freely. The water saturation is proportional to the fraction of void spaces (porosity) and the resistivity of the rock. Therefore, 100 percent saturated rock has a lower resistivity value, while same unsaturated rock has a higher resistivity value. The salinity or water quality is also proportional to the resistivity of the water filling the pore spaces of the

rock at a certain temperature. In other words, the water resistivity value can be converted to a salinity in terms of part per million (PPM) of dissolved solids. Schlumberger Company has prepared a chart for resistivity of NaCl aqueous solutions as a function of a corresponding salinity (PPM) and temperature (Figure 6). From this chart the water salinity (PPM) can be obtained directly at any temperature, if the water resistivity is known. In any event, an empirical formula was introduced by G.E. Archie (1942), expressing the relationship between bulk resistivity of a rock, porosity, resistivity of water filling pore spaces, and cement of the rock as the following:

$$R_t = R_w \phi^{-m} \qquad (7)$$

where R_t = the bulk (true) resistivity of a rock,

R_w = the resistivity of water in pore spaces,

ϕ = the porosity (fraction of void spaces), and

m = is the cementation factor.

From this empirical relation, the high porous rocks have a lower cementation factor than the lower porous rocks (Pirson, 1963). Another parameter which relate to the texture of the rock was investigated by Humble, Wyllie and others to improve Archie's formula as the following:

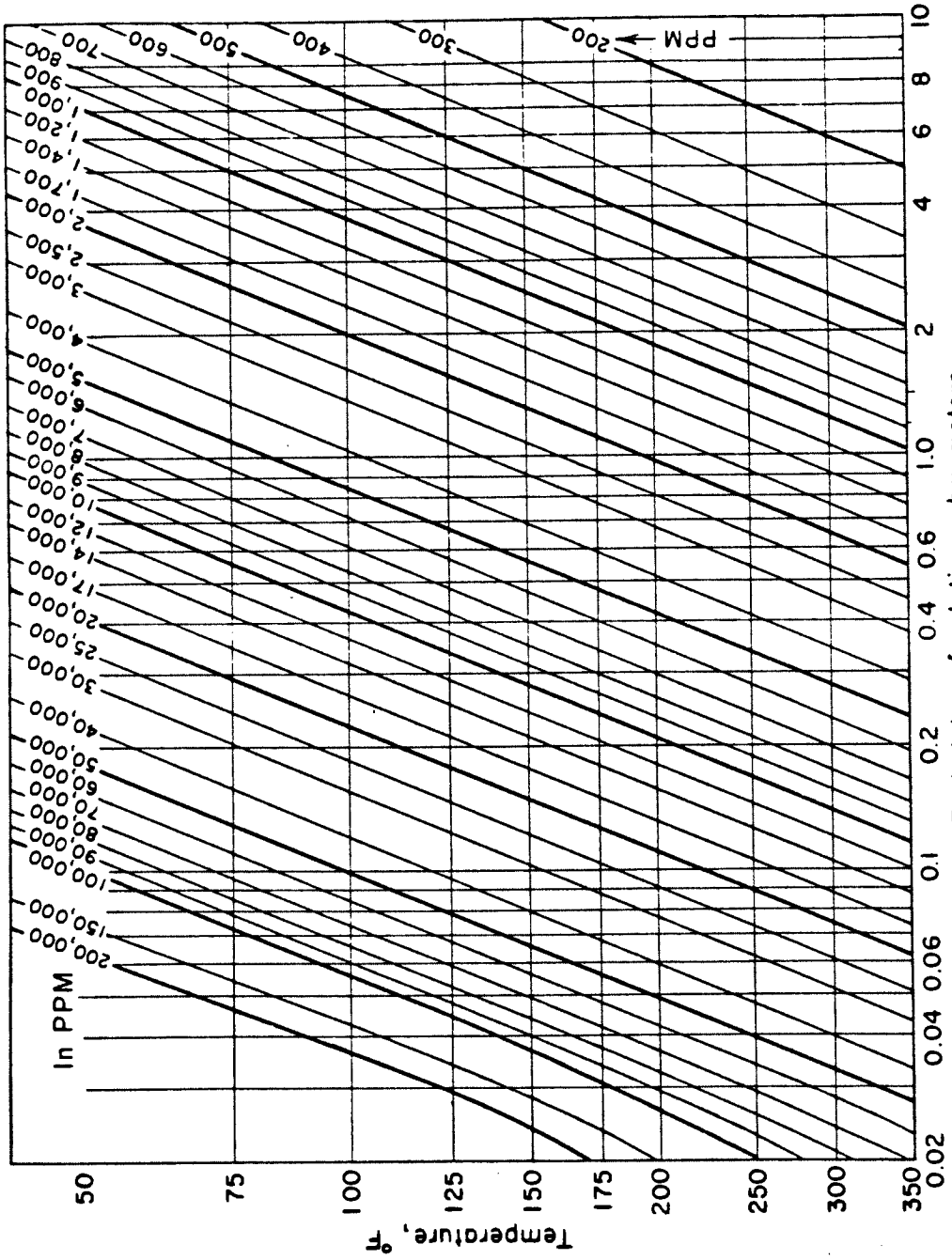

Figure 6. Resistivity-salinity conversion chart (after Schlumberger, 1972).

$$R_t = n R_w \phi^{-m} \quad (8)$$

where n = the parameter which relates to texture, also known as tortuosity factor.

The parameter n ranges from 0.6 to 1.3 in marine environment sedimentary rock, while the cementation factor, m, ranges from 1.3 in weakly cemented detrital rocks to about 2.2 in highly cemented rocks (Keller, 1967). In this case, different factors can be used for different environments of disposition. Therefore, the following formula was chosen to determine the water salinity of a limestone aquifer of a Middle-Miocene age with an average porosity of 25 percent:

$$R_t = 0.62 R_w \phi^{-1.72} . \quad (9)$$

These n and m factors were obtained generally for moderately cemented Mesozoic sandstones and limestones, with porosity range from 18 to 35 percent (Keller, 1967). A good graphical view can be obtained from plotting a porosity log vs. the resistivity log on a linear log paper in order to see any significant change in the relationship between porosity, resistivity, and the salinity simultaneously. This is known as a cross-plot technique, which is usually used for well log formation evaluation in the oil industry where gas-oil-water phases have to be distinguished using a combination of different logs to get more reliable results. The cross-plot

technique was used in this study for salinity estimation using the long normal resistivity log, and the neutron log as a porosity tool.

Principles of Neutron Logs

The neutron log is used basically to determine porosity of the formation. The response of this log is directly proportional to the amount of hydrogen present in the pore spaces of the formation. Therefore, water, oil, and gas zones can be defined with the aid of another resistivity log. The water and the oil have approximately the same amount of hydrogen. In this case the neutron log response decreases in the gas zone, and another porosity log or a core analysis is needed for comparison to identify the gas zones. A combination of different porosity tool logs with the neutron log is practically used for accurate determination of porosity values (Schlumberger, 1972).

The neutrons are simply produced by a chemical source. This source is a mixture of beryllium with radium, polonium, plutonium, or americium (Pirson, 1963). The neutron log source which was used by Condrill AB Company is a mixture of americium and beryllium. The neutrons are continuously emitted at energy about four million-electron-volts (MEV)

from such a source. The mass of the meutron is equivalent to the mass of the hydrogen atom. When the neutron log is run in a borehole, the emitted neutrons collide with the nuclei of the surrounding media. The neutron loses its maximum energy when it collides with a nucleus of an equivalent mass such as hydrogen. Therefore, the neutrons' energy loss depends on the amount of hydrogen in the surrounding media. The neutron energy reaches a thermal velocity stage within microseconds if the formation is highly saturated with hydrogen (Schlumberger, 1972). The neutrons at the thermal velocity stage, which corresponds to an energy of about .025 electron volts (EV), are captured by chlorine, silicon, or hydrogen nuclei.

Gamma rays are emitted as a result of capturing the neutrons at the thermal velocity stage. Different neutron logging tools are used to detect either the emitted gamma rays, the thermalized neutrons, or both. The neutron log response basically depends on the amount of hydrogen surrounding the sonde. Therefore, large amounts of hydrogen cause the neutrons to reach their thermal velocities and to become captured near the source, and small amounts of hydrogen give the neutrons the opportunity to scatter at farther distances before reaching their thermal velocities and becoming captured. Thus, different source-detector spacings

are technically used according to this reason. The types of neutron logs include the GNT series, the compensated neutron log (CNL), and the epithermal side wall neutron log (SNP).

FIELD DATA PROCEDURE AND MEASUREMENTS

The DC resistivity data, subsurface borehole logging, well coring, aquifer permeability tests, and water quality analysis were performed by Condrill AB Company from Sweden. The other geophysical methods mentioned previously were performed by CGG (Compagnie Generale de Geophysique). All of these measurements have been carried out within about four years (1977-1981). The DC resistivity data is the most recent work in the area and has produced useful information, while other methods (electromagnetic and gravity) have come up short, with insufficient data. This is primarily due to the cultural noise which could be avoided by using the DC resistivity method, but the electromagnetic method was affected by this noise and the geologic noise caused by lateral change in resistivity.

The DC Resistivity Soundings and Profilings

An ABEM SAS 300 Terrameter instrument, enhanced by an SAS 2000 Booster, was used to perform 16 soundings and three profilings covering approximately four square kilometers near the Blue Lagoon area (Figure 7). The Schlumberger electrode configuration was used for both sounding and profiling. The field work lasted from April 26 to May 14, 1981.

This portion of the area is particularly characterized by lateral change in the resistivity at the surface, because of the occurrence of the Sebkha area, the Blue Lagoon, rock fissures, and roads. This may cause difficulties in driving sufficient current to a reasonable depth, especially at the Sebkha area which is the most conductive surface layer. However, the capability of the booster to drive a current up to 500 mA through the ground made the measurements possible, with AB electrode spacing up to 500 meters. The cultural noise from power lines and industrial plants was eliminated by a compensating device designed in the instrument.

The 16 electric soundings were carried out from 1 up to 300-500 m AB electrode spacing. Most of these soundings were made parallel and close to the highway. This could be due either to tracing of a possible karst connecting the Ayn Zayanah spring or to the fact that it is the easy way to spread out the electrodes. The three electric profilings were performed with AB=200 and MN=20 meters spacing along the profiles RP-1, RP-2, and RP-3 (Figure 7). The profiling electrode spacing was chosen from the sounding data curve results where a conductive zone is approached.

The survey may be assembled to three sets as the following:

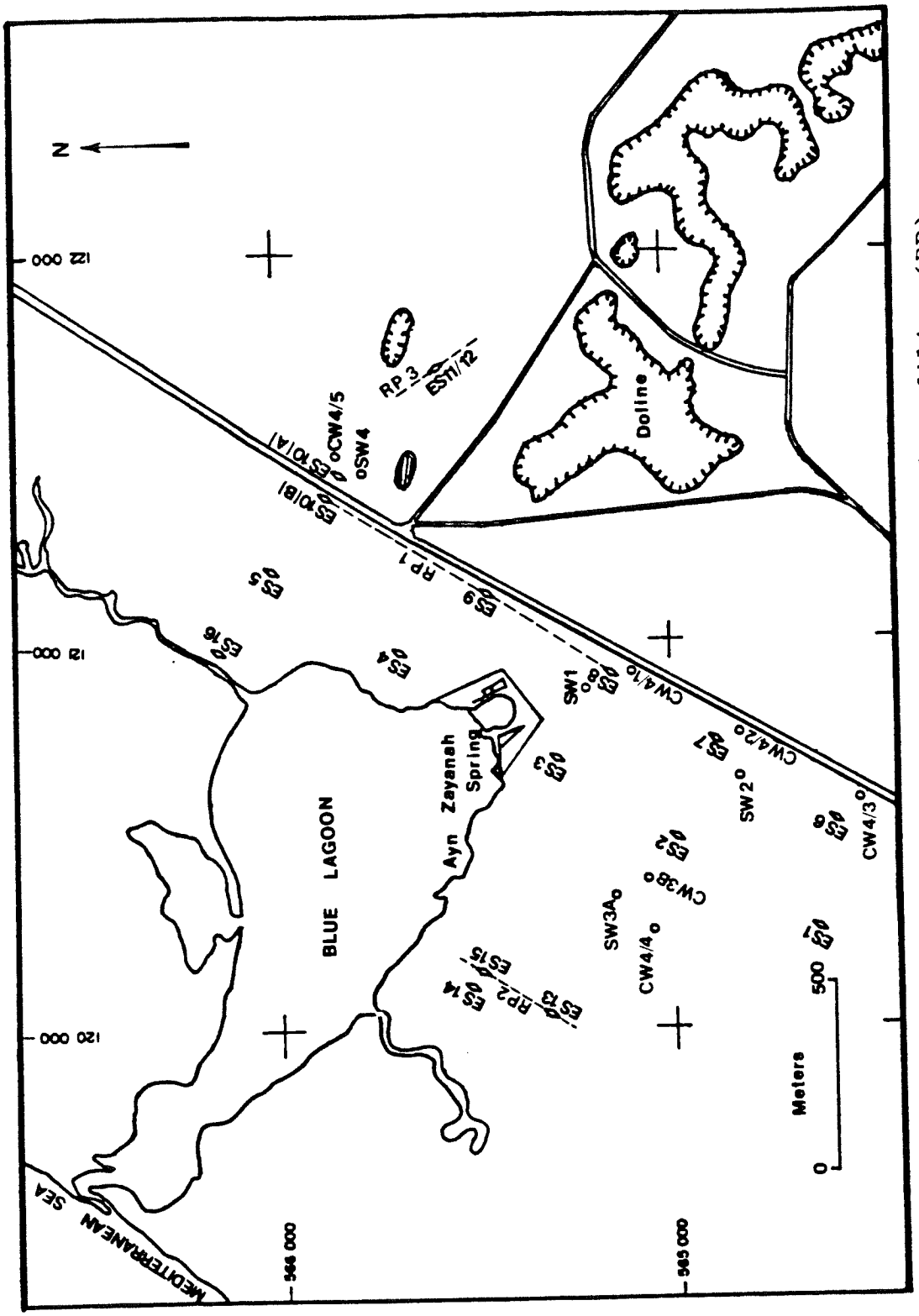

Figure 7. Electrical sounding (ES) and profiling (RP) locations.

Set 1: The electrical soundings lie between the Blue Lagoon and the highway and include ES-1 through ES-5 line, ES-6 through ES-10(A), ES-10(B), ES-16, and the resistivity profile RP-1 from ES-8 position to ES-10(B).

Set 2: The electrical soundings lie in the Sebkha area near the Blue Lagoon and include ES-13, ES-14, ES-15, and the resistivity profile RP-2.

Set 3: The electric sounding ES-11/12, and the resistivity profile RP-3.

The following electrode spacings were arranged for the electric soundings according to a complete measurement test at ES-8:

MN = 0.4 m for AB/2 = 1.0, 1.5, 2, 3, 4, 5, 6, 8, and 10 m;
MN = 4.0 m for AB/2 = 10, 15, 20, 30, 40, and 50 m;
MN = 20.0 m for AB/2 = 50, 60, 80, 100, 150, 200, and 250 m.

There is a common AB/2 spacing at each single change of the potential electrode's MN spacing (Appendix 1). The Schlumberger array is designed to measure approximately the potential gradient or the electric field using a closely

spaced measuring electrode. However, the potential gradient or electric field is an infinitesimal amount which is beyond the instrument accuracy to be measured. Therefore, the potential gradient is defined as the voltage measured with two electrodes at an infinitesimal spacing. This is the pracical reason for increasing MN measuring electrodes spacing occasionally to maintain sufficient voltage.

The resistivity profiling data were recorded as the following:

MN potential electrode spacing was fixed 20 m.

AB current electrode spacing was fixed 200 m.

Five readings were taken at each single movement of AB current electrodes by moving MN potential electrodes 5 meters twice to the left and twice to the right with respect to the midpoint 0 or $\frac{AB}{2}$ point, plus the original position reading. The AB current electrodes were displaced 20 meters along the profile after each set of readings. The resistivity profiling was an attempt to trace any major karst or subsurface lateral change in resistivity in the area.

Well Coring

According to the Condrill AB drilling report, a total of nine core wells were drilled, with depths ranging between 25

and 200 m for more detailed study in the area (Figure 2). The drilling program lasted from January 25, 1978 until March 13, 1979, where borehole logging, pressure permeability testing, and water quality analysis were performed as well. All of the core wells were run by logging tools, except core well CW3. However, the well log record of CW4/6 is also not available to the author. The following table explains each core well drilled depth and its sector:

SDWR Project #	Well #	T.D (m)	Sector
3389-3/906	CW1	200	Boukarma-Jumard pits
3389-3/907	CW2	150	Near Mirisi gallery
3389-3/908	CW3	75	NE Coeffiah village
3389-3/909	CW4/1	50	Ayn Zayanah
3389-3/927	CW4/2	25	Ayn Zayanah
3389-3/928	CW4/3	25	Ayn Zayanah
3389-3/929	CW4/4	25	Blue Lagoon area
3389-3/930	CW4/5	25	NE Coeffiah village
3389-3/931	CW4/6	25	SW Coeffiah village

The other 24 supply wells, noted by SW on the map, have been drilled with depths ranging from 5 to 50 m in the cored well vicinity in order to provide atmospheric pressure through the aquifers for the pressure permeability tests. The core wells were equipped with short casing pipes and screwed well caps (Appendix 3). They were left as open holes in the aquifer formation, except core well CW1 in the deep confined aquifer region which was completed with a cement plug in order to

isolate the upper karst from the deep karst, which was the saline water carrier from the confined aquifer. Eight of the supply wells were equipped with well caps to use them as additional observation points for water level and salinity changes. The following were the supply wells used as observation points:

SDWR Project #	Well #	T.D (m)	Sector
3389-3/933	SW1	21.0	Ayn Zayanah
3389-3/934	SW2	6.7	Ayn Zayanah
3389-3/935	SW3A	21.0	Blue Lagoon
3389-3/936	SW3B	26.0	Blue Lagoon
3389-3/937	SW4	33.0	NE Coeffiah village
3389-3/938	SW5	52.0	SW Coeffiah village
3389-3/939	SW6	25.0	SW Coeffiah village
3389-3/940	SW7	15.0	NE Coeffiah village

Four other supply wells were found to be nonproductive, because they were drilled in impervious regions; two were located in the Blue Lagoon sector, and two were in the NE Coeffiah village sector. The remaining two supply wells were drilled without completion in the Boukarma and Mirisi sectors. An addition seven observation wells, denoted by AW, are being used to measure the change of water level frequently in the area. Unfortunately, there is no drilling report about these wells so far. Generally, all wells in the area are being used as observation points (Table 5).

Throughout the coring and drilling project, two different groundwater levels were defined by packer test in well CW1. This is related to two different hydrostatic heads of two confined and unconfined aquifers in the area. The higher groundwater hydrostatic head is the unconfined aquifer, which has relatively brackish or less water salinity that the deep confined aquifer. The confined aquifer has a relatively lower hydrostatic head level, which was defined through well CW1 only, in the Moukarma and Mirisi sectors (Figure 2).

The Borehole Logs

Spontaneous potential (SP), short normal-long normal resistivity, neutron, gamma ray, temperature, and caliper logs have been run in the cored wells, except well CW3. The Condrill AB Company has no comment about excluding core well CW3 from the borehole logging program. These borehole logs were run to get more detailed investigation about water salinity change with depth, porosity, permeability, lithology, and structure such as karst or cavity which possibly has not been recurved by coring. The well logging program was completed two years before the DC resistivity method was performed in the area. This may explain the importance of the

DC resistivity method in groundwater prospecting and tracing of sea-water fronts regarding drilling cost and time consumption.

Permeability Tests

Pressure permeability tests were used for defining high permeability zones which indicate the occurrence of karstic formation. These were performed by injecting water through the formation at 5-10 meters depth with the 5-meter stage length packers. The tests provided quantitative analysis to the upper and the deep major karstic systems in the area. Also, minor karsts, fissures, and fractures were defined from the tests (Appendix 3).

Water Quality

Chemical analysis of water samples was performed in the SDWR laboratory. All samples were analyzed for Na, Ca, Mg, K, HCO_3, CI, SO_4, electrical conductivity, and total dissolved solids (TDS) in parts per million (PPM) (Table 4). The water samples were taken after pumping water out of the core well for about six hours in order to discharge all water injected during the pressure permeability tests. Packer tests were made in core wells CW1 and CW2 only, to get samples from

two main formations where the major karstic system occurs. These were performed by separating Middle-Miocene and Oligo-Eocene formations using a packer, and pumping water out in two stages individually. Core well CW3 was not tested for water quality.

INTERPRETATION OF FIELD DATA

The DC Electrical Sounding Data

The interpretation of the apparent resistivity sounding data may take some stages before a final earth's resistivity model can be considered. The first stage usually starts at the field measurements, where a quick estimation of the earth's resistivity and thickness parameters are needed in order to know the suitable electrode separation which can be used to reach a target horizon. This can be done by theoretical curve matching, or by asymptotes approach in case H and K type curves. The four types of curves, H, A, K, and Q, are shown in Figure 8. After these quick results, the interpretation can be improved by using a partial or a complete theoretical curve matching with three layers, in order to keep up to date more approximated results which can be followed through the field operations for more consistent measurements. The discontinuity of the sounding curve could result from the occasional change of the potential electrode's MN spacing, lateral change in resistivity of surface layer, or measurement errors (Zohdy, 1974). From all field survey data, other geophysical surveys, if available, and geology

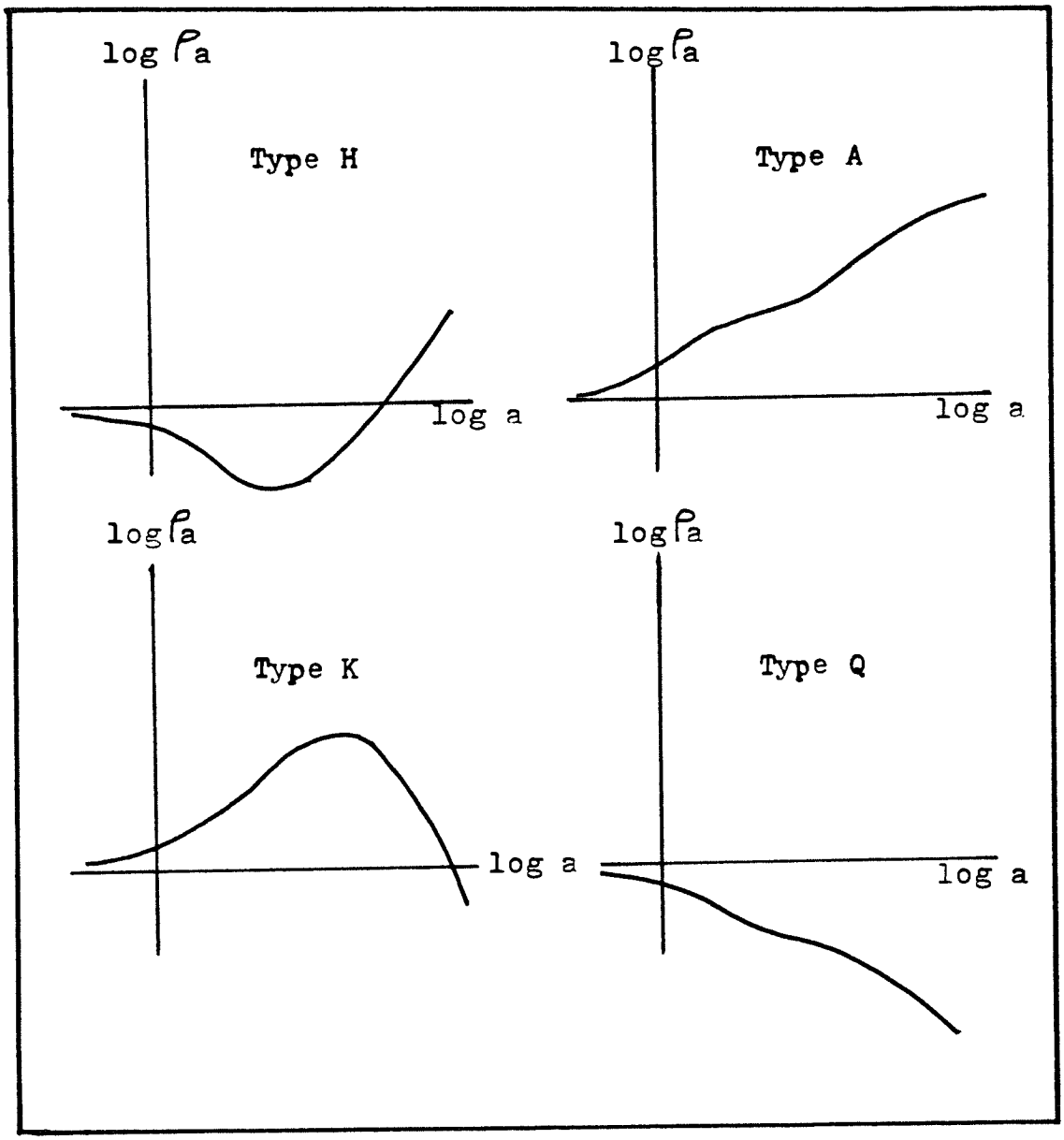

Figure 8. Types of electrical sounding curves.

of the area, a final interpretation can be reached at this stage.

Recently, an inversion technique using a computer program to calculate a theoretical curve for a given earth's model has been used as the best approach for more accurate interpretation, rather than manual curve matching. The inversion technique was used to interpret the electrical resistivity sounding data of this research.

An interactive computer inversion program called SARI (Semi-Automatic Resistivity Inversion), written by C.H. Stoyer (1979) of the Department of Geophysics, Colorado School of Mines, was used for the field data interpretation. SARI is a second generation from another inversion program called CRIMPA (Complete Resistivity Interpretation and Modeling Package - Automatic), which also was written by Stoyer (1977). The inversion technique is basically the generation of calculated resistivity values corresponding to the actual field resistivity values for a given earth's model of different layered media, and the matching of these calculated values with the field data using the least squares method to determine the errors. Matrix properties are used for matching and determining the change of all model parameters needed to improve the model. This procedure is repeated until the errors con-

verge to a minimum possible value, then a best earth's model which fits the actual field data is reached. The SARI is an interactive computer program with useful operating commands, through which all field data can be input and saved in a file. A suitable earth's model for the field data sounding curve is given to the computer program, which automatically generates a set of theoretical data for the assumed earth's model corresponding to the same electrode spacings in the field data. Both the theoretical and field data are matched and the errors are determined. The computer program automatically iterates this step until the best model is reached, with minimum possible errors. The SARI program has fixing and editing key commands which can be used in fixing earth's model parameters and adding or deleting data points. The fixing command has been used to fix one of the intermediate layer parameters in type H and K curves due to the principle of equivalence. Fixing parameters gives relatively higher error percentage than leaving them to alter freely through the computer program iterations. The editing command has been successfully used in deleting some data points which cause discontinuity in the resistivity sounding data curve. Deleting discontinuous data points improves the error percentage generally, but may delete useful information, since the corresponding theoretical data would be affected as well.

In any event, the application of the inversion technique in resistivity sounding data interpretation is generally more accurate than using a catalog of theoretical results (Keller, 1977).

The interpretation of the field resistivity sounding data has been done with regard to three important features, which are consistent results through all resistivity soundings, the resistivity well logs, and the geology of the area. The geology of the area has been followed through the geomorphology and the lithology obtained from the core well analysis. The geomorphology provides useful surface features supporting the lateral change in resistivity noticed in the thin surface layer as a result of the interpretation. The lithology study has confirmed the occurrence of the major karstic system through which the groundwater circulation activity takes place. A great support for the interpretation of the resistivity sounding data was obtained from the resistivity well logs. Unfortunately, all core wells in the vicinity of the sounding profiles were shallow compared with the deep core wells CW1 and CW2. However, the core well CW4/1, which was drilled adjacent to Ayn Zayanah spring up to 50 meters depth, was a major support to the interpretation (Appendix 2). The other shallow core wells, CW4/2 through CW4/5, provided consistent resistivity values in the second

and the third layer of the interpretation.

The consistency of the results was obtained through two stages of interpretation. The first stage of interpretation was obtained by assuming suitable earth's models with regard to the data curve shape and the resistivity log of the most adjacent well. Most of the 16 electric sounding data curves were of K and Q type (Appendix 1). According to the principle of equivalence, all K- and Q-type curves were interpreted by fixing one of the middle layer parameters. After this stage was completed (Table 1), an average resistivity of 2.5 ohm-m/layer was noticed through all model results. This layer represents that the most conductive lower zone was reached by the electric soundings. Four geo-electric sections were drawn, as shown in the map (Figure 9), in order to see the interpreted earth's models and the theoretical salt-fresh water interface, presumably by following the last conductive layer in the sections (Figures 10 through 13). In the second state of interpretation, this 2.5-ohm-m layer was fixed through all earth's models with regard to the previous stage process. A final earth's model resulted in an average error of 6.7 percent (Table 2). An isoresistivity contour map of the 2.5-ohm-m zone was made in the electric soundings region in order to delineate the salt-fresh water fronts caused by the seawater intrusion (Figure 14).

Table 1. Results of electrical resistivity interpretation (1).

ES #	Model Layers	Ω-m ρ_1	m h_1	ρ_2	h_2	ρ_3	h_3	ρ_4	Error %
1	4	1.2	0.69	35.0	8.5	10.1	22.5	1.8	3.9
2	4	31.3	0.8	58.0	3.41	19.1	33.6	2.68	4.8
3	4	905	0.24	31.1	1.6	13.6	36.2	2.13	5.7
4	4	264	0.87	29.0	10.4	5.71	13.2	3.26	8.2
5	4	8.18	1.73	16.2	6.82	7.48	31.4	2.46	2.7
6	4	1.16	0.74	15.3	5.7	35.0	18.4	0.76	4.1
7	4	1370	0.28	32	9.7	14.3	33.6	3.39	4.8
8	4	4.12	0.22	18.9	2.03	25	29.8	2.78	8.03
9	4	173	3.44	25	16.4	5.29	31.4	4.02	7.3
10(A)	4	7.48	1.77	50.0	6.84	6.61	59.6	1.78	8.5
10(B)	4	9.09	1.48	50.0	1.76	8.02	71.1	3.00	3.06
11/12	4	1170	0.27	146.0	11.6	27.0	26.9	2.96	7.05
13	3	405	1.07	0.51	6.0	2.06			12.89
14	3	0.32	2.63	15.0	2.59	2.06			4.81
15	3	0.33	2.37	10.0	7.22	2.11			2.98
16	3	0.82	1.05	14.0	14.6	2.65			3.46
							Average % Error		5.76

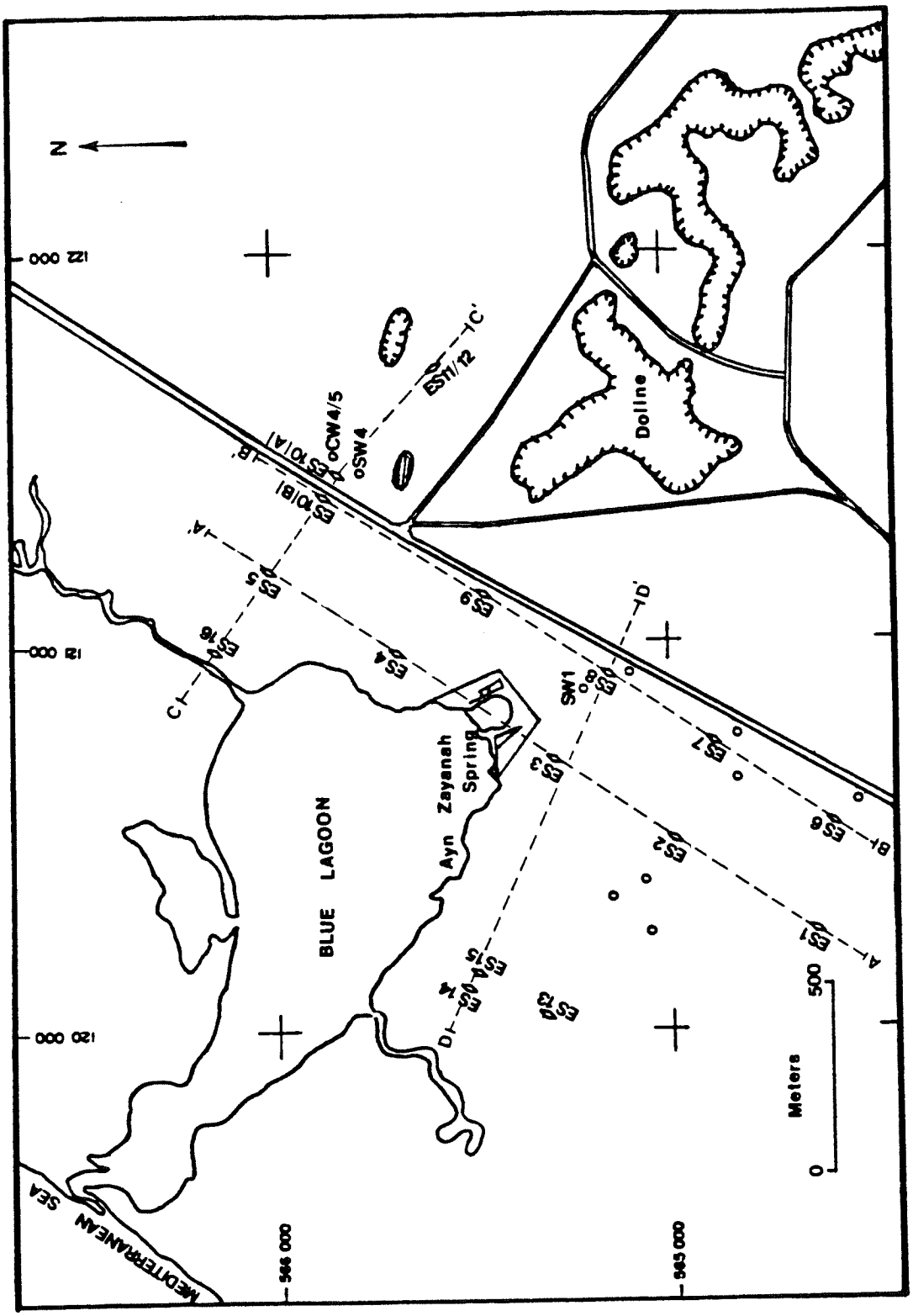

Figure 9. Geo-electric sounding sections.

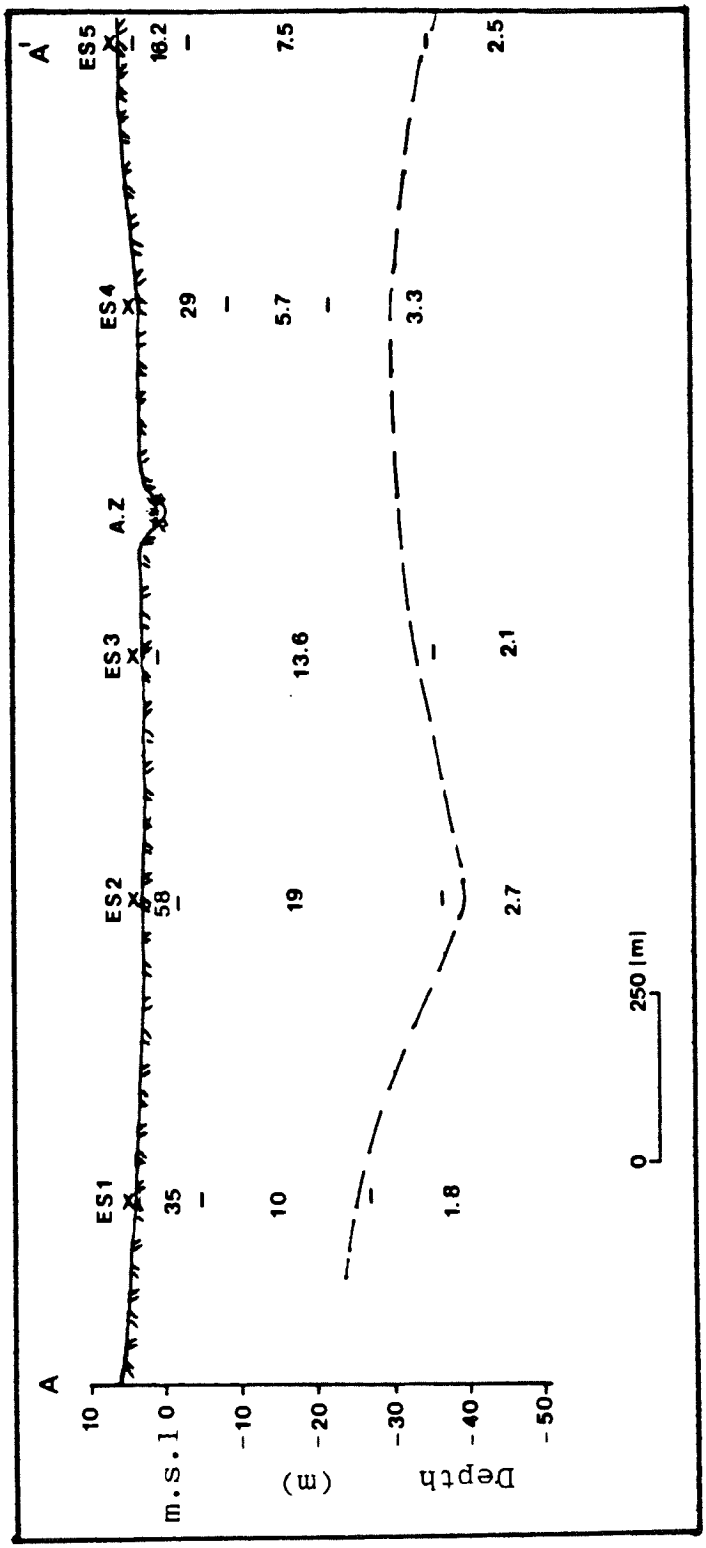

Figure 10. AA' geo-electric sounding section.

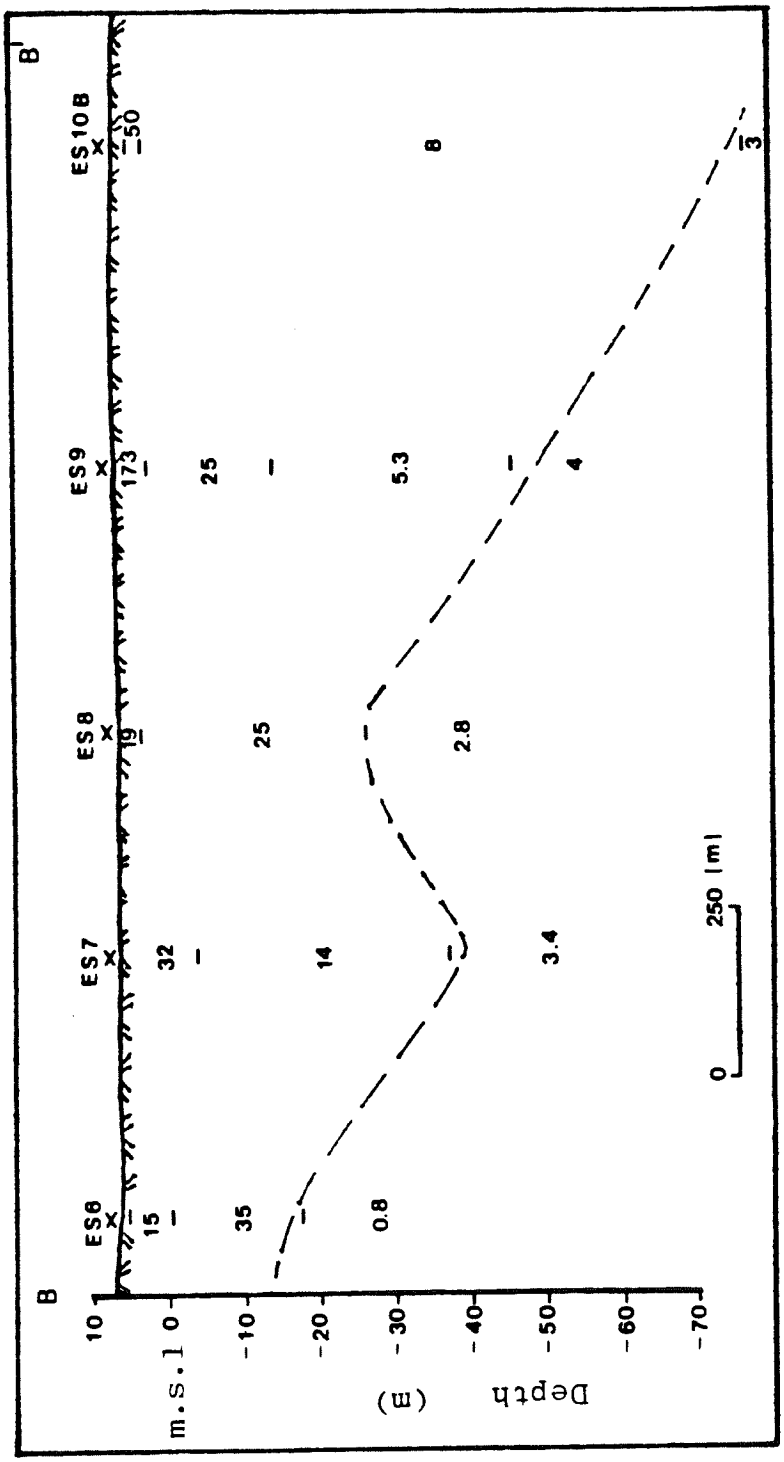

Figure 11. BB' geo-electric sounding section.

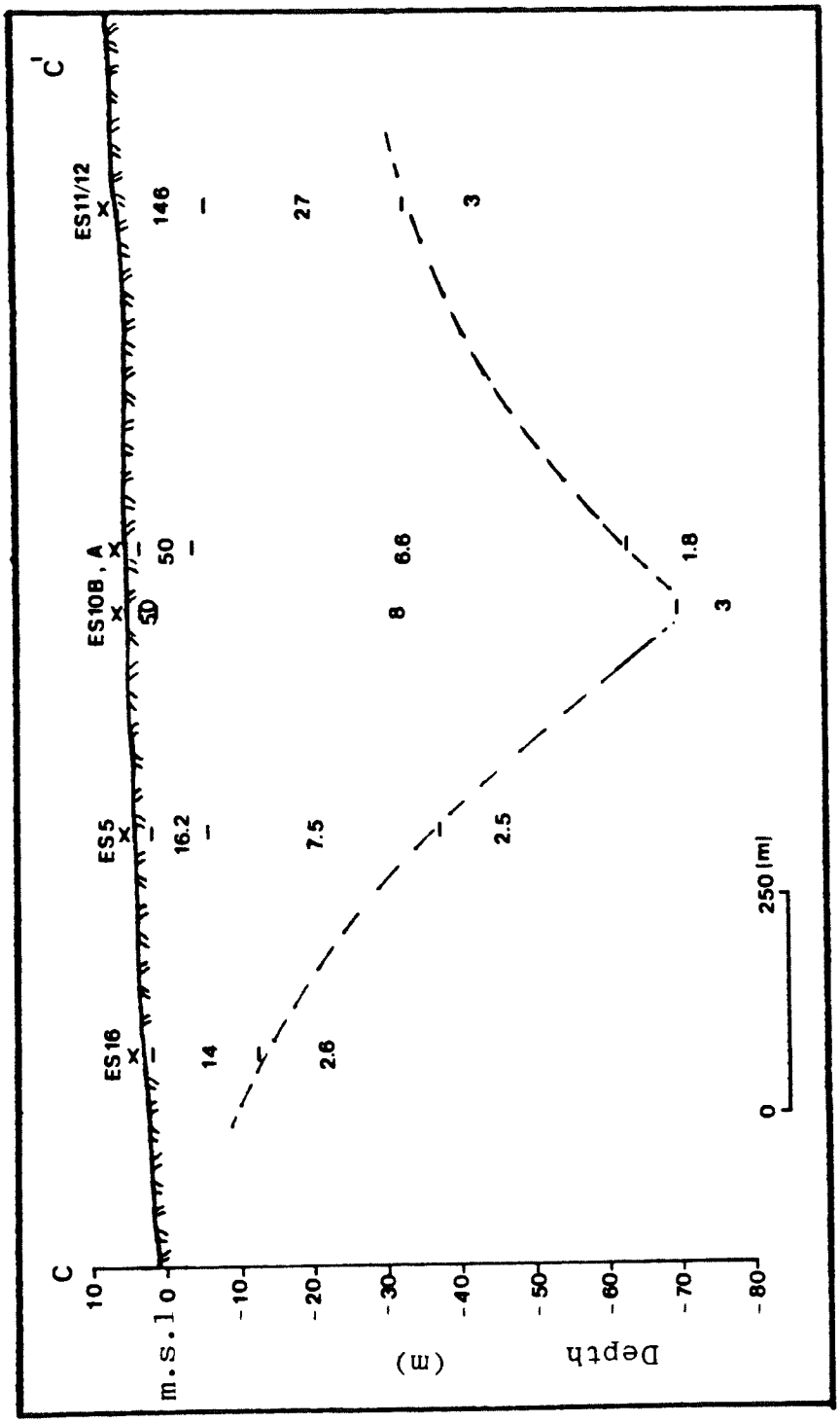

Figure 12. CC' geo-electric sounding section.

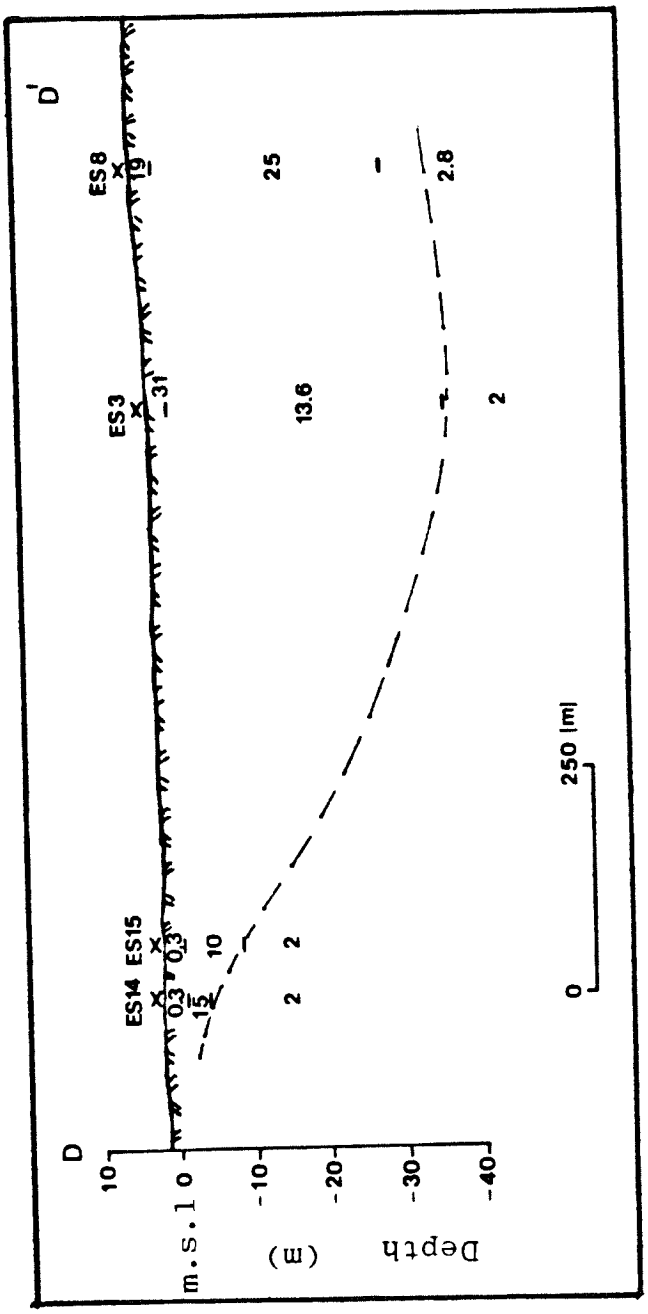

Figure 13. DD' geo-electric sounding section.

Table 2. Results of electrical resistivity interpretation (2).

ES #	Model Layers	ρ_1	h_1	ρ_2	h_2	ρ_3	h_3	ρ_4	Error %	Depth to 2.5 ohm-m Zone
1	4	1.18	0.7	37.0	5.7	27	9.5	2.5	7.5	15.9
2	4	40.6	1.6	58.4	3.02	18.2	37.1	2.5	4.84	41.72
3	4	331	0.28	31.1	1.5	14.5	22.8	2.5	6.19	35.5
4	4	243	0.88	29	10.1	5.88	21.8	2.5	6.24	32.78
5	4	8.15	1.67	16	6.91	7.55	30.4	2.5	2.64	38.98
6	4	1.12	0.7	13.9	3.7	35	15.2	2.5	8.63	19.6
7	4	1390	0.28	32.3	10.8	12.6	42.3	2.5	3.77	53.38
8	4	5.49	0.3	19.2	2.3	25.6	30.1	2.5	8.4	32.7
9	4	172	3.4	26.1	12.2	7.9	39.5	2.5	9.26	55.1
10(A)	4	4.67	1.96	53.4	5.87	7.2	44.18	2.5	6.02	52.01
10(B)	4	5.6	1.45	50.1	1.76	7.9	77.7	2.5	3.02	80.9
11/12	4	868	0.3	138	13.1	19.8	32.3	2.5	7.39	45.7
13	3	403	1.07	0.37	4.96	2.5			13.33	6.03
14	3	0.3	2.37	11.5	1.75	2.5			6.94	4.12
15	3	0.32	2.19	6.3	8.02	2.5			6.12	10.21
16	3	0.81	1.02	13.3	16.5	2.5			3.21	17.52
							Average % Error		6.7	

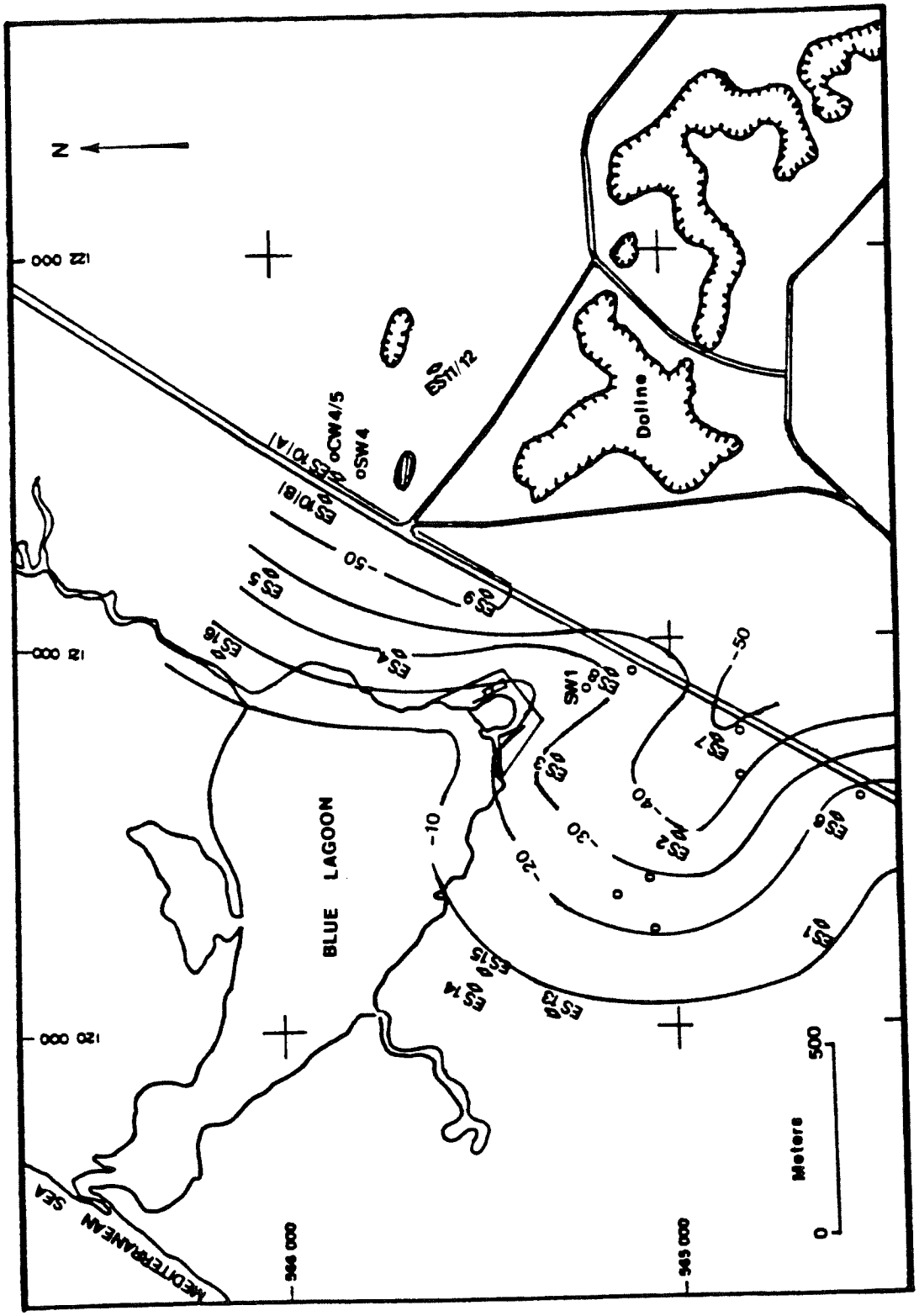

Figure 14. Isopach contour map of (2.5 ohm-m) zone.

The DC Electrical Profiling Data

The DC electrical profilings were performed to trace any significant anomalies due to sea-water intrusion or karst in the area. Unfortunately, the data of the three resistivity profiles did not define any significant change in resistivity (Figures 15 through 17). However, the resistivity profiles explained the subsurface lateral change in resistivity, where resistivity decreases as the resistivity profile approaches the coast (Figures 16 and 17). This resistivity change is due to the slope of salt-fresh water transition interface. The resistivity profile (1) (Figure 15) showed slight changes in resistivity because of some noise sources (pipeline culverts and road).

Well Log Data Analysis

The well log data were used for quantitative and qualitative interpretation. The long normal resistivity and neutron logs were used for the quantitative interpretation for estimating groundwater salinity. The cross-plot technique was used with the neutron log vs. the normal resistivity log (Figures 18 through 24) in order to see, graphically, the relationship between resistivity, porosity, and water salinity.

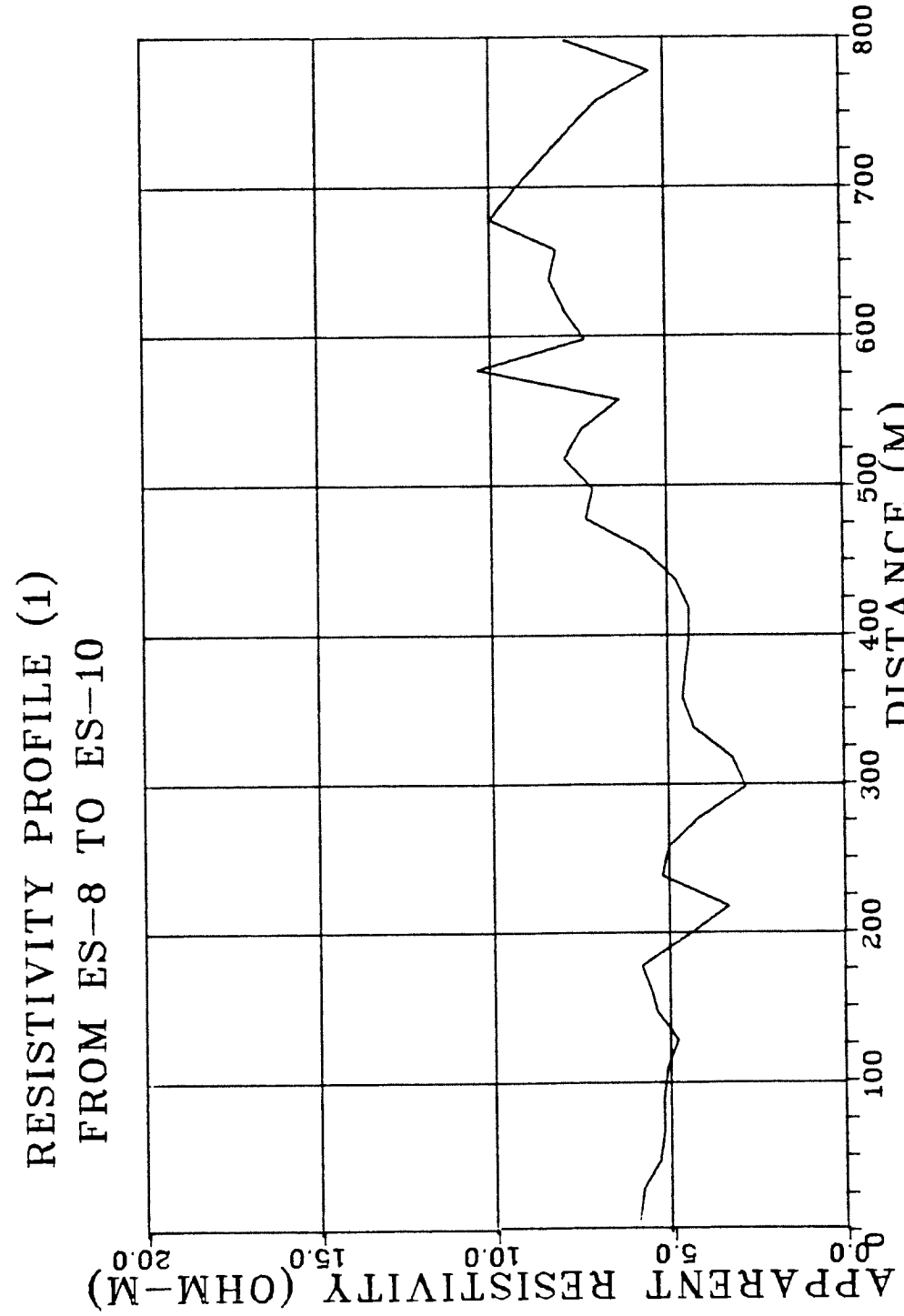

Figure 15. RP-1 resistivity profile (1).

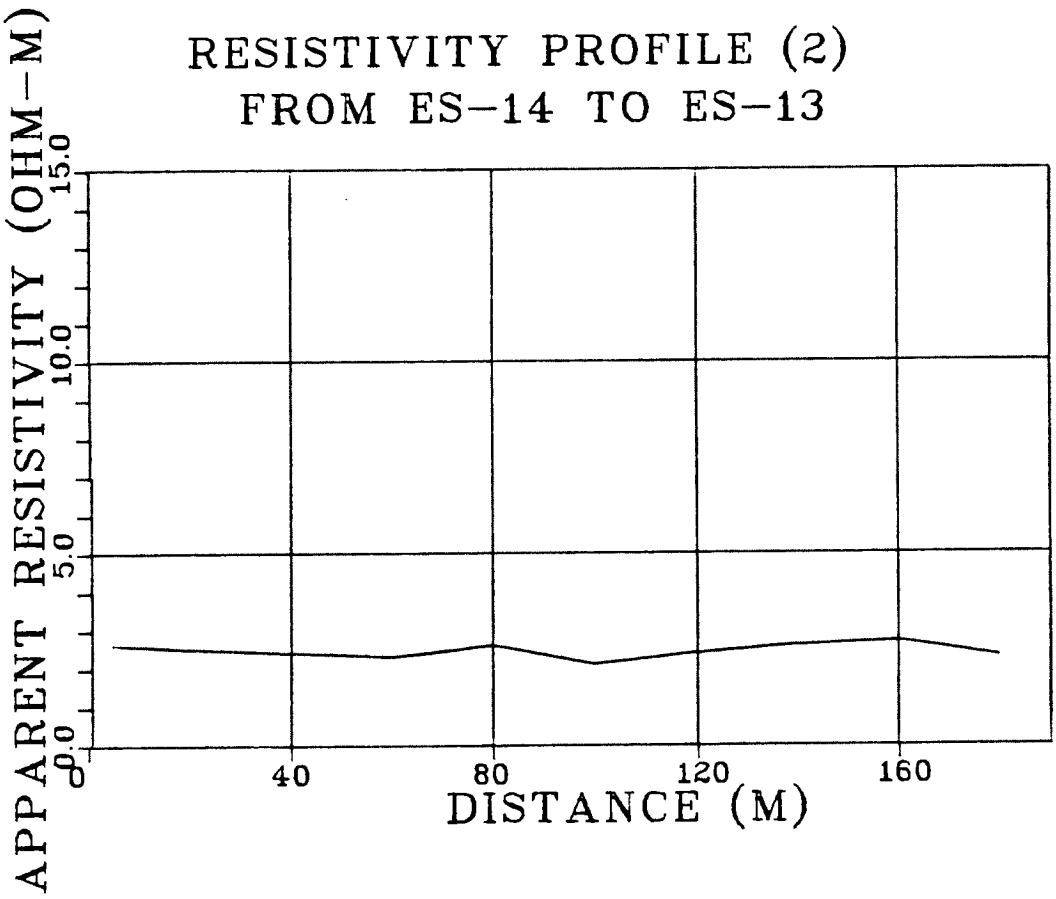

Figure 16. RP-2 resistivity profile (2).

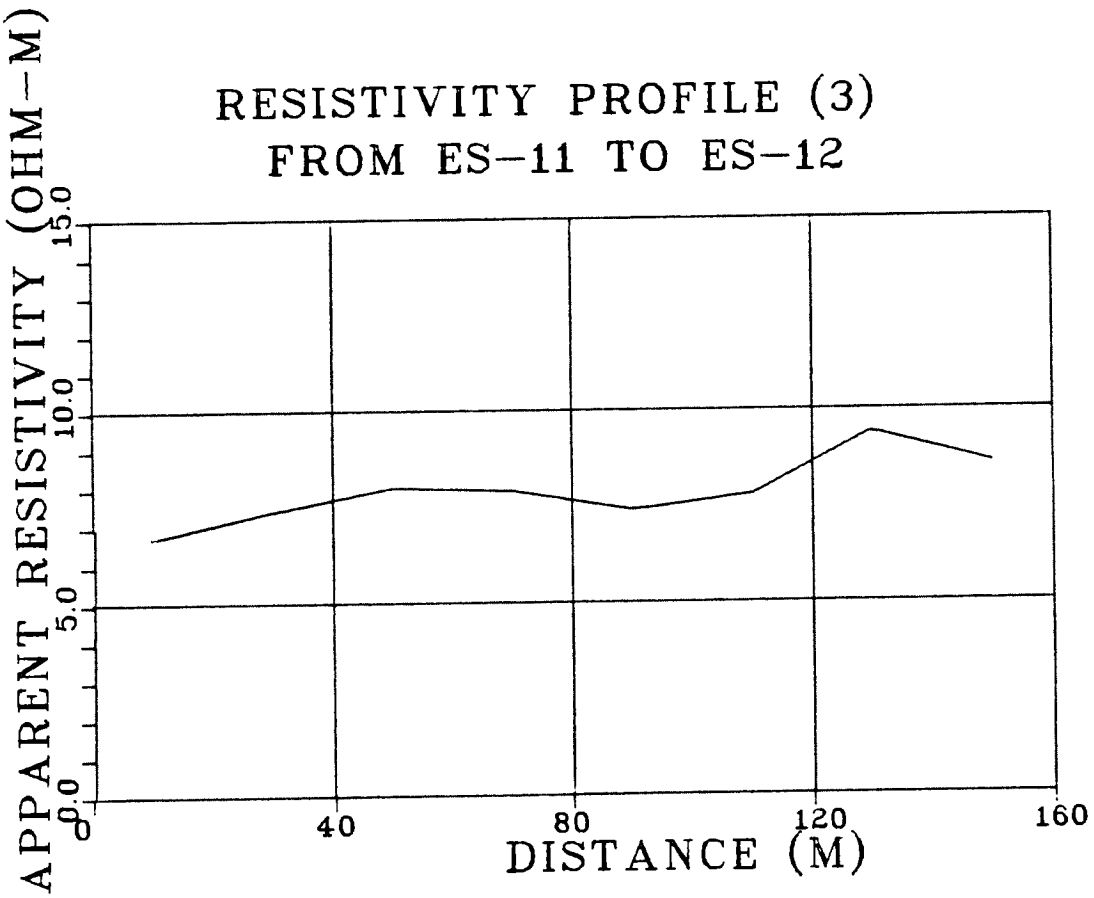

Figure 17. RP-3 resistivity profile (3).

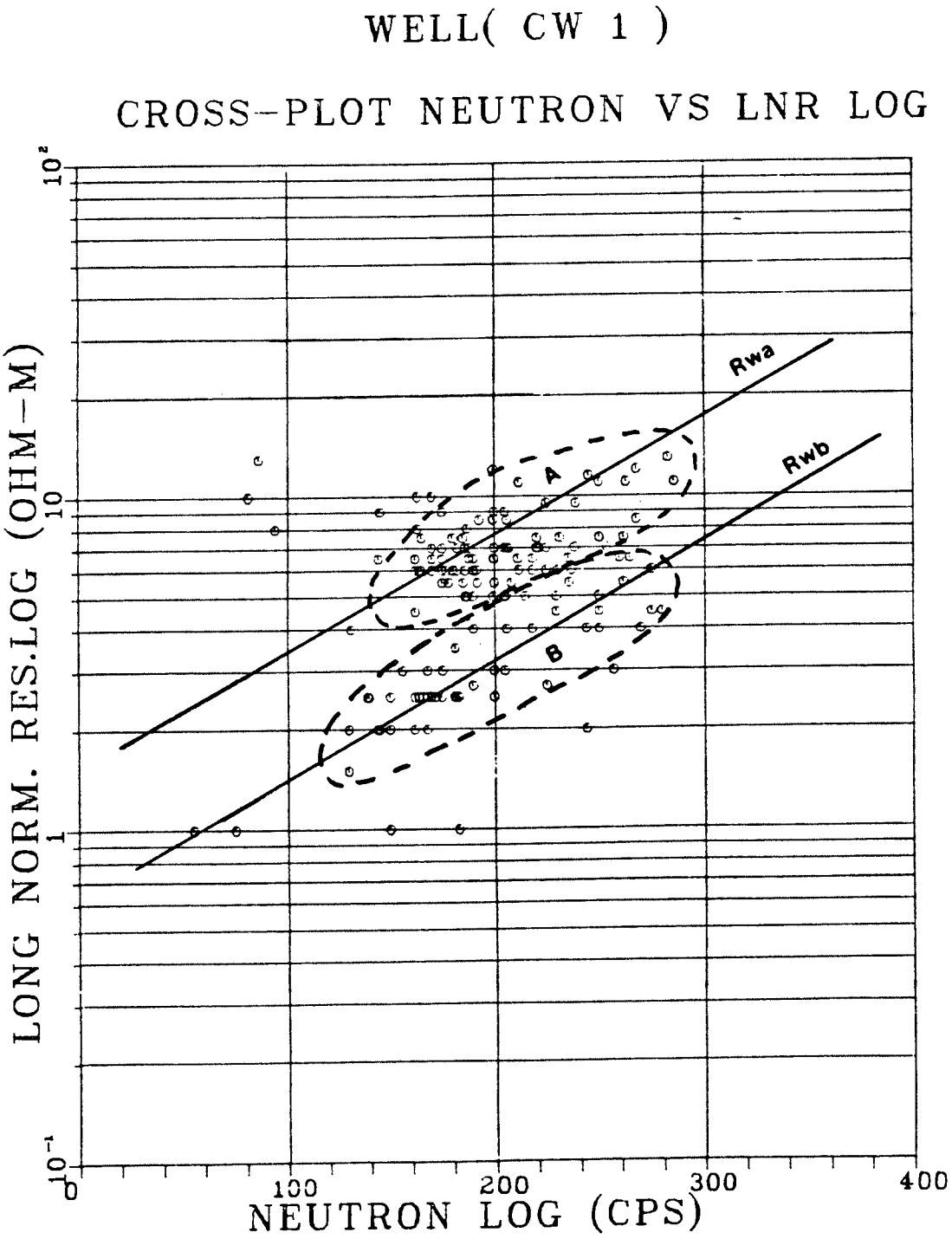

Figure 18. Core well CW1 cross-plotting.

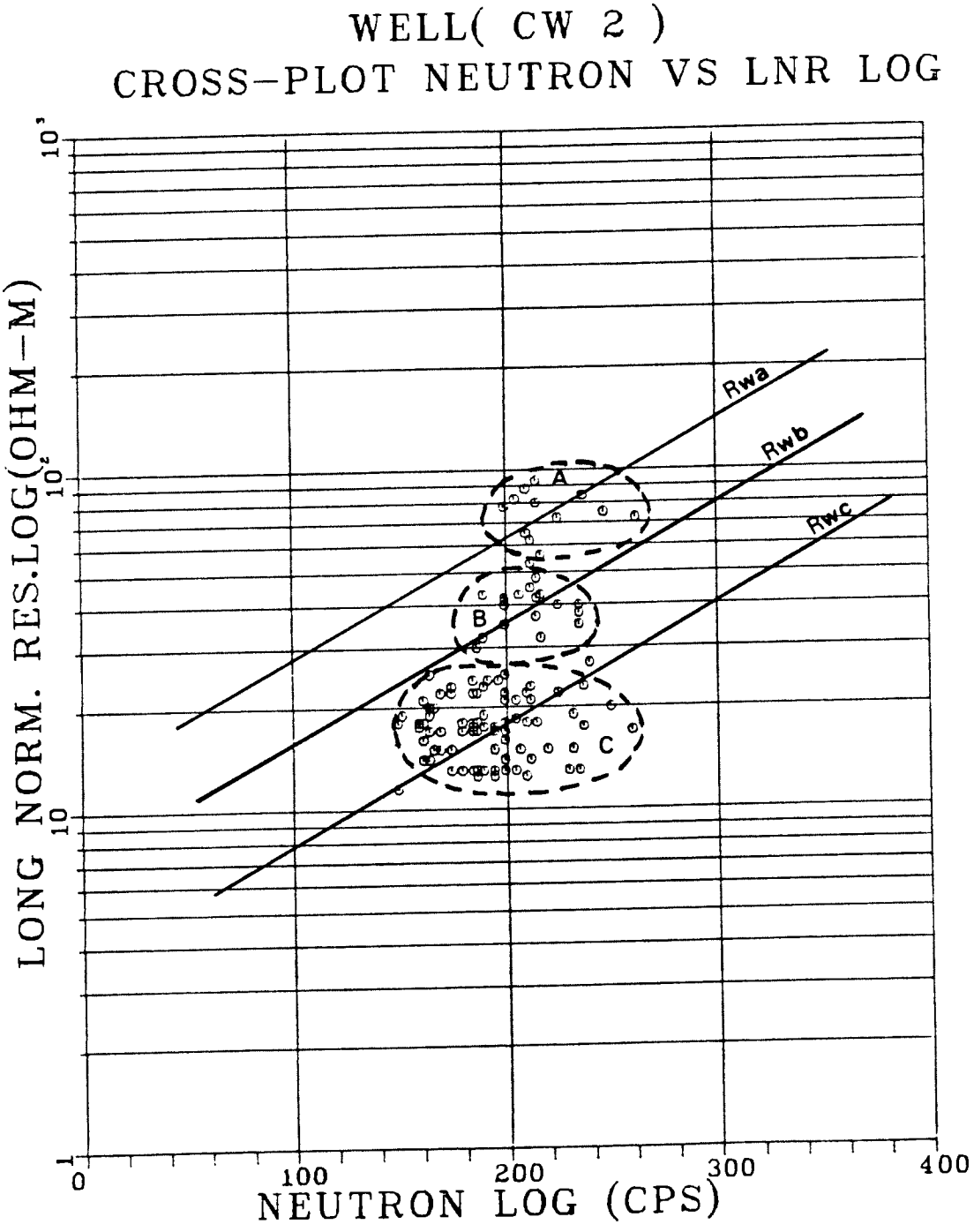

Figure 19. Core well CW2 cross-plotting.

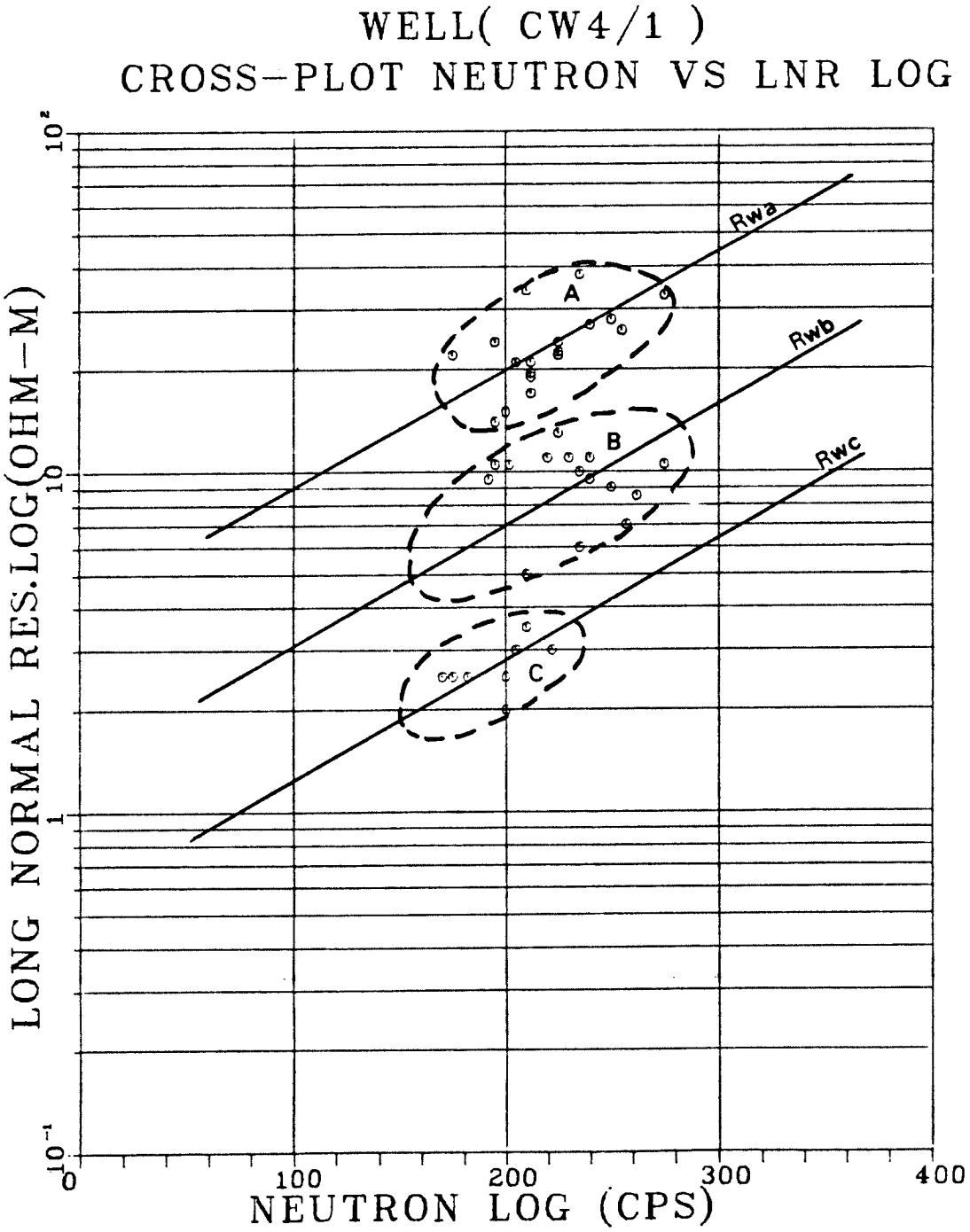

Figure 20. Core well CW4/1 cross-plotting.

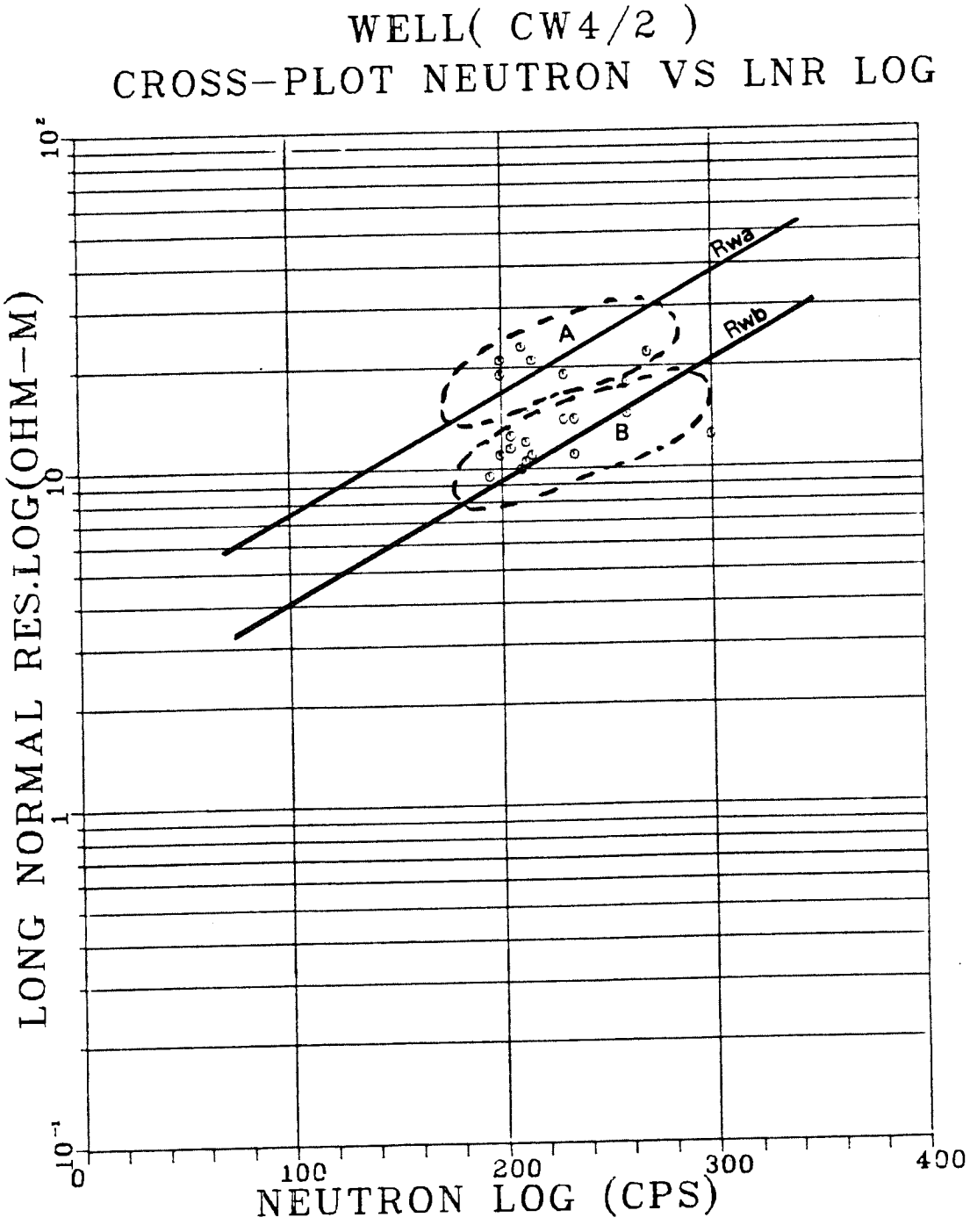

Figure 21. Core well CW4/2 cross-plotting.

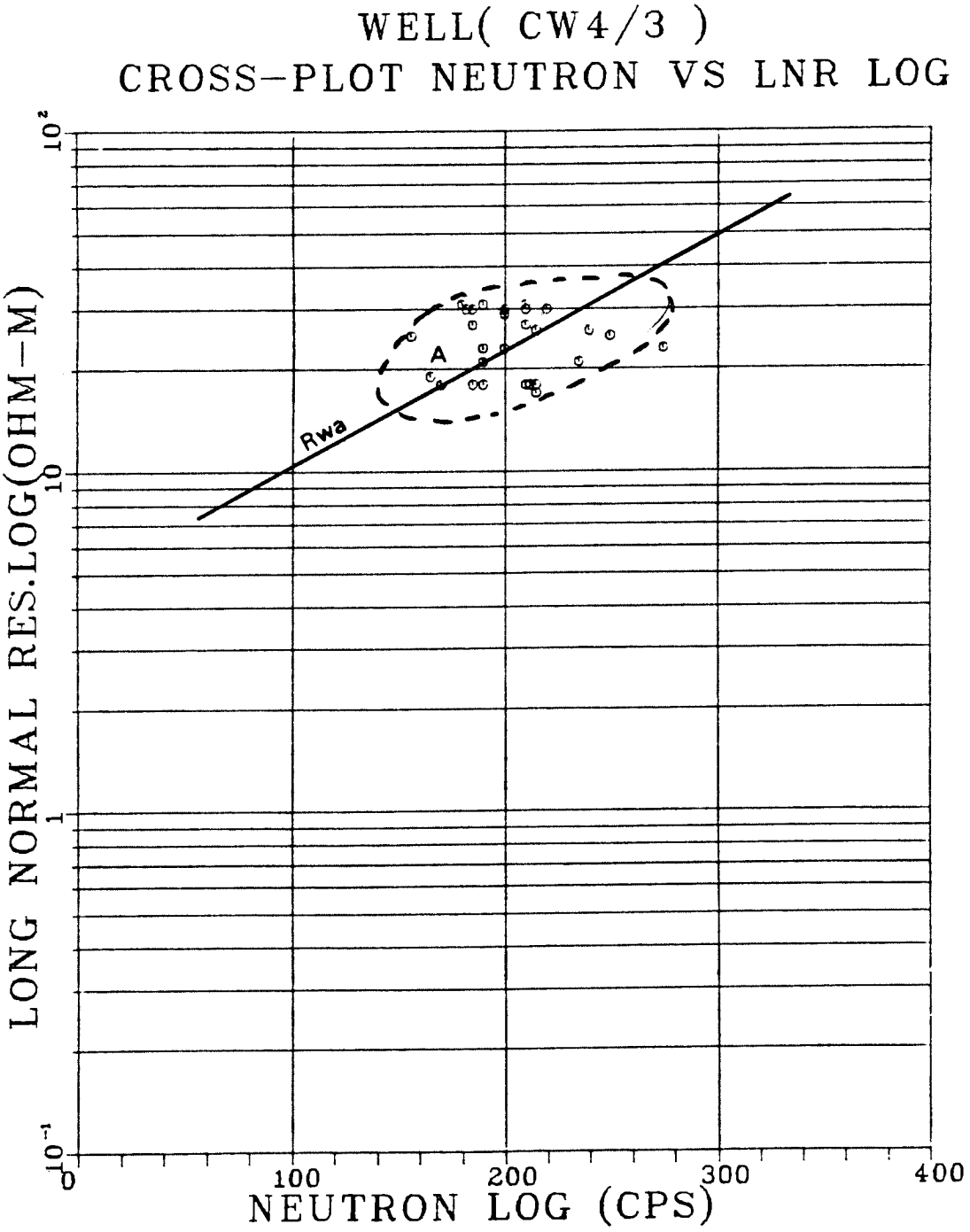

Figure 22. Core well CW4/4 cross-plotting.

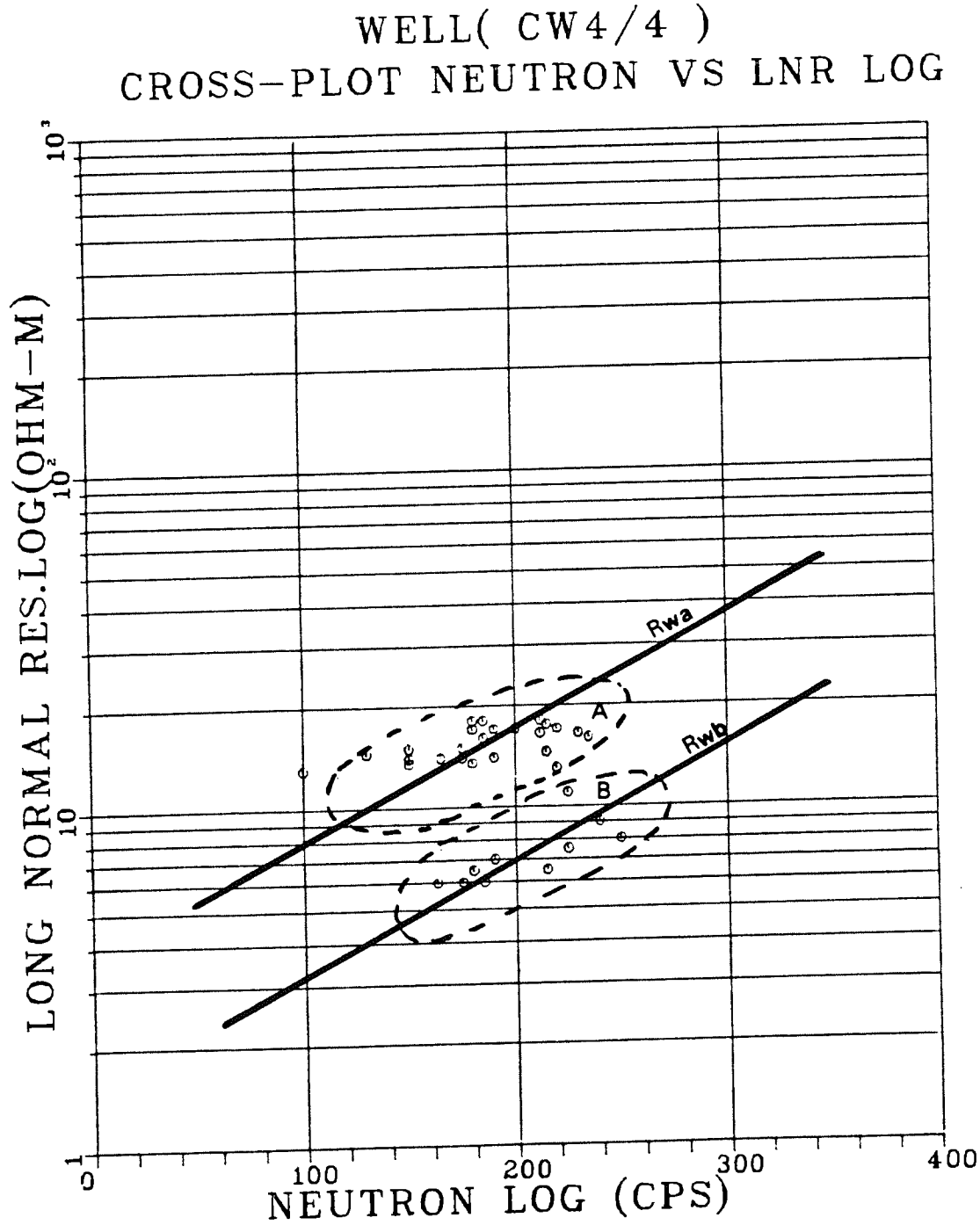

Figure 23. Core well CW4/4 cross-plotting.

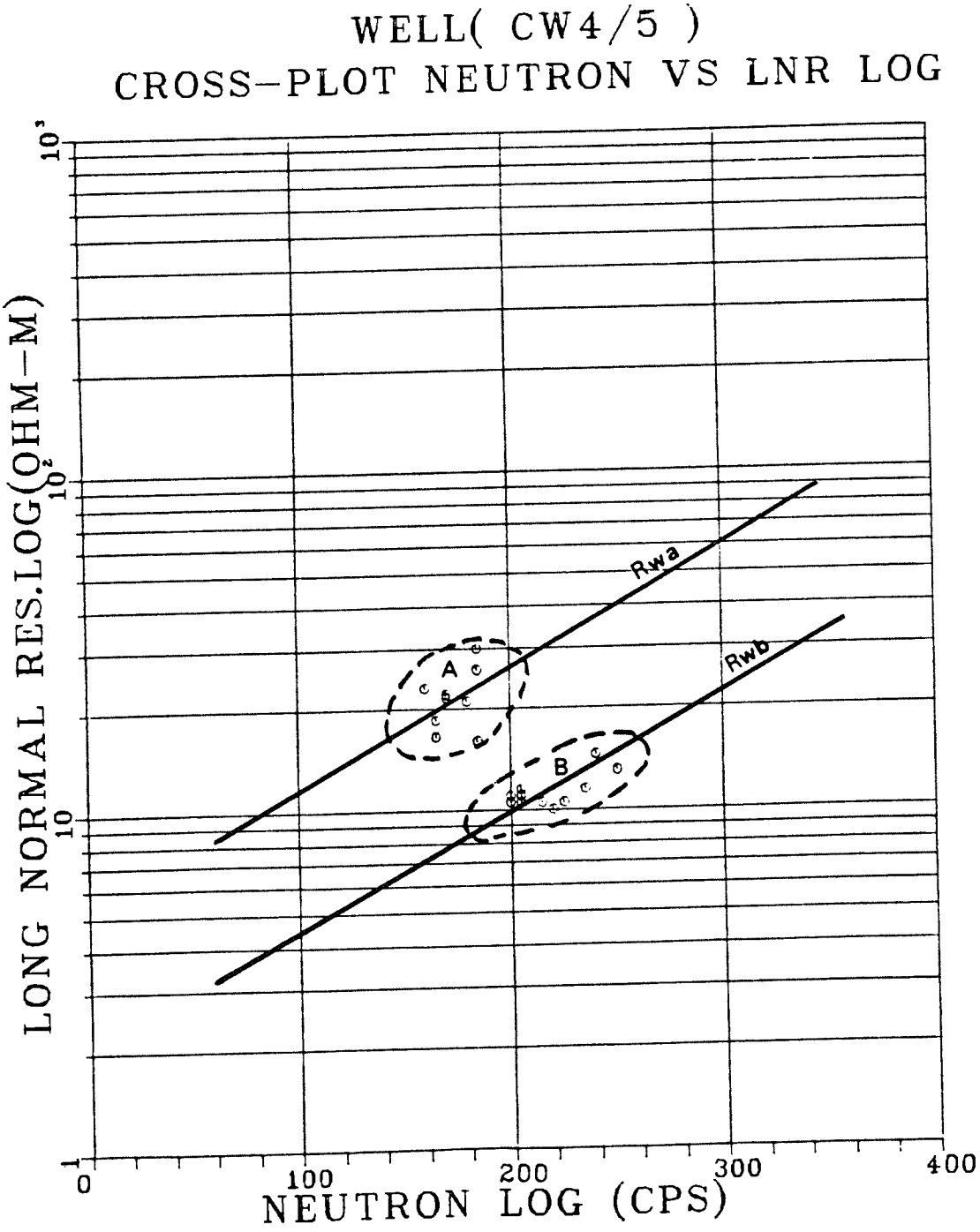

Figure 24. Core well CW4/5 cross-plotting.

The porosity of the limestone media varied between 20 percent and 35 percent, with higher frequency values between 25 percent and 30 percent, according to the Condrill AB Company report. The average porosity value of 25 percent has been chosen to determine the water resistivity using equation (9). The porosity values can be estimated within a 20-35 percent range from the neutron log response. The Schlumberger Company has established a nomography to invert neutron responses (CPS) to direct porosity values, but this has been designed for special types of neutron tools which are used by the company. All well logs, except the temperature and the caliper logs, have been digitized with a rate of one sample per meter in order to correlate all logs qualitatively and to provide all data needed for cross-plots (Appendix 2). All cross-plots have been made using a plotting-assisted computer program called GRAPH, which is available in the DEC-10 system library.

Using equation (9) and a porosity value of 25 percent corresponding approximately to 200 CPS on the neutron log, the water resistivity, R_w, has been for different zones, A, B, and C, defined by the gathering data points on the plots (Figures 18 through 24). The water resistivity values have been inverted to salinity values using the Schlumberger chart prepared for equivalent resistivity of NaCl aqueous

solutions as a function of salinity (PPM) and temperature (Figure 6) (Table 3).

Other cross-plots for long normal vs. short normal logs (Figures 25 through 27) have been made to compare both log responses, which appear to have approximately the same responses. This means that there is no invasion from the water in the well to the surrounding media, so either the long normal or the short normal log data can be used for water salinity determination.

Qualitatively speaking, the resistivity and SP logs generally show salinity increase with depth. The neutron log response has inverse relation with porosity, where low response corresponds to high porosity value due to the attenuation of neutron particles in porous, saturated media. The gamma ray log defines some shale streaks in the limestone formation, especially in the deep core wells CW1 and CW2. The two major karstic systems have been indicated by the caliper log in core well CW1, as well as some other minor karstification through the shallow core wells. The temperature logs have normal thermal gradients through the deep core wells, and seem to have a constant temperature through the shallow core wells.

Core Well No.	Total Depth TD (m)	BHT °F	ST °F	Zone			Corresponding TDS (PPM)		
				A	B	C	Zone		
				Rwa	Rwb	Rwc	A	B	C
CW1	200	87	78	1.14	0.47	-	5,000	10,500	-
CW2	150	82	-	9.21	5.2	2.67	550	1,000	2,000
CW4/1	50	70	68	2.97	1.04	0.42	2,000	6,000	15,500
CW4/2	25	72	68	2.45	1.34	-	2,500	5,000	-
CW4/3	25	73	68	3.42	-	-	1,700	-	-
CW4/4	25	70	77	2.38	1.04	-	2,500	6,000	-
CW4/5	25	75	68	3.86	1.49	-	1,550	4,000	-

Table 3. Results of water salinity from well log cross-plots at an average porosity of 25% ≅ 200 CPS on neutron log.

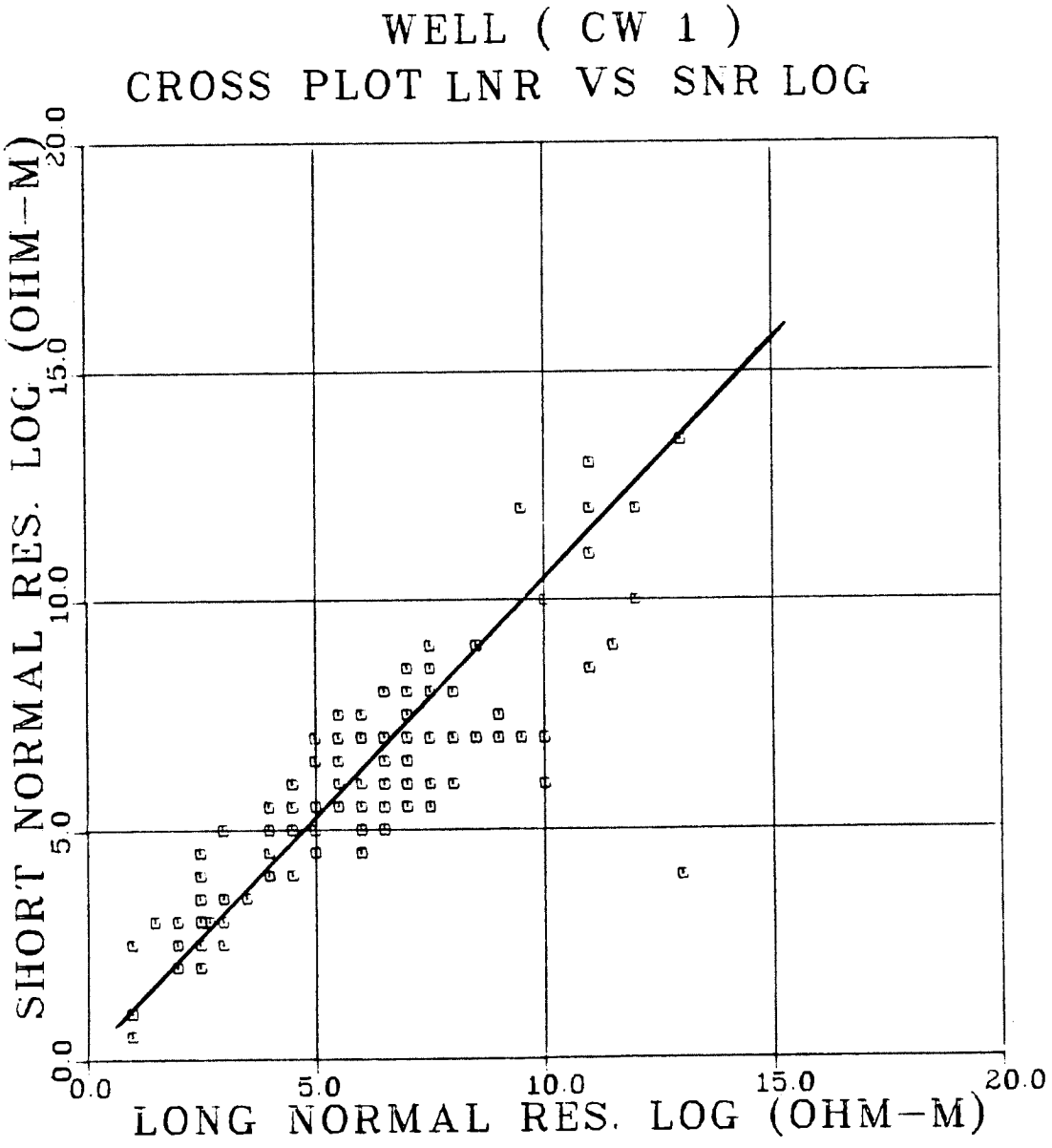

Figure 25. Core well CW1 resistivity cross-plotting.

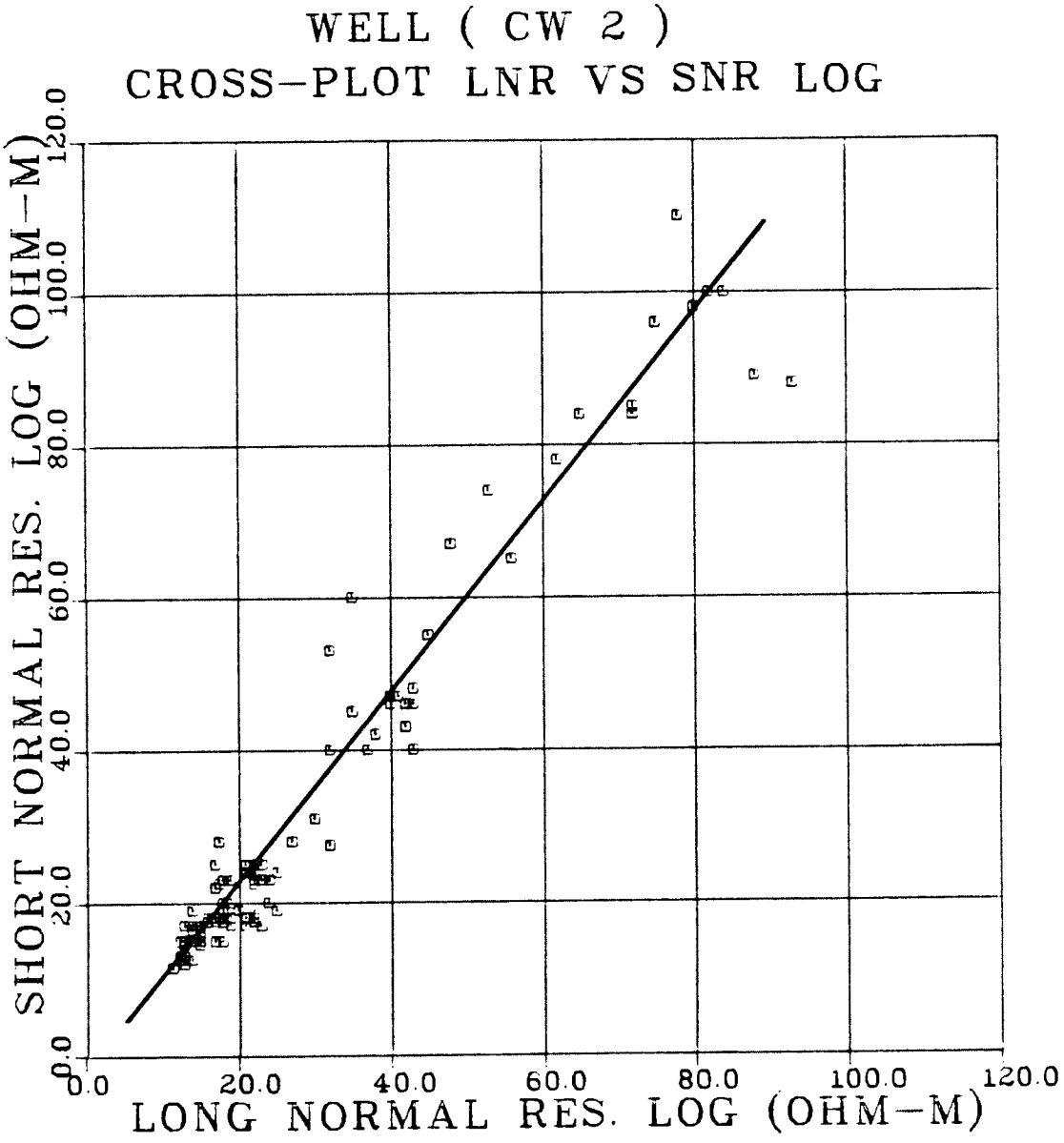

Figure 26. Core well CW2 resistivity cross-plotting.

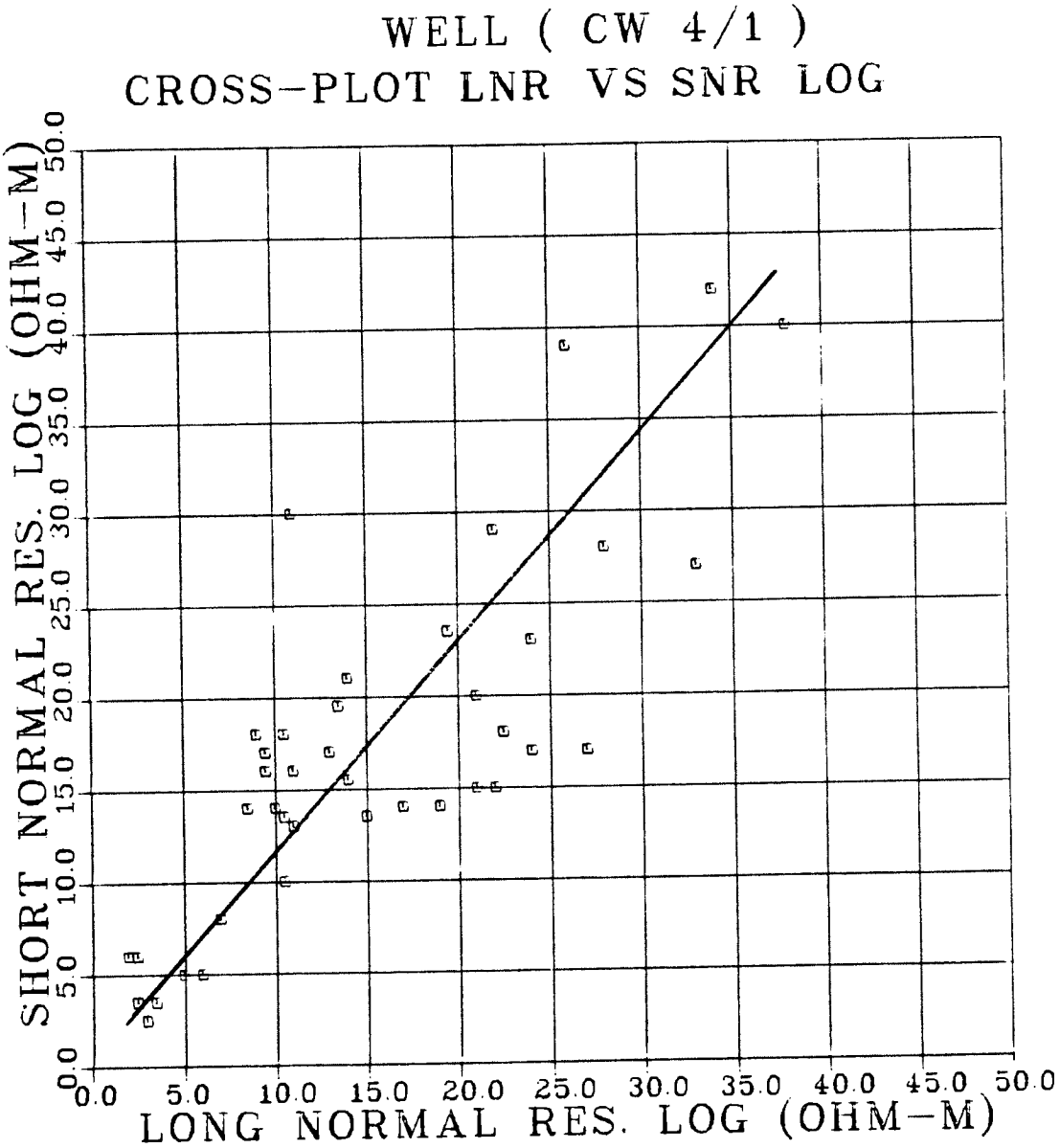

Figure 27. Core well CW4/1 resistivity cross-plotting.

Water Quality

The chemical analysis of the water samples shown in Table 4 provides generally high salinity, with some restrictions in the results of well CW2's sampling test. This test shows a significant amount of potassium dissolved, while all other samples taken have the least amount. Also, the chemical analysis results of the two water samples from well CW2 show unexpected reverse salinity values; this could be because the water samples were taken in the upper section of the well, without isolating the lower section, or it could be that the two water samples were switched by mistake. Comparing the resistivity logs of the well with the other wells, we may notice that it has relatively higher resistivity values than the others, which means well CW2 should have the least water salinity in the area. All these water samples were taken after the pressure permeability test, where water was injected through the formation during the test. This may have disturbed the aquifer and given altered samples. Also, the water samples were taken within extensive depth intervals ranging from 25 to 75 m, which obviously is the main reason for the high salinity results. However, the chemical analysis of the water samples indicates NaCl and $CaCO_3$ as the higher amounts of dissolved solids, which re-

Pump Set-up

Core Well No.	Sample Depth Interval	Cations +				Anions -			Hardness	PH Value	TDS PPM	Conductivity μ mhos/cm
		Ca	Mg	K	Na	Cl	SO_4	HCO_3	$CaCO_3$			
CW1	126-200 (Isolated)	540	1289	391	9945	18758	2064	207	6634	7.15	33194	-
CW2	at 40 m (No isolation)	220	379	2342	1725	5532	865	244	2144	7.45	13312	20800
	120-150 (Isolated)	180	364	2033	1541	4893	817	232	1942	7.45	11981	18720
CW4/1	All Water Column	120	182	41	1045	1844	528	275	1046	7.55	5232	8175
CW4/2	All Water Column	130	176	5	1253	2128	528	281	1046	7.0	5930	9265
CW4/3	All Water Column	180	146	82	1099	2003	480	269	1049	7.3	3259	8720
CW4/4	All Water Column	260	316	45	2494	4645	624	281	1946	7.1	8665	17472
CW4/5	All Water Column	240	268	92	2352	4326	576	281	-	7.7	8135	15808
CW4/6	All Water Column	140	85	21	632	1170	240	244	698	7.2	2532	4742

Table 4. Water quality chemical analysis.
(Source: SDWR Laboratory)

late to the sea-water intrusion and the ionization of $CaCO_3$ from the limestone aquifer, respectively.

The Karstic Formation

The karst development in the limestone formation has been defined through the core analysis and the pressure permeability tests (Appendix 3). The difference in depth of the core wells does not provide enough information about well interconnection and its relation to karst development on a large scale. The two major karstic systems were indicated from core well CW1 at depth intervals of 30-35 meters, and 110-116 meters below ground level. Unfortunately, only one major karstic system was indicated from core well CW2 at a depth interval of 46-56 meters below ground level. Other minor karstic features were recovered in the all shallow core wells at depth intervals ranging from 10 to 20 meters. The minor karstic features include fissures, fractures, and fossiliferous limestone. Therefore, the karstic formation can be classified by upper and deep karst. The upper karst occurs in the unconfined Middle-Miocene aquifer of mainly fresh to brackish groundwater. The deep karst occurs in the confined Oligo-Eocene aquifer which is characterized by original saline water. This saline water zone can be defined as a 1.0 ohm-m resistivity zone from the long normal resistivity

log in CW1 at intervals ranging from 112 to 116 meters, which is exactly the deep major karst zone.

Other vertically developed karsts were defined at Boukarma and Jumard dolines (Figure 2); these are characterized by high-salinity, brackish water, which means that these vertical karsts have connection with the deep karst defined in well CW1. On the other hand, the vicinity of well CW1 is influenced locally by this high-salinity water from the two vertical karsts. Therefore, this zone is suffering from local, high-salinity water circulation.

The Hydrostatic Water Level

All the drilled wells shown in Table 5 are being used as observation points to measure and evaluate the change of the hydrostatic heads due to piezometry in karsts, fissures, and fractures. There are reference points or datum at all well heads which are used to take the measurements. All these reference points have been marked by SDWR survey section, but according to the Condrill AB Company report, the leveling of these reference points was not made accurately because of the use of unfixed benchmarks. However, the measurements shown in Table 5 indicate a general change in the water level pattern during the January to April period, with an average increase of 25 cm during this rainfall season.

Observation Point	Type of Point	Elevation of RM or Datum (m) a.m.s.l.	Measurements 1/23/79 Depth to Water Level (m)	Measurements 1/23/79 Elev. of Water Level (m)	Measurements 4/1/79 Depth to Water Level (m)	Measurements 4/1/79 Elev. of Water Level (m)
Jabbah cave	Upper karst	3.30	1.650	1.650	-	-
Boukarma cave	Deep karst	3.45	2.055	1.395	-	-
Ayn Zayanah	Upper karst	1.92	1.435	0.485	1.035	0.885
Blue Lagoon	Lagoon	0.81	0.535	0.275	-	-
AW1	Upper karst	23.28	-	-	-	-
AW2	Upper karst	23.28	21.900	1.380	21.590	1.69
AW3	Deep karst	24.63	23.245	1.385	23.00	1.63
AW4	Upper karst	25.47	24.080	1.390	23.81	1.66
AW5	Upper karst	26.19	24.740	1.450	24.46	1.73
AW6	Upper karst	28.04	-	-	-	-
AW7	Upper karst	27.92	26.470	1.450	26.24	1.68
CW1	Upper karst	27.705	26.490	1.215	-	-
CW2	Upper karst	23.940	22.565	1.375	-	-
CW3	Limestone media	14.795	(13.45)	1.345	-	-
CW4/1	Limestone media	6.730	5.490	1.240	5.16	1.57
CW4/2	Limestone media	5.670	4.670	1.000	4.40	1.27
CW4/3	Limestone media	4.855	3.655	1.200	3.38	1.50
CW4/4	Limestone media	1.860	0.955	0.905	(1.065)	(0.795)
CW4/5	Limestone media	6.520	5.285	1.235	5.000	1.52
CW4/6	Limestone media	12.885	11.480	1.405	-	-
SW1	Limestone media	(4.372)	3.540	0.832	3.14	1.23
SW2	Limestone media	3.650	2.645	1.005	2.42	1.23
SW3A	Limestone media	2.090	1.390	0.700	1.255	0.835
SW3B	Limestone media	3.000	2.030	0.970	1.965	1.035
SW4	Upper karst	5.670	4.425	1.245	4.11	1.56
SW5	Limestone media	12.165	10.750	1.415	-	-
SW6	Limestone media	12.505	11.125	1.380	-	-
SW7	Upper karst	10.065				

Table 5. Groundwater level measurements.

The water level at well CW4/4 indicates an uncertain decrease in the vicinity of the Blue Lagoon; unfortunately, there is no measurement at the Blue Lagoon with which to compare. Also, the water level at the Ayn Zayanah spring and the Blue Lagoon is remarkably lower than the surrounding area. The Ayn Zayanah spring and the Blue Lagoon represent the discharge zone of groundwater circulation in the upper karst pattern.

Other measurements have been taken (Table 6) to find the relation between water level changes in the Ayn Zayanah, the Blue Lagoon, and the Mediterranean Sea and the discharge rates at the Ayn Zayanah and the Blue Lagoon. Also, conductivity measurements were taken at the same time at the surface and at the bottom of the Ayn Zayanah and the Blue Lagoon. From all these measurements, it has been noticed that the Blue Lagoon discharge rate obeys oppositely to the sea-water level changes, where a minimum discharge rate was measured during the positive increase on the mean sea level. Also, the water salinity at the Blue Lagoon is directly proportional to the discharge rate.

On the other hand, the Ayn Zayanah water level and discharge rate are not obviously influenced by the tidal effect, but variations similiar to the Blue Lagoon discharge rates have been recorded with approximately two hours' leading time.

Reference	Water Levels (m)			Discharge Rates (m^3/sec)		
Time	H_{sea}	H_{BL}	H_{Az}	Q_{BL}	Storage Flow Rate	Q_{Az}
10.05	-0.14	0.285	0.470	5.27	-0.28	4.99
11.30	-0.10	0.280	0.465	4.94	-0.40	4.54
12.40	-0.06	0.275	0.470	4.52	+0.32	4.84
15.45	+0.02	0.285	0.485	4.66	+4.66	5.15
17.40	-0.01	0.295	0.490	4.75	+1.23	5.98
19.35	-0.08	0.300	0.500	5.80	+0.11	5.91

Reference time = mid time of the gauging period, hrs. and min.

H_{sea} = sea level in meters from m.s.l.

H_{BL} = water level at Blue Lagoon m.s.l.

H_{Az} = water level at Ayn Zayanah m.s.l.

Q_{BL} = discharge rate at Blue Lagoon outlet in m^3/sec.

Q_{Az} = discharge rate at Ayn Zayanah in m^3/sec.

Conductivity Measurements (in micromhos/cm):

Reference Time	Ayn Zayanah		Blue Lagoon
	Surface	Bottom	
10.05	27,000	28,000	31,000
11.30	25,500	28,000	29,800
12.40	25,500	28,000	30,000
15.45	25,500	27,500	29,000
17.40	26,500	27,800	31,500
19.35	26,800	28,000	31,500

Table 6. Tidal effect on hydrological measurements in Ayn Zayanah and the Blue Lagoon discharge area.

Therefore, the maximum discharge rate at Ayn Zayanah was recorded two hours after the maximum positive increase of the sea level.

Comparing the tidal effect with the difference of the discharge rates between Ayn Zayanah and the Blue Lagoon, we may conclude that the discharge rate and water salinity reach their maximum amount during the period of low tide, and the discharge rate and water salinity reach their minimum amount during the period of high tide.

SUMMARY AND DISCUSSION OF THE RESULTS

The interpretation of the resistivity soundings data was supported by the resistivity logs, particularly well CW4/1's resistivity log, where this well was drilled to an adequate depth to achieve a suitable layered earth's model. Three- and four-layered earth's models were chosen to interpret the resistivity soundings data for the best fit (Table 2). The resistivity of the surface layer varies from 0.3 to 1390 ohm-m, which depends on the change of the surface features (sebkha, sand, dry limestone, and lagoon). The intermediate layers (the second in the three-layer model, and the second and third in the four-layer model case) represent the moistured formation, with fresh to brackish groundwater with resistivity ranging from 58-6 ohm-m. The last layer represents the most consistent resistivity zone in the area with 2.5 ohm-m, which obviously contains saline water derived from the sea.

The isoresistivity contour map (Figure 14) delineates the saline water fronts in the Blue Lagoon and Sebkha vicinities, where the sea-water intrusion is expected. Also, the geoelectric cross-sections trace the slope of the salt-fresh water interface, however the interface is actually a transition zone which can be seen through the resistivity logs.

The resistivity profiling was affected by the lateral change in resistivity of the surface layer, therefore no significant resistivity change due to occurrence of karst or subsurface channels could be detected. The resistivity contrast and dimensions of the karst are important factors in detecting significant anomalies. However, comparing the resistivity profiling (2) (Figure 16) with the resistivity profiling (3) (Figure 17), a lateral increase in the resistivity towards the resistivity profiling (3) is noticed due to the slope of the salt-fresh water transition zone.

The quantitative interpretation of well log data using the cross-plot technique of the neutron log vs. the long normal resistivity log has provided all possible water quality analysis in terms of total dissolved solids (TDS) in parts per million (PPM). This analysis emphasizes the salinity problems in fresh, brackish, and saline zones (Table 3). Generally, the salinity increases towards the coast and the vicinity of the Blue Lagoon, where the contamination with the sea water takes place. Also, the SP log qualitatively indicates salinity increase with depth. The estimation of water salinity from the cross-plot and equation (9) was based on an average porosity value of 25 percent, corresponding to about 200 CPS on the neutron log. This average porosity value was obtained from the core analysis. The estimation of the

water salinity could be more accurate if the neutron log could have been calibrated to obtain porosity values or if another direct porosity tool was used.

The chemical analysis of the water samples obtained generally high salinity values compared with the water salinity results from the cross-plot technique. This should be expected because of disturbing the aquifer by pumping out the water, where the fresh water is just a lense floating on the brackish/saline water. The quantitative interpretation of water quality gave a good approximated result and differentiated the water salinity in different regions, where wells CW2 and CW4/6 are located in less salinity, while wells CW4/1 and CW4/4 are located in a high-salinity region. The well CW1 region can be considered a special case for its high water salinity because of the occurrence of the vertically developed karst in the Boukarma and Jumard dolines, which are interconnected with the deep saline water.

Karsts, fissures, and fractures usually occur in limestones through which the groundwater movement takes place. The study of these features has been achieved by the core analysis and the pressure permeability tests (Appendix 3). The occurrence of the major karstic galleries have been confirmed in the Coeffiah area only, where high permeability

zones due to fissures or fractures associated with fossiliferous limestone media were defined in the Ayn Zayanah area.

The groundwater level measurements (Table 5) indicate an average water level of 1.24 meters above mean sea level in the Coeffiah and Ayn Zayanah areas, which are denoted as upper karst and limestone media, respectively. The water level of the Ayn Zayanah spring and the Blue Lagoon is remarkably lower than the surrounding limestone media. This could be the reason for the intrusion problem, because the hydraulic gradient would be smaller in the Blue Lagoon zone.

The relation between the Ayn Zayanah and the Blue Lagoon discharge rate and the sea tidal effect has concluded that the discharge rate and the water salinity reach their minimum amount during the period of high tide and their maximum amount during the period of low tide. Actually, the hydraulic gradient controls the discharge rate as a function of the difference between the sea and the discharge area water level. Therefore, the hydraulic gradient towards the sea decreases as the water level difference decreases, or the sea level increases. The opposite is true during low tide -- the hydraulic gradient increases, so that the discharge rate increases. In this case, the water salinity would naturally increase as the discharge rate increases, and disturbance occurs in the saline water which underlies the thin, fresh-water layer.

Under all of these hydrological circumstances, the area poses a great salinity problem due to the sea-water intrusion. The low water level in the discharge area causes a sea-water wedge underneath the Ayn Zayanah area. Therefore, the proposed dam project, to raise the water level in the Blue Lagoon to about 3.5 meters above the mean sea level in order to increase the hydraulic gradient towards the sea, is necessary to prevent the sea-water wedge from further inlandward transgression.

CONCLUSIONS

The application of the resistivity method to study and delineate saline water bodies intruding into fresh water of a coastal limestone aquifer has met with great success. Also, the interpretation of the resistivity sounding data, with the support of the resistivity logs, has come up with consistent results. However, the subsurface resistivity log response contains only the longitudinal resistivity parameter in horizontally layered medium, while the surface resistivity measurements are affected by the longitudinal and the transverse resistivity, also (Flathe, 1976). On the other hand, the lithology of the area is mainly limestones, and there is no place for other continental sedimentary rocks. Therefore, the change of water salinity with depth is the main factor in resistivity measurements which can be directly obtained from the resistivity log response. The surface layer represents a heterogeneous medium (sand, swamp, lake, and limestone), which has been interpreted as arbitrary from the resistivity sounding data.

The delineated saline water bodies in Figure 14 represent the sea-water wedge underlying the Blue Lagoon and the Sebkha area. This sea-water wedge appears to be relatively close to the surface, according to the Ghyben-Herzberg formula,

because the water level at the Blue Lagoon is approximately 30 cm. Therefore, this zone is considered to be the main gateway to the sea-water intrusion problem to the whole area. Nevertheless, similar sea-water intrusion problems are facing most of the worldwide coastal regions.

Karsts, fissures, and fractures serve as routes and passageways through which the groundwater movements take place. The major karstic system has been defined only in the Coeffiah area by the core analysis of wells CW1 and CW2 and pressure permeability tests. Unfortunately, there are no resistivity measurements in this region by which to trace these major karsts. All the resistivity profilings have been performed in the Ayn Zayanah and the Blue Lagoon area, where only fissures and fractures associated with fossiliferous limestones were defined. However, the resistivity profilings indicate lateral change in the resistivity between RP-2 and RP-3 as a result of the sloping salt-fresh water interface. The resistivity profiling can be successfully performed if the resistivity contrast between two extensive zones is high, but thin, dimensional structures may not be defined, even if high resistivity contrast exists (Keller, 1966).

The fresh-water zone in the area is only the uppermost few meters; this information has been obtained from the re-

sistivity logs and the cross-plot technique. The gradual salinity increase with depth was noticed in all the resistivity logs forming the salt-fresh water transition zone.

The uncertain water salinity at the CW1 well region due to the occurrence of the vertically developed karst in the Boukarma and Jumard dolines introduces another problem, because these vertical karsts are possibly interconnected with the deep saline confined aquifer. This problem may become worse if the vertical karst is interconnected with the upper karst system.

The groundwater circulation is towards the drainage area, which includes the Ayn Zayanah spring and the Blue Lagoon. The water level at the drainage area is remarkably lower than the average water level in the surrounding limestone area. Therefore, the hydraulic gradient is smaller in the drainage area, where the sea-water wedge occurs. The water salinity of the drainage area is about 15,000 and 18,000 PPM at the Ayn Zayanah spring and the Blue Lagoon, respectively. This indicates the effect of the sea-water wedge on the water salinity.

The result of the tidal effect on the drainage area has defined an inverse proportionality at the Blue Lagoon, but not a direct relation with the Ayn Zayanah, so more periodic measurements are recommended to determine this

relationship, particularly with the Ayn Zayanah spring. The relation between the tidal effect and the Blue Lagoon discharge rate is a direct result of the hydraulic gradient changes.

The proposed dam project on the Blue Lagoon will raise the water level in the Blue Lagoon to about 3.5 meters and the Ayn Zayanah water level to 4.0 meters. This will provide a significant increase in the hydraulic gradient towards the sea to prevent the sea-water wedge from further inlandward transgression; also, the water salinity would be improved.

The dam project will prevent the groundwater from being drained into the sea, but may cause water flooding in some doline areas which would be lower than the water level expected at the dam.

NOMENCLATURE

AB	Current electrodes spacing (m)
AW	Additional well (e.g., AW2, AW5)
Cps	Counts per second
CW	Core well
ES	Electrical sounding (e.g., ES-1, ES-2)
GR	Gamma ray log (Cps)
H	Water level at m.s.l. (e.g., H_{AZ} = water level at Ayn Zayanah)
h_s	Depth of sea water or salt water below mean sea level
h_w	Elevation of groundwater above mean sea level
I	Current (Am)
K	Geometric factor (e.g., K_s, K_w)
m	Cementation factor
MN	Potential electrodes spacing (m)
m.s.l.	Mean sea level
n	Tortuosity factor
ND	Neutron log deflections (Cps)
Q	Discharge rate (m^3/sec)
RLN	Long normal resistivity log (ohm-m)
RP	Resistivity profiling (e.g., RP-1, RP-2)
RSN	Short normal resistivity log (ohm-m)
R_t	Formation bulk (true) resistivity (ohm-m)

R_w	Water resistivity in pore spaces
SDWR	Secretariat of Dams and Water Resources
SP	Spontaneous potential (mv)
SW	Supply well (e.g., SW1, SW3)
TDS	Total dissolved solids in parts per million (PPM)
T_f	Density of fresh water
T_s	Density of sea water

Greek Symbols

ϕ	Formation porosity (fraction of void spaces), %
ρ_a	Apparent resistivity (ohm-m)
ΔU	Potential difference (volts)

REFERENCES CITED

Archie, G.E., 1942, The electrical resistivity log as an aid in determining some reservoir characteristics: Trans. AIME, Petrol. Br., v. 146, pp. 54-62.

_____, 1947, Electrical resistivity - an aid in core analysis interpretation: Bull. Am. Assoc. Petrol. Geologists, v. 31, no. 2.

_____, 1957, Classification of carbonate reservoir rocks and petrophysical considerations: Bull. Am. Assoc. Petrol. Geologists, v. 36, no. 2

Aley, T.J., Williams, J.H., and Massello, J.W., 1972, Groundwater contamination and sinkhole collapse: Engineering Geology Series No. 5, 32 pp.

Ayers, M.L., Dobyns, R.P., and Bussell, R.Q., 1952, Resistivities of water from subsurface formations: Petrol. Eng., v. 24, no. 13, pp. 1336-1348.

Banks, H.O., and Richter, R.C., 1953, Sea-water intrusion into groundwater basins bordering the California coast and inland bays: Trans. Amer. Geoph. Union, v. 34, no. 4, pp. 575-582.

Bezuidenhout, C.A., and Enslin, J.F., 1970, Surface subsidence and sinkholes in the Far West Rand, Transvaal, Republic of South Africa: Land Subsidence, v. 2, pp. 482-495.

Bhattacharya, P.K., and Patra, H.P., 1968, Direct current geoelectric sounding - principles and interpretation: New York, Elsevier Publishing Co., 135 pp.

Breusse, J.J., 1963, Modern geophysical methods for subsurface water exploration: Geophysics, v. 28, no. 4, pp. 633-657.

Chombart, L.G., 1980, Well log interpretation in carbonate reservoirs: Geophysics, v. 25, pp. 779-853.

Condrill AB Company, 1981, Resistivity survey of Blue Lagoon, field data report: Benghazi, Libya, Secretariat of Dams and Water Resources.

Davis, W.M., 1930, Origin of limestone caverns: Geol. Soc. Amer. Bull., v. 41, pp. 475-628.

Davis, S.N., and DeWiest, R.J.M., 1966, Hydrogeology: New York, John Wiley & Sons, 463 pp.

Dixey, F., and Shaw, S.H., 1961, Hydrology with reference to salinity: salinity problems in the arid zone: Proceedings of the Teheron Symposium, UNESCO, pp. 15-18.

Dunlap, H.F., and Hawthorne, R.R., 1951, The calculation of water resistivity from chemical analysis: Trans. AIME, v. 192, pp. 373-375.

Erwin, J.W., 1953, Resistivity methods applied to groundwater prospecting on the Big Sandy Creek in parts of Lincoln and Elbert Counties, Colorado: Golden, CO, Colorado School of Mines, Thesis T-786.

Flack, J.E., and Howe, C.W., 1973, Salinity in water resources, Proceedings of the 15th Annual Western Resources Conference at University of Colorado, July 1973: Boulder, CO, Merriman Publishing Co.

Flathe, H., 1955, Possibilities and limitations in applying geoelectrical methods to hydrogeological problems in coastal areas of north-west Germany: Geophysical Prospecting, v. 3, pp. 95-110.

_____, 1963, Five-layer master curves for the hydrogeological interpretation of geoelectrical resistivity measurements above a two-story aquifer: Geophysical Prospecting, v. 6, pp. 472-508.

_____, 1967, Interpretation of geoelectrical resistivity measurements for solving hydrogeological problems: mining and groundwater geophysics: Geol. Survey of Canada, Econ. Geol. Report 26, pp. 580-597.

_____, 1976, The role of a geologic concept in geophysical research work for solving hydrogeological problems: Geoexploration, v. 14, pp. 195-206.

Floegel, H., 1979, Sea-water intrusion study in Gefara plain: Tripoli, Libya, Secretariat of Agricultural Reclamation and Land Development, September 1979, 55 pp.

Foose, R.M., 1967, Sinkhole formation by groundwater withdrawal, Far West Rand, South Africa: Science, v. 157, pp. 1045-1048.

_____, 1981, Sinking can be fast or slow: Geotimes, v. 26, no. 8, pp. 21-24.

Frear, G., and Johnston, J., 1929, The solubility of calcium carbonate (calcite) in certain aqueous solutions at 25°C: Journal Am. Chem. Soc., v. 51, pp. 2082-93.

Gass, T., 1981, Sinkholes: Water Well Journal, v. 35, no. 9, pp. 36-37.

Gray, C., ed., 1971, Symposium on the geology of Libya; Paper presented at the Symposijm held at Tripoli, April 14-18, 1969: Faculty of Science, University of Tripoli, Libya.

Guerre, A., and Jewell, F., 1978, Ayn Zayanah project - geophysical survey, report of CGG Co.: Benghazi, Libya, Secretariat of Dams and Water Resources, Nov. 1978.

Guerre, A., 1981, Ayn Zayanah project - results of the core wells campaign, annex 2: Benghazi, Libya, Secretariat of Dams and Water Resources, May 1979.

Guyod, H., 1944, Fundamental data for the interpretation of electric logs: Oil Weekly, v. 115, Oct. 30, 1944.

Heiland, C.A., 1937, Prospecting for water with geophysical methods: Trans. Amer. Geophys. Union, pp. 574-588.

Henriet, J.P., 1976, Direct applications of Dar Zarrouk parameters in groundwater surveys: Geophysical Prospecting, v. 24, pp. 344-353.

Hill, H.J., and Milburn, J.D., 1955, Effect of clay and water salinity on electrochemical behavior of rocks: Trans. Am. Inst. Mining Met. Engrs., 207, Tech. Publ. 4223.

Jakosky, J., 1950, Exploration geophysics: Los Angeles, Trija Publishing Co., 1195 pp.

Jennings, J.N., 1971, Karst: Cambridge, MA and London, England, The M.I.T. Press, 252 pp.

Jones, P.H., and Buford, T.B., 1950, Electrical logging applied to groundwater exploration: Geophysics,

Keller, G.V., and Frischknecht, F.C., 1966, Electrical methods in geophysical prospecting: New York, Pergamon Press, 517 pp.

Keller, G.V., 1967, Applications of resistivity methods in mineral and groundwater exploration programs: Mining and Groundwater Geophysics, Geol. Survey of Canada, Econ. Geol. Report 26, pp. 51-66.

_____, 1968, Electrical prospecting for oil: Quarterly of the Colorado School of Mines, v. 63, no. 2, 268 pp.

_____, 1977, Electrical resistivity methods: subsurface geology: Golden, CO, Colorado School of Mines, pp. 459-465.

Kiersch, G.A., and Hughes, P.W., 1952, Structural localization of groundwater in limestones - Big Bend District - Texas-Mexico: Econ. Geol., v. 47, pp. 794-806.

Koefoed, O., 1976, An approximate method of resistivity sounding interpretation: Geophys. Prosp., v. 24, pp. 617-632.

_____, 1979, Geosounding principles, 1 - resistivity sounding measurements: New York, Elsevier Scientific Publishing Co., 276 pp.

Krulc, Z., and Mladenovic, M.L., 1969, The application of geoelectrical methods to groundwater exploration of unconsolidated formations in semi-arid areas: Geoexploration, v. 7, pp. 83-85.

LaMoreaux, P.E., and Powell, W.J., 1960, Stratigraphic and structural guides to the development of water wells and well fields in a limestone terrain: International Assoc. Sci. Hydrology Pub. No. 52, pp. 363-375.

Lennox, D.H., and Carlson, V., 1967, Integration of geophysical methods for groundwater exploration in the Praire provinces, Canada: Mining and Groundwater Geophysics, Geol. Survey of Canada, Econ. Geol. Report 26, pp. 517-535.

Maillet, R., 1947, The fundamental equations of electrical prospecting: Geophysics, v. 12, pp. 529-556.

McDonald, H.R., and Wantland, D., 1961, Geophysical procedures in groundwater study: Amer. Soc. of Civil Eng. Trans., no. 3137, pp. 123-135.

Meidav, T., 1960, An electrical resistivity survey for groundwater: Geophysics, v. 25, no. 5, pp. 1077-1093.

Mooney, H.M., and Wetzel, W.W., 1956, The potentials about a point electrode and apparent resistivity curves of a two-, three-, and four-layered earth: Minneapolis, The University of Minnesota Press.

Murray, R.C., 1960, Origin of porosity in carbonate rocks: Jour. Sed. Petrology, v. 30, pp. 59-84.

Noguchi, T., Tokumitsu, Y., and Takahashi, R., 1970, Small sinking holes in limestone area, with special reference to drainage of coal mines: Land Subsidence, v. 2, pp. 467-474.

Ogilvy, A.A., 1967, Geophysical prospecting for groundwater in the Soviet Union: Mining and Groundwater Geophysics, Geol. Survey of Canada, Econ. Geol. Report 26, pp. 536-543.

Parkhomenko, E.I., translated from Russian and edited by Keller, G.V., 1967, Electrical properties of rocks: New York, Plenum Press, 314 pp.

Paver, G.L., 1950, The geophysical interpretation of underground water supplies; a geological analysis of observed resistivity data: Journal Inst. Water Engrs., v. 4, pp. 237-266.

Pettijohn, F.J., 1975, Sedimentary rocks, 3rd ed.: New York, Harper & Row Publishers, 628 pp.

Pickett, G.R., 1973, Pattern recognition as a means of formation evaluation: Trans. SPWLA, paper A.

Pickett, G.R., and Rowle, G., 1976, Rock properties - volume I & II: Tulsa, Amoco Production Company.

Pirson, S.J., 1957, Formation evaluation by log interpretation: World Oil, April, May, June.

_____, 1963, Handbook of well log analysis: Englewood Cliffs, NJ, Prentice-Hall, Inc., pp. 275-292.

Polak, E.J., 1953, The application of resistivity methods in establishing the base of the water-bearing rocks in the Cannock Chase Coalfield: Geophys. Prosp., v. 1, pp. 197-204.

Ritter, D.F., 1978, Process geomorphology: Wm. C. Brown Company, 603 pp.

Roy, A., and Apparao, A., 1971, Depth of investigation in direct-current methods: Geophysics, v. 36, no. 5, pp. 943-959.

Satpathy, B.N., and Kanungo, D.N., 1975, Groundwater exploration in hard rock terrain - a case history: Geophys. Prosp., v. 24, pp. 725-736.

Sayre, A.N., and Stephenson, E.L., 1937, The use of resistivity methods in the location of salt-water bodies in the El Paso, Texas area: Trans. Amer. Geophys. Union, v. 18, pt. 2, pp. 393-398.

Schlumberger, C., and Leonardon, E.G., 1934, A new contribution to subsurface studies by means of electrical measurements in drill holes: Trans. AIME, v. 110, pp. 273-289.

Schlumberger, LTD., 1972, Log interpretation, volume I - principles: New York, NY, Schlumberger Limited.

_____, 1974, Log interpretation, volume II - applications: New York, NY, Schlumberger Limited.

Serres, Y.F., 1969, Resistivity prospecting in a United Nations groundwater project of Western Argentina: Geophys. Prosp., v. 17, pp. 450-467.

Shaw, S.H., 1935, A study of the resistivity method in connection with the investigation of underground water supplies in the Nata Reserve, Southern Rhodesia: Trans. Inst. Min. and Met., v. 44, pp. 3-47.

Shiftan, Z.L., 1967, Integration of geophysics and hydrogeology in the solution of regional groundwater problems: Mining and Groundwater Geophysics, Geol. Survey of Canada, Econ. Geol. Report 26, pp. 507-516.

Sutton, G.H., Berckhemer, H., and Nafe, J.E., 1957, Physical analysis of deep sea sediments: Geophysics, v. 22, p. 779.

Sweeting, M.M., 1973, Karst landforms: Columbia University Press, 362 pp.

_____, ed., 1981, Karst geomorphology; Benchmark Papers in Geology, v. 59; A Benchmark book series: Stroudsburg, PA, Hutchinson Ross Publishing Co., 427 pp.

Tattam, C.M., 1937, The application of electrical resistivity prospecting to groundwater problem: Quarterly of the Colorado School of Mines, v. 32, no. 1, pp. 119-138.

Telford, W.M., Geldart, L.P., Sheriff, R.E., and Keys, D.A., 1976, Applied geophysics: Cambridge, Cambridge University Press, 860 pp.

Todd, D.K., and Asce, J.M., 1955, Investigating groundwater by applied geophysics: Amer. Soc. of Civil Eng. Proc., v. 81, pp. 625-1 - 625-12.

Todd, D.K., 1959, Groundwater hydrology: New York, John Wiley & Sons, Inc., 336 pp.

Van Dam, J.C., and Meulenkamp, J.J., 1967, Some results of the geoelectrical resistivity method in groundwater investigations in Netherlands: Geophys. Prosp., v. 15, no. 1, pp. 92-115.

Van Dam, J.C., 1976, Possibilities and limitations of the resistivity method of geoelectrical prospecting in the solution of geohydrological problems: Geoexploration, v. 14, pp. 179-193.

Vincenz, S.A., 1968, Resistivity investigations of limestone aquifers in Jamaica: Geophysics, v. 33, no. 6, pp. 980-994.

Weiss, O., 1946, Geophysical prospecting for water in the dolomite: Journal of Chem., Met., and Min. Soc. of South Africa, v. 47, no. 4, pp. 155-163.

Workman, L.E., and Leighton, M.M., 1937, Search for groundwaters by the electrical resistivity method: Trans. Amer. Geophys. Union, v. 18, pt. 2, pp. 403-409.

Worthington, P.F., 1975, Procedures for the optimum use of geophysical methods in groundwater development programs: Bull. Assoc. Eng. Geologists, v. 12, no. 1, pp. 23-38.

_____, 1977, Geophysical investigations of groundwater resources in the Kalahari Basin: Geophysics, v. 42, no. 4, pp. 838-849.

Wyllie, M.R.J., and Rose, W.D., 1950, Some theoretical considerations related to the quantitative evaluation of the physical characteristics of reservoir rock from electrical log data: Trans. AIME, v. 189.

Wyllie, M.R.J., 1963, The fundamentals of well log interpretation: New York, Academic Press, Inc., 238 pp.

Yevjevich, V., ed., 1976, Karst hydrology and water resources; Proceedings of the U.S.-Yugoslavian Symposium, Dubrovnik, June 2-7, 1975: Fort Collins, CO, Water Resources Publications, two volumes, 873 pp.

Zohdy, A.A.R., and Jackson, D.B., 1969, Application of deep electrical resistivity soundings for groundwater exploration in Hawaii: Geophysics, v. 34, pp. 584-600.

Zohdy, A.A.R., 1969, The use of Schlumberger and equatorial soundings in groundwater investigations near El Paso, Texas: Geophysics, v. 34, pp. 713-728.

Zohdy, A.A.R., Eaton, G.P., and Mabey, D.R., 1974, Application of surface geophysics to groundwater investigations: Techniques of Water-Resources Investigations of the U.S.G.S., chapter D1, book 2, 116 pp.

APPENDIX 1

Schlumberger Resistivity Sounding and Profiling Data

ES-1

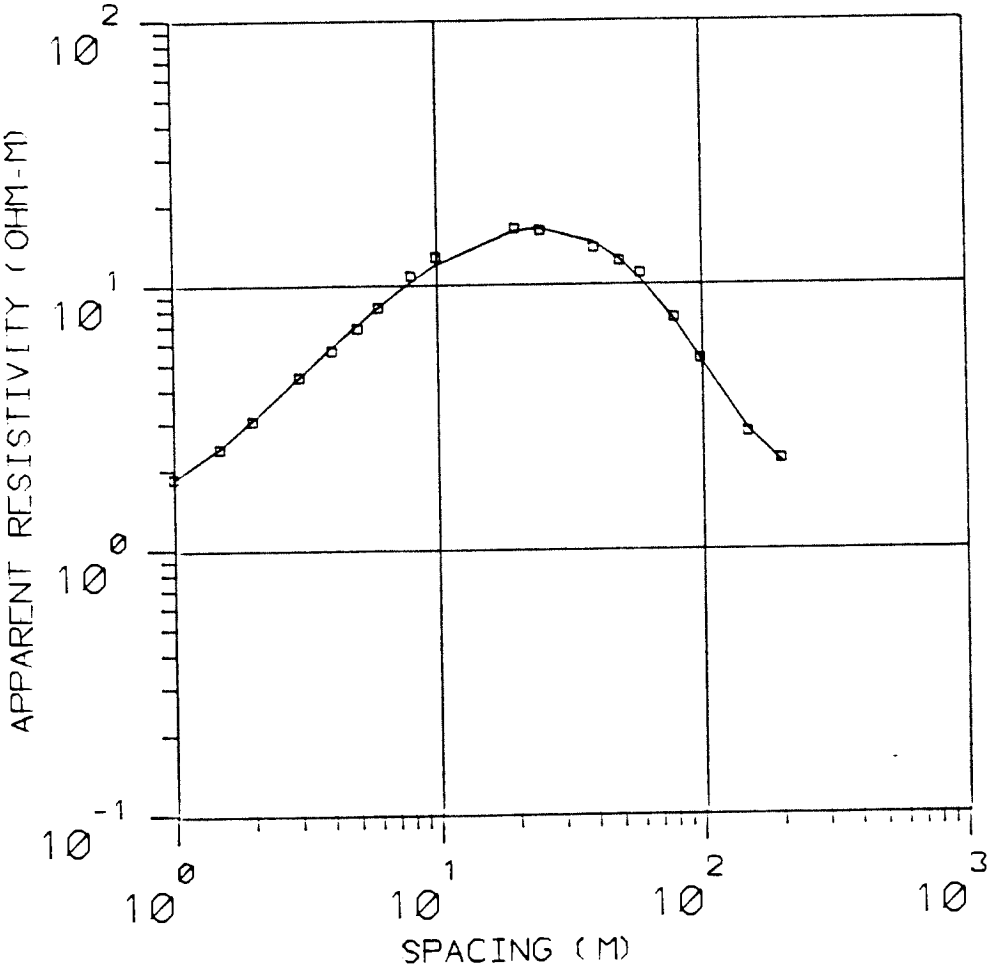
APPARENT RESISTIVITY (OHM-M)
10^2
10^1
10^0
10^-1
10^0
10^1
10^2
10^3
SPACING (M)

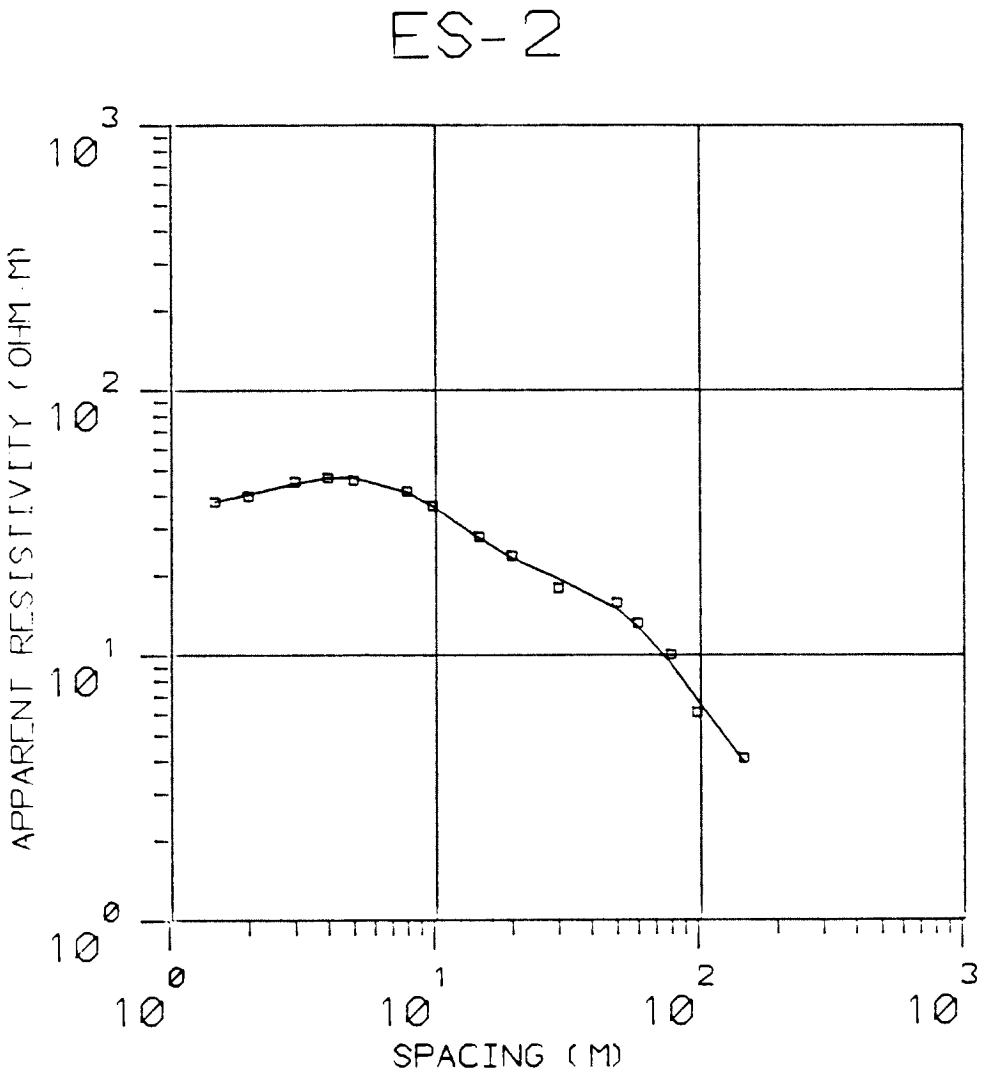
ES-2
APPARENT RESISTIVITY (OHM-M)
SPACING (M)
10^3
10^2
10^1
10^0
10^0
10^1
10^2
10^3

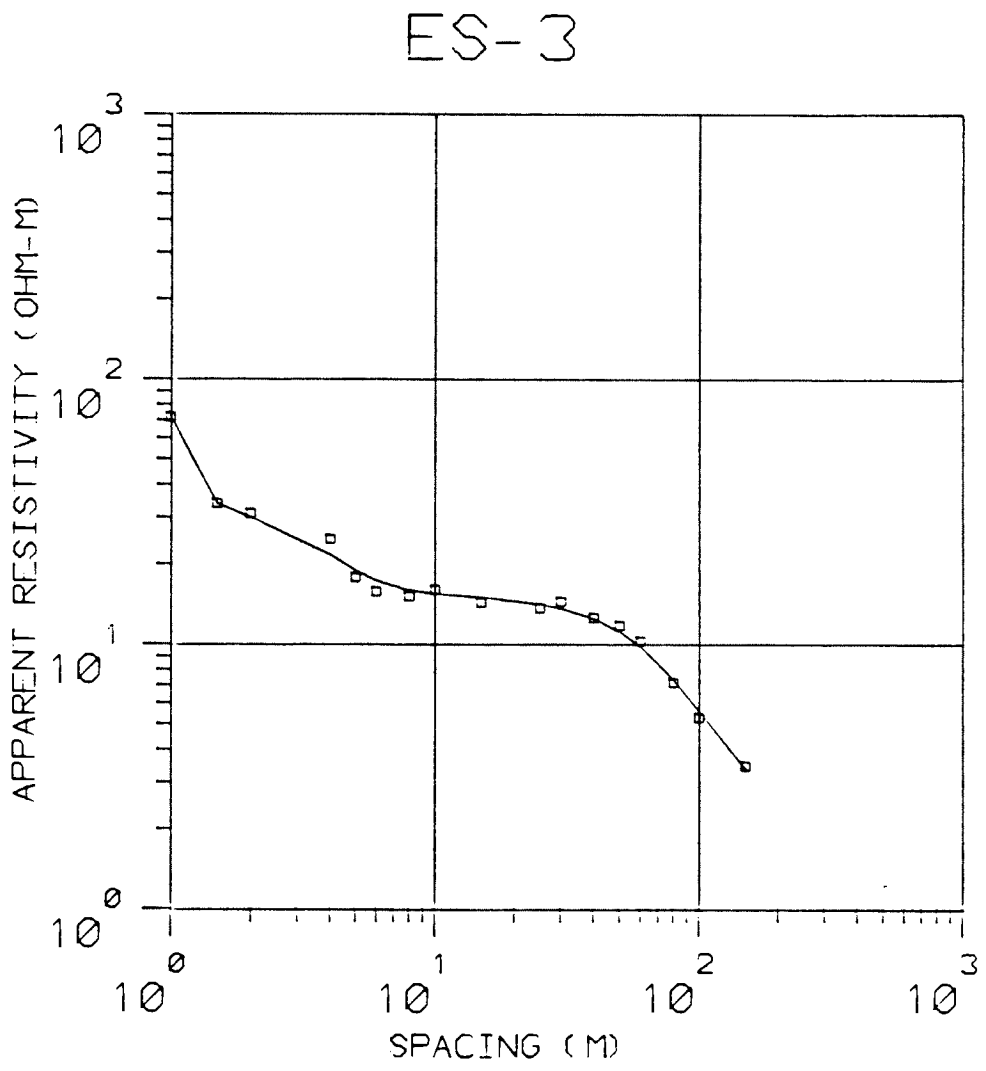
ES-3
APPARENT RESISTIVITY (OHM-M)
SPACING (M)
10^3
10^2
10^1
10^0
10^0
10^1
10^2
10^3

ES-4

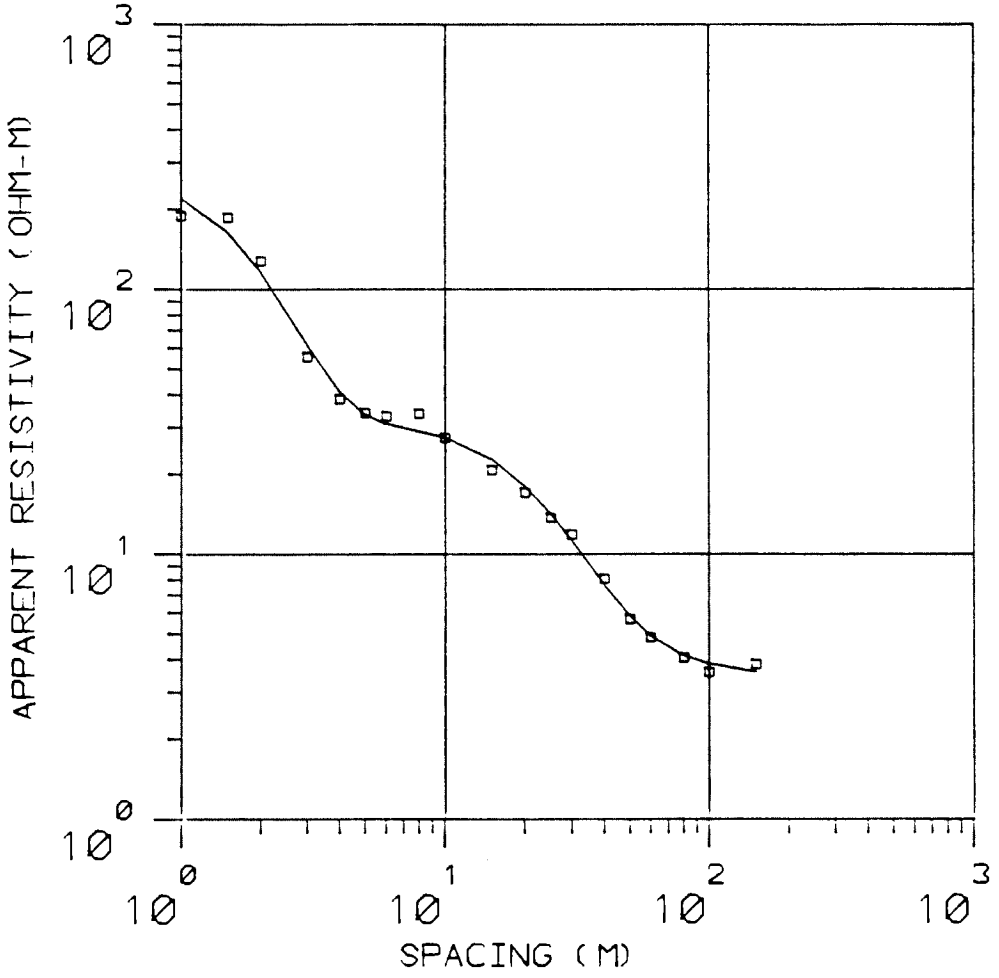
APPARENT RESISTIVITY (OHM-M)
10^3
10^2
10^1
10^0
10^0
10^1
10^2
10^3
SPACING (M)

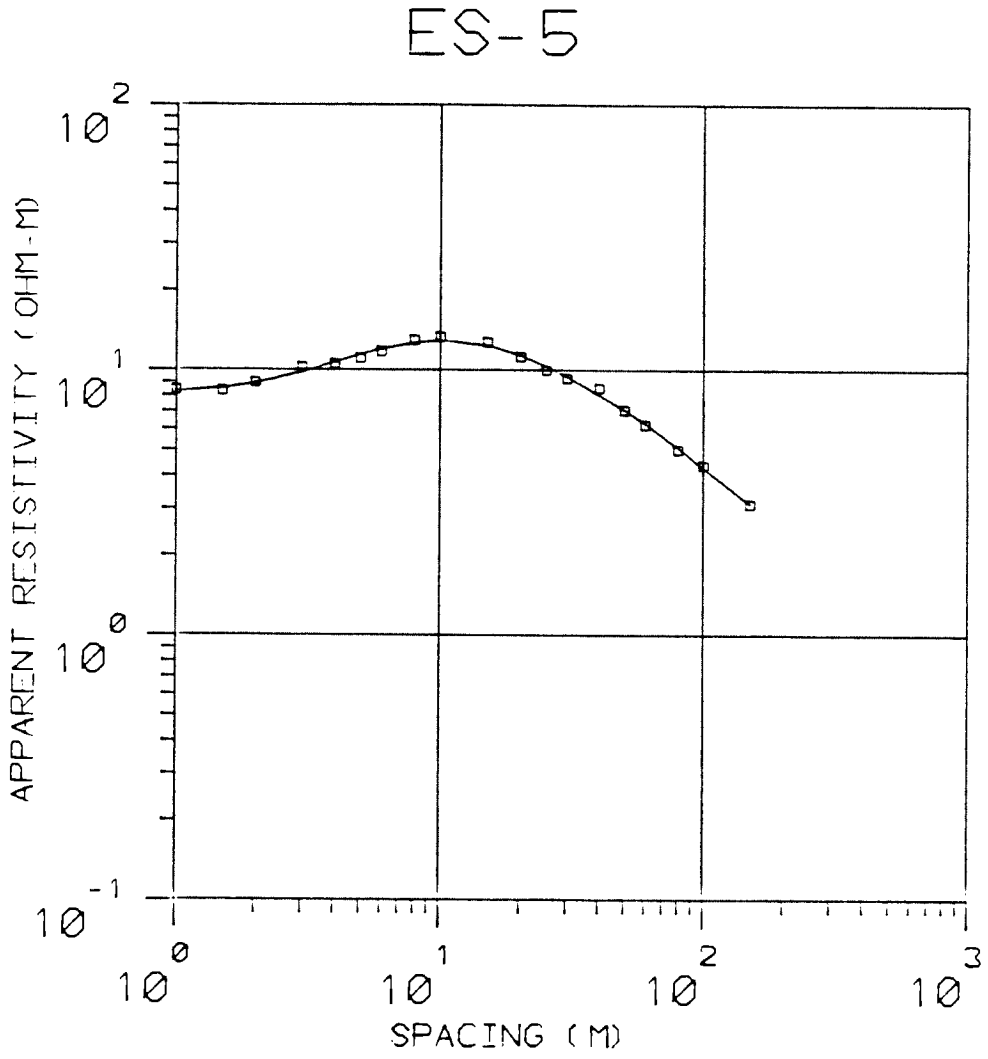
ES-5
APPARENT RESISTIVITY (OHM-M)
10^2
10^1
10^0
10^-1
10^0
10^1
10^2
10^3
SPACING (M)

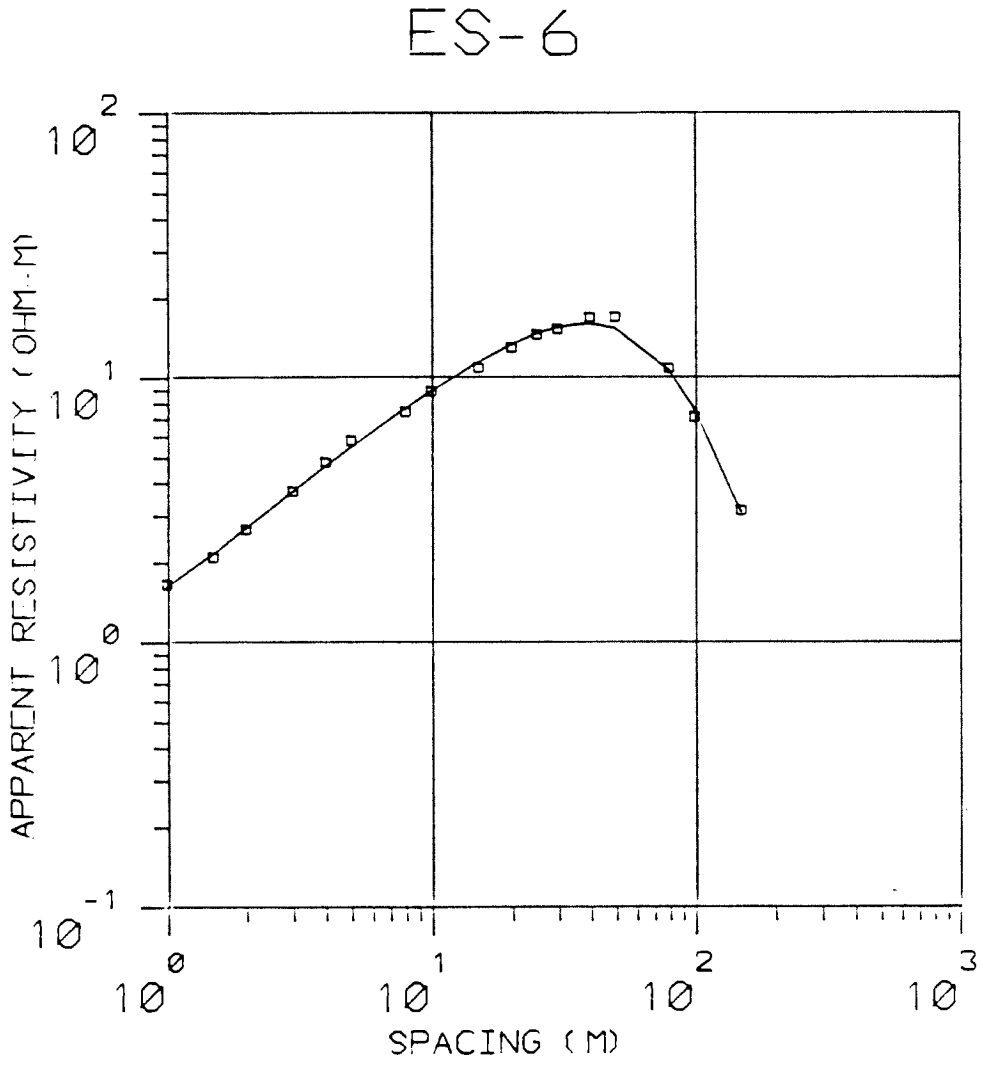
ES-6
APPARENT RESISTIVITY (OHM-M)
10^2
10^1
10^0
10^-1
10^0
10^1
10^2
10^3
SPACING (M)

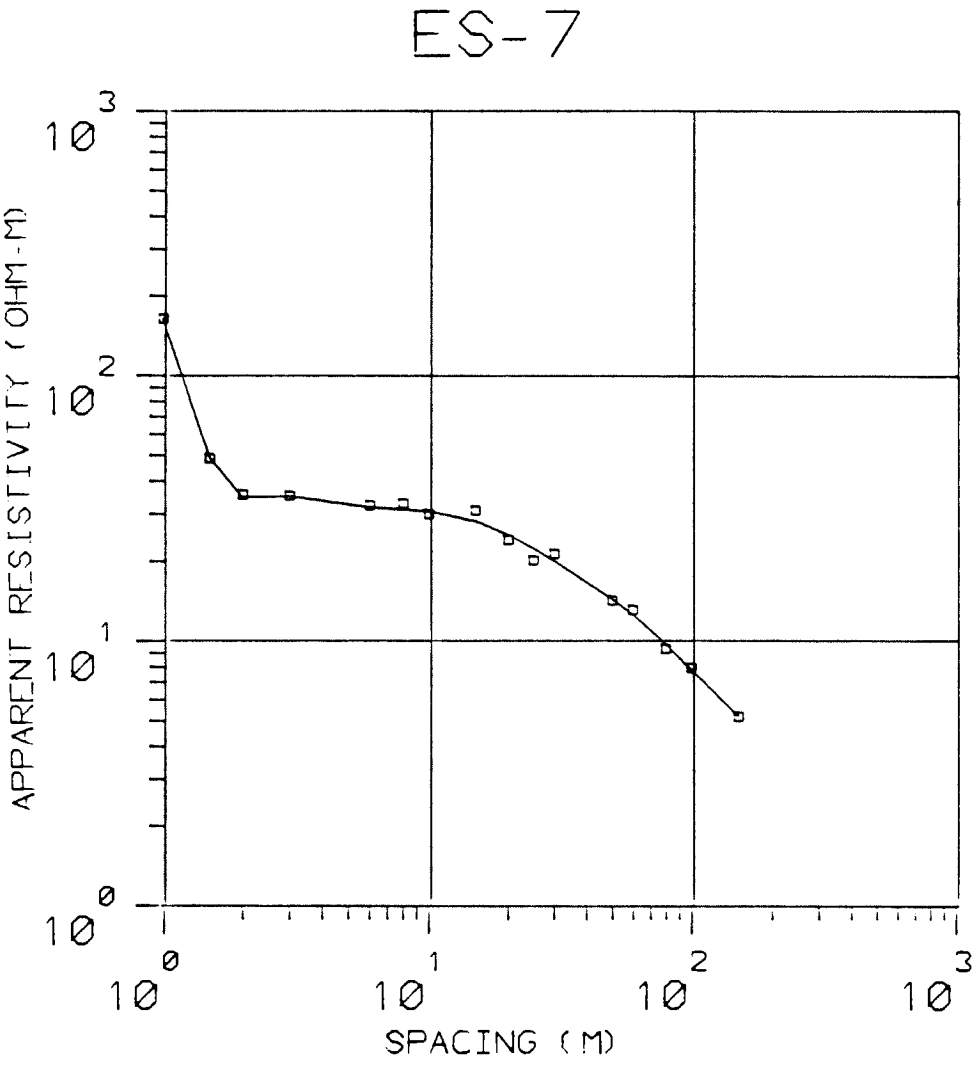
ES-7
APPARENT RESISTIVITY (OHM-M)
10^3
10^2
10^1
10^0
10^0
10^1
10^2
10^3
SPACING (M)

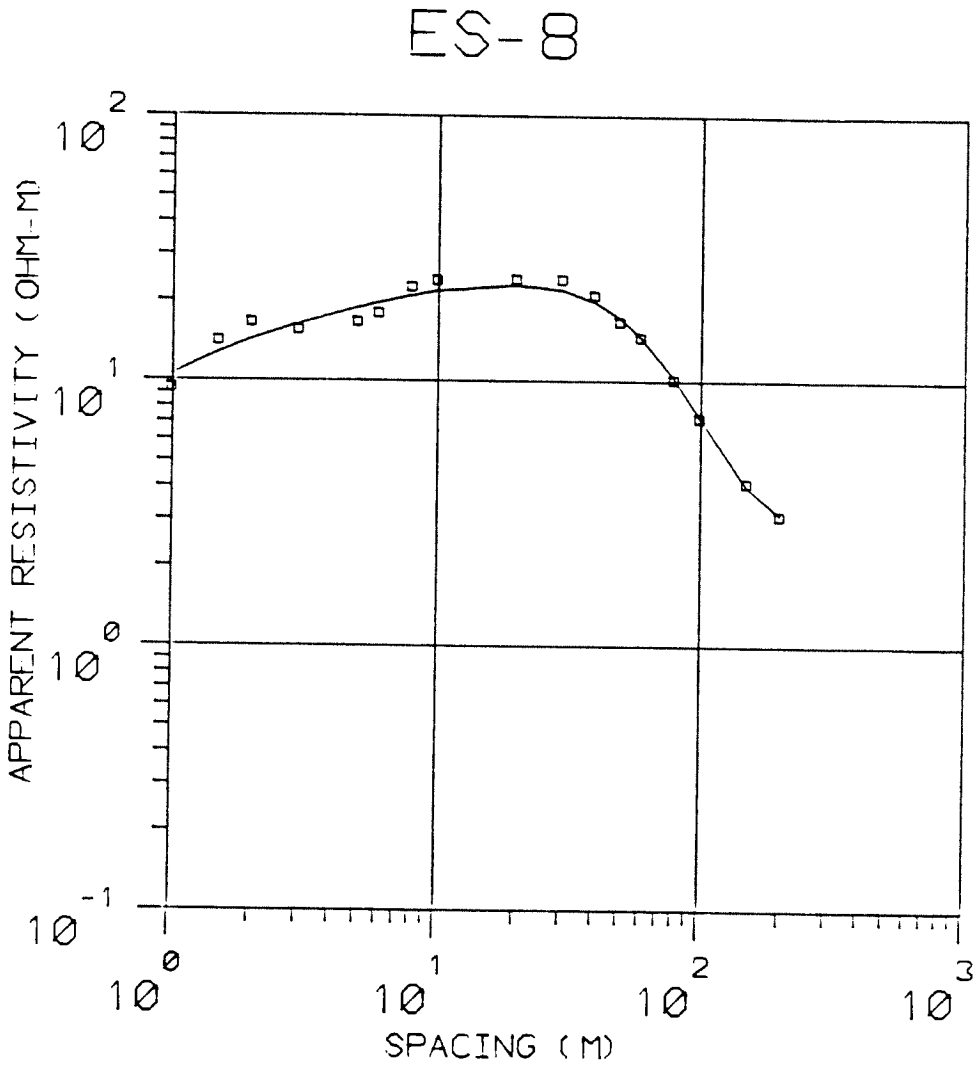
ES-8
APPARENT RESISTIVITY (OHM-M)
10^2
10^1
10^0
10^-1
10^0
10^1
10^2
10^3
SPACING (M)

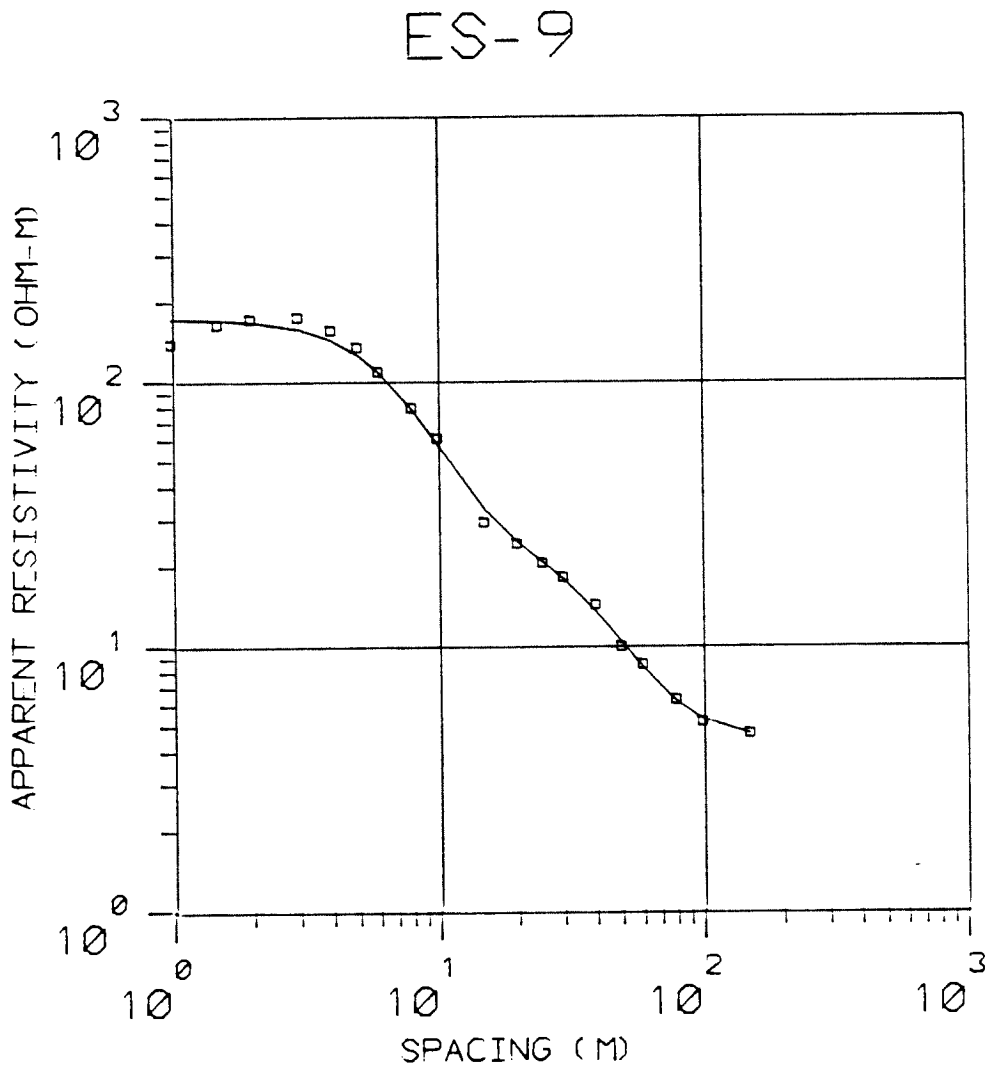
ES-9
APPARENT RESISTIVITY (OHM-M)
10^3
10^2
10^1
10^0
10^0
10^1
10^2
10^3
SPACING (M)

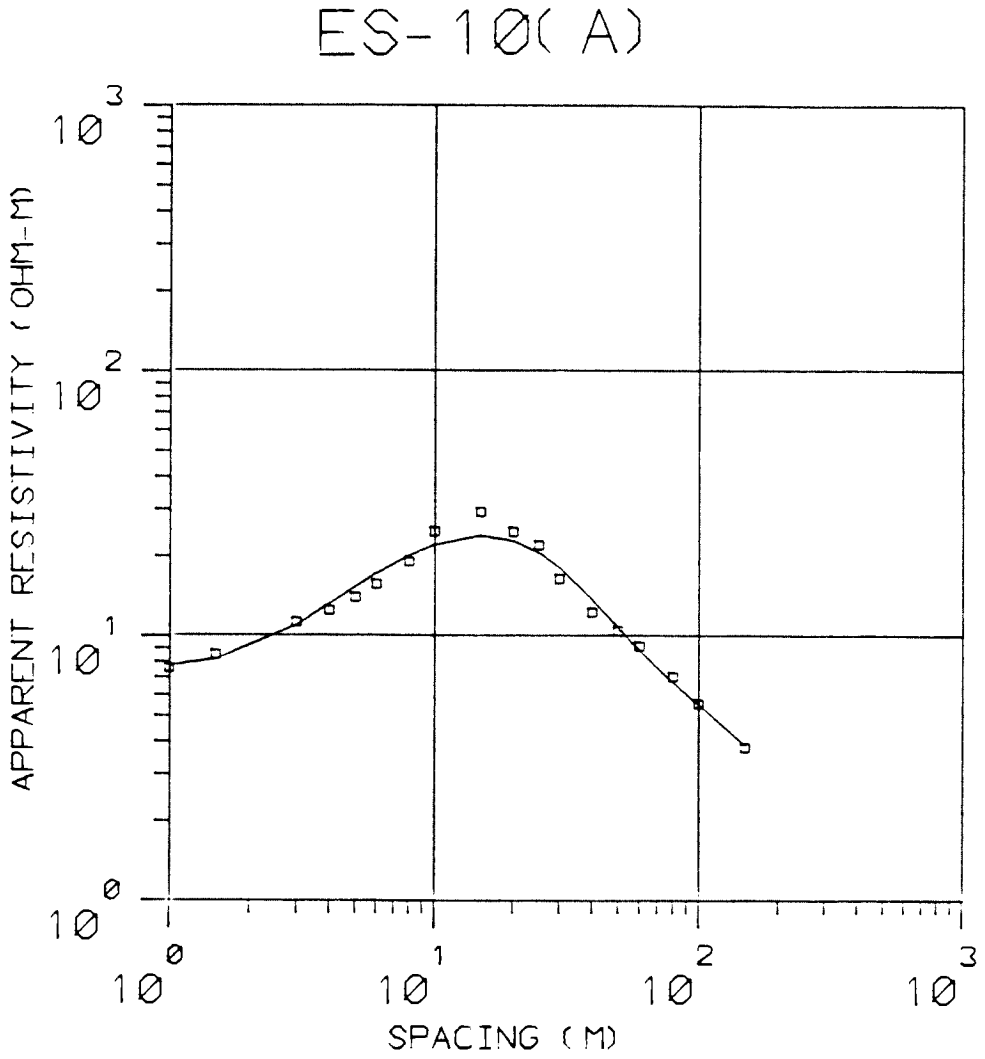
ES-10(A)
APPARENT RESISTIVITY (OHM-M)
10^3
10^2
10^1
10^0
10^0
10^1
10^2
10^3
SPACING (M)

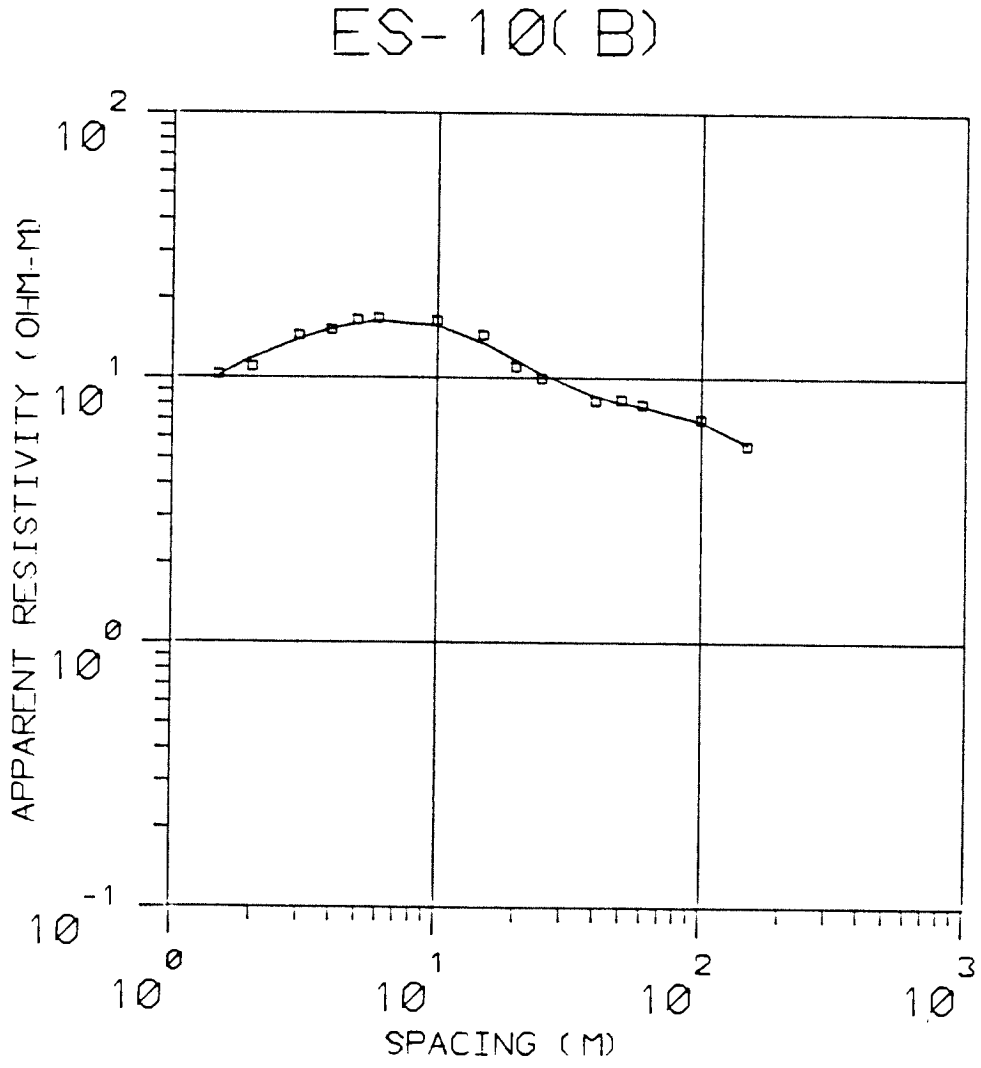
ES-10(B)
APPARENT RESISTIVITY (OHM-M)
10^2
10^1
10^0
10^-1
10^0
10^1
10^2
10^3
SPACING (M)

ES-11/12

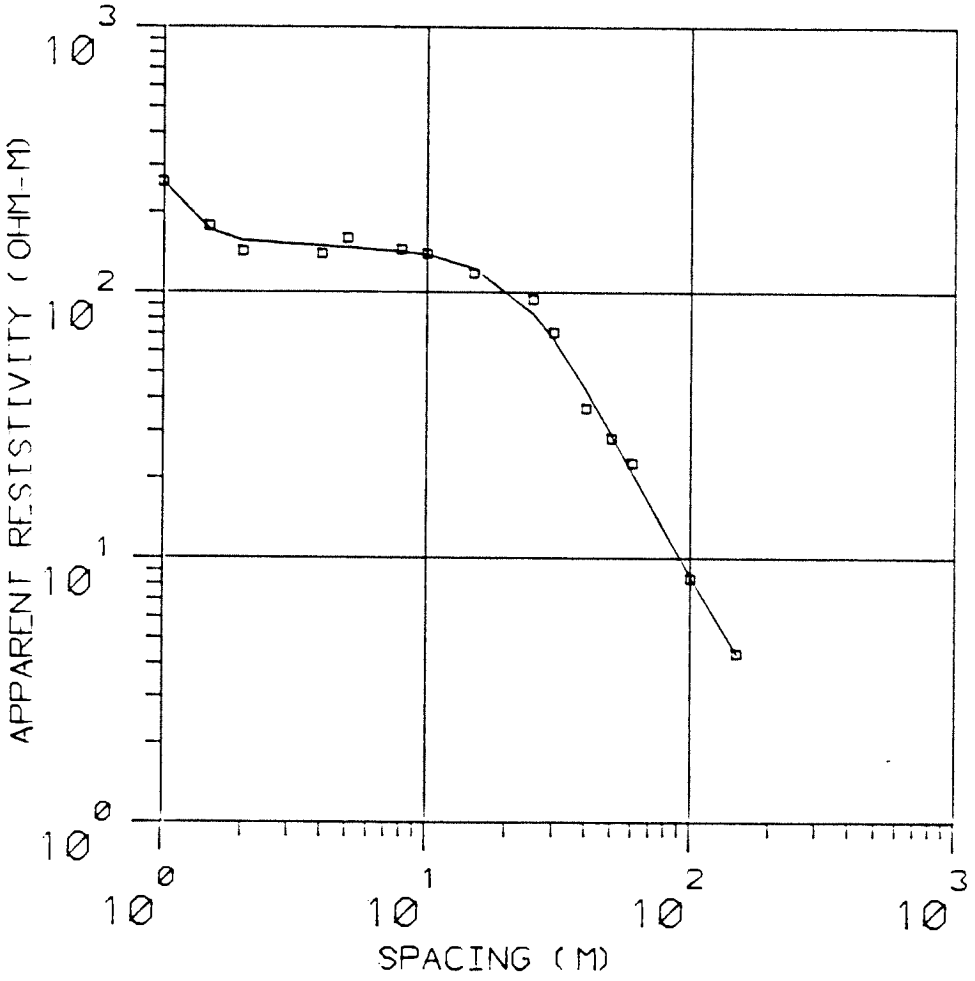
APPARENT RESISTIVITY (OHM-M)
10^3
10^2
10^1
10^0
10^0
10^1
10^2
10^3
SPACING (M)

ES-13

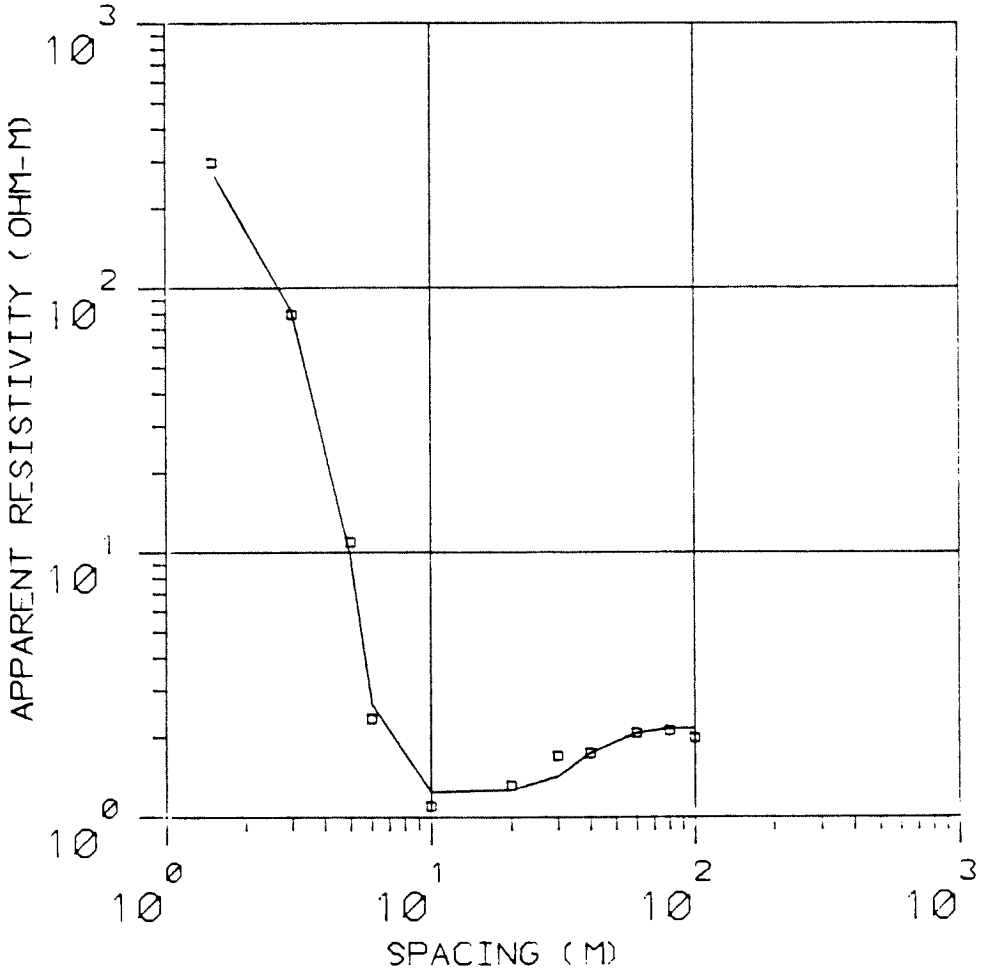
APPARENT RESISTIVITY (OHM-M)
10^3
10^2
10^1
10^0
10^0
10^1
10^2
10^3
SPACING (M)

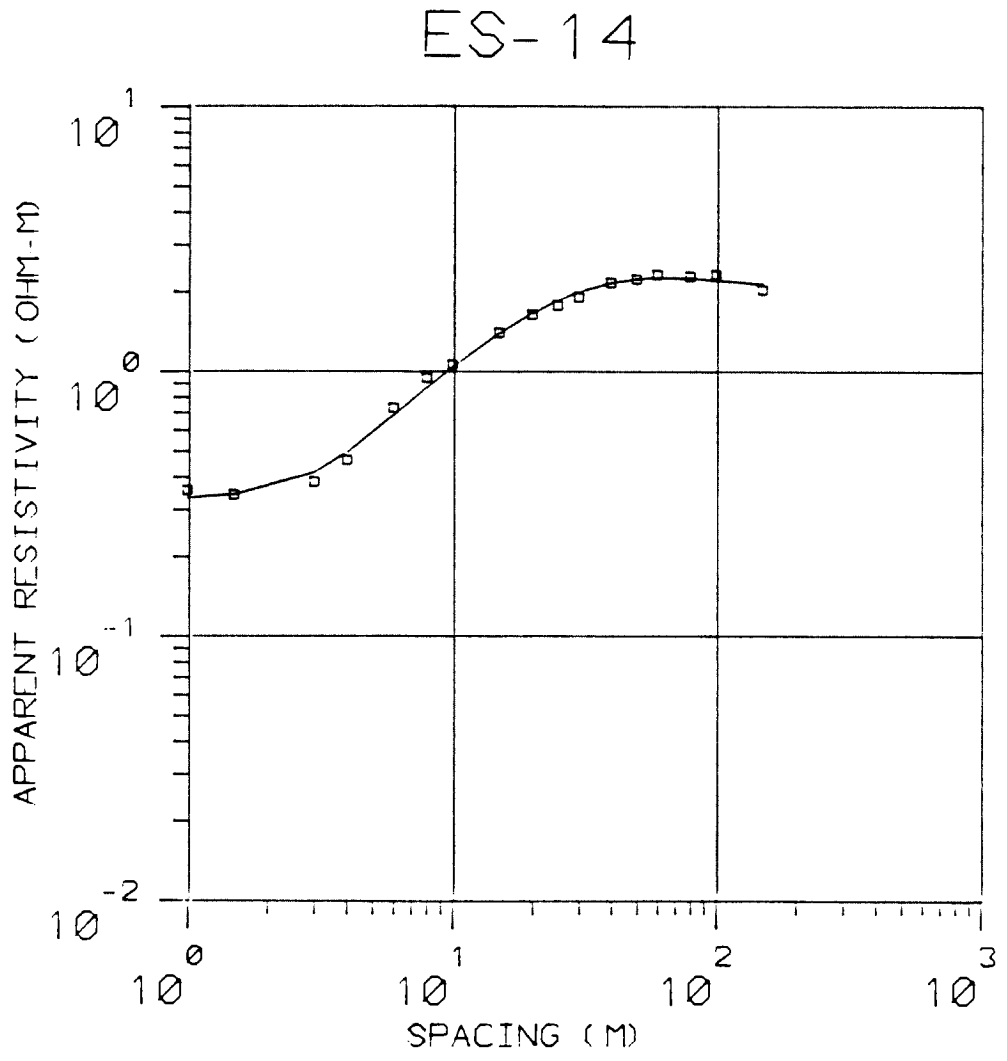
ES-14
APPARENT RESISTIVITY (OHM-M)
10^1
10^0
10^-1
10^-2
10^0
10^1
10^2
10^3
SPACING (M)

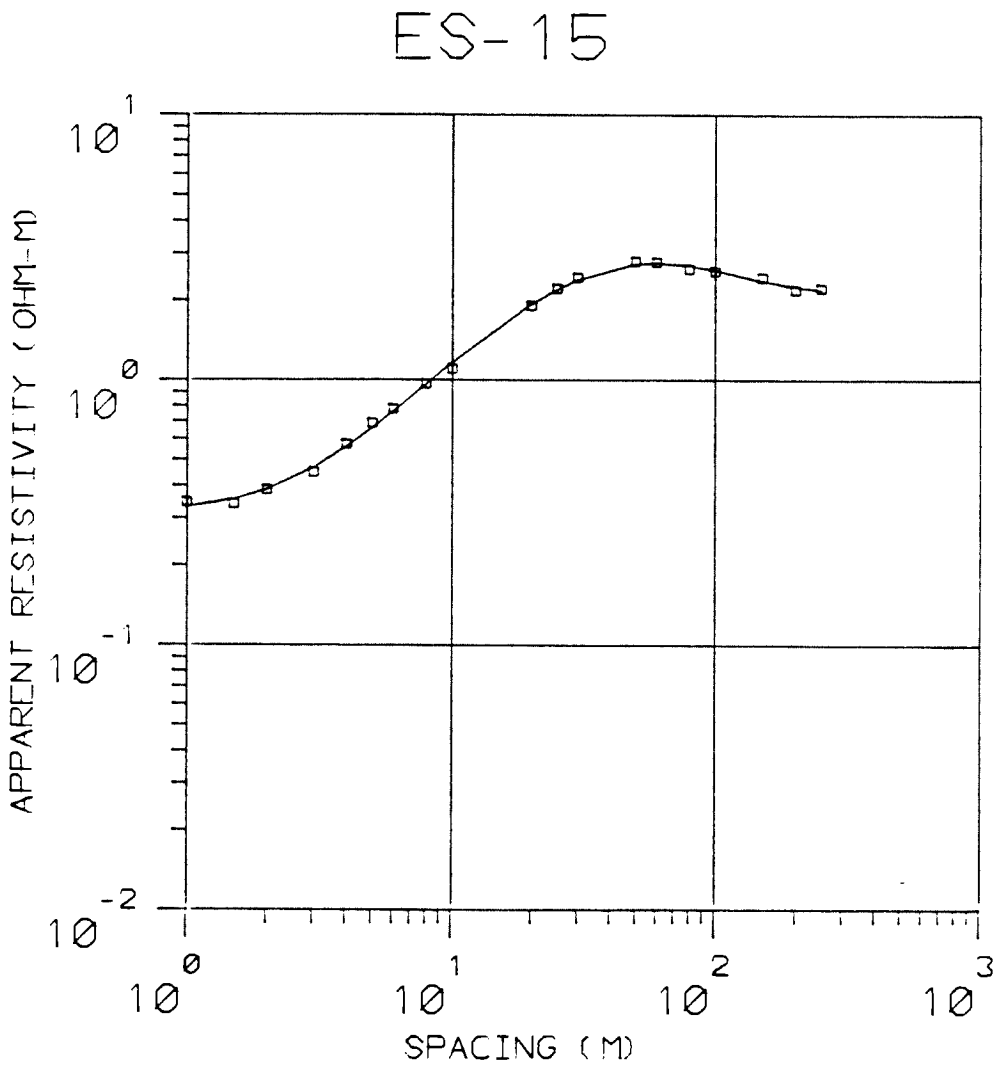
ES-15
APPARENT RESISTIVITY (OHM-M)
10^1
10^0
10^-1
10^-2
10^0
10^1
10^2
10^3
SPACING (M)

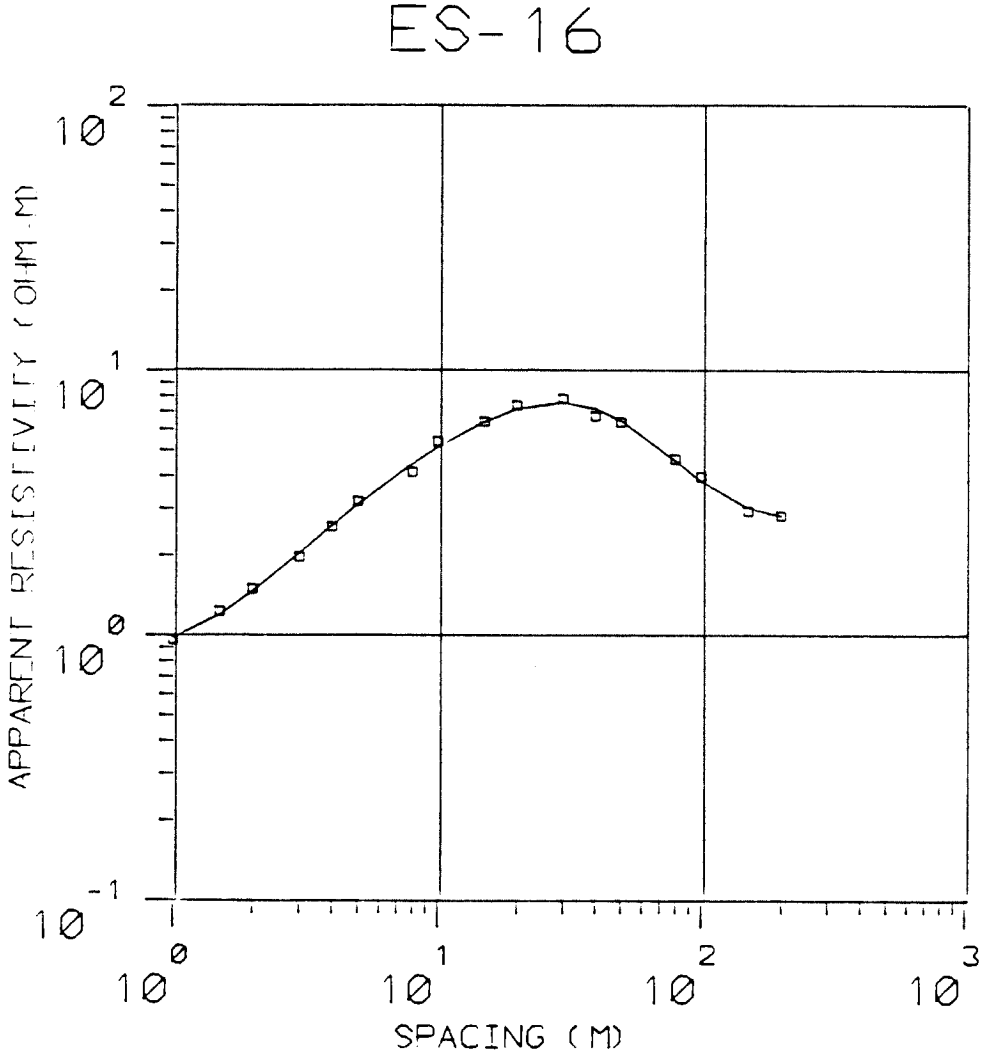
ES-16
APPARENT RESISTIVITY (OHM-M)
10^2
10^1
10^0
10^-1
10^0
10^1
10^2
10^3
SPACING (M)

Schlumberger Resistivity Sounding Data
by Condrill AB Company

Electrical Sounding # ES-1 Date: April 29, 1981

MN (meters)	AB/2 (meters)	$K = \pi(\frac{a^2}{b} - \frac{b}{4})$	$\Delta U/I$ (milli-ohms)	ρ_a (ohm-m)	ρ_a corrected (ohm-m)
0.40	1.0	7.540	218.0	1.64	1.85
"	1.5	17.36	122.2	2.12	2.39
"	2	31.10	86.4	2.69	3.04
"	3	70.37	56.0	3.94	4.45
"	4	125.3	39.7	4.97	5.61
"	5	196.0	30.7	6.02	6.80
"	6	282.4	25.5	7.20	8.13
"	8	502.3	18.93	9.51	10.7
"	10	785.1	14.25	11.2	12.6
4.0	10	75.40	160.8	12.1	12.6
"	15	173.6	97.4	16.9	17.7
"	20	311.0	49.6	15.4	16.1
"	25	487.7	31.0	15.1	15.8
"	30	703.7	21.3	15.0	15.7
"	40	1,253	10.37	13.0	13.6
"	50	1,960	5.89	11.54	12.1
20.0	50	377.0	32.0	12.06	12.1
"	60	549.8	19.87	10.9	10.9
"	80	989.6	7.48	7.40	7.40
"	100	1,555	3.33	5.18	5.18
"	150	3,519	0.778	2.74	2.74
"	200	6,267	0.345	2.16	2.16
"	250	9,802	-	-	-

Schlumberger Resistivity Sounding Data
by Condrill AB Company

Electrical Sounding # ES-2 Date: April 28, 1981

MN (meters)	AB/2 (meters)	$K = \pi(\frac{a^2}{b} - \frac{b}{4})$	$\Delta U/I$ (milli-ohms)	ρ_a (ohm-m)	ρ_a corrected (ohm-m)
0.40	1.0	7.540	5,750	43.4	46.2
"	1.5	17.36	2,040	35.4	37.7
"	2	31.10	1,192	37.1	39.5
"	3	70.37	598	42.1	44.8
"	4	125.3	347	43.5	46.3
"	5	196.0	217	42.5	45.3
"	6	282.4	144.4	40.8	43.4
"	8	502.3	76.8	38.6	41.1
"	10	785.1	43.3	34.0	36.2
4.0	10	75.40	480	36.2	36.2
"	15	173.6	159.6	27.7	27.7
"	20	311.0	75.6	23.5	23.5
"	25	487.7	34.4	16.8	16.8
"	30	703.7	25.2	17.7	17.7
"	40	1,253	13.57	17.0	17.0
"	50	1,960	8.00	15.7	15.7
20.0	50	377.0	41.4	15.6	15.6
"	60	549.8	23.8	13.1	13.1
"	80	989.6	10.06	9.96	9.96
"	100	1,555	3.87	6.02	6.02
"	150	3,519	1.15	4.05	4.05
"	200	6,267	-	-	-
"	250	9,802	-	-	-

Schlumberger Resistivity Sounding Data
by Condrill AB Company

Electrical Sounding # ES-3 Date: April 28, 1981

MN (meters)	AB/2 (meters)	$K = \pi(\frac{a^2}{b} - \frac{b}{4})$	$\Delta U/I$ (milli-ohms)	ρ_a (ohm-m)	ρ_a corrected (ohm-m)
0.40	1.0	7.540	6,400	48.3	71.7
"	1.5	17.36	1,312	22.8	33.8
"	2	31.10	671	20.9	31.0
"	3	70.37	290	20.4	30.3
"	4	125.3	133.4	16.7	24.8
"	5	196.0	61.2	12.0	17.8
"	6	282.4	37.7	10.6	15.7
"	8	502.3	20.4	10.2	15.1
"	10	785.1	13.71	10.8	16.0
4.0	10	75.40	245	18.5	16.0
"	15	173.6	95	16.5	14.3
"	20	311.0	62.7	19.5	16.9
"	25	487.7	32.1	15.7	13.6
"	30	703.7	23.6	16.6	14.4
"	40	1,253	% road	-	-
"	50	1,960	6.89	13.5	11.7
20.0	50	377.0	31.1	11.7	11.7
"	60	549.8	18.48	10.2	10.2
"	80	989.6	7.20	7.13	7.13
"	100	1,555	3.38	5.26	5.26
"	150	3,519	0.984	3.46	3.46
"	200	6,267	-	-	-
"	250	9,802	-	-	-

Schlumberger Resistivity Sounding Data
by Condrill AB Company

Electrical Sounding # ES-4 Date: April 29,1981

MN (meters)	AB/2 (meters)	$K = \pi(\frac{a^2}{b} - \frac{b}{4})$	$\Delta U/I$ (milli-ohms)	ρ_a (ohm-m)	ρ_a corrected (ohm-m)
0.40	1.0	7.540	35,100	265	189
"	1.5	17.36	15,090	262	186
"	2	31.10	5,740	179	127
"	3	70.37	1,105	77.8	55.3
"	4	125.3	429	53.8	38.3
"	5	196.0	244	47.8	34.0
"	6	282.4	165.1	46.6	33.1
"	8	502.3	94.4	47.4	33.7
"	10	785.1	49.1	38.5	27.4
4.0	10	75.40	358	27.0	27.4
"	15	173.6	117.3	20.4	20.7
"	20	311.0	53.9	16.8	17.0
"	25	287.7	27.6	13.5	13.7
"	30	703.7	16.50	11.6	11.8
"	40	1,253	6.33	7.93	8.04
"	50	1,960	2.85	5.59	5.67
20.0	50	377.0	15.03	5.67	5.67
"	60	549.8	8.81	4.84	4.84
"	80	989.6	4.10	4.06	4.06
"	100	1,555	2.30	3.58	3.58
"	150	3,519	1.087	3.83	3.83
"	200	6,267	-	-	-
"	250	9,802	-	-	-

Schlumberger Resistivity Sounding Data
by Condrill AB Company

Electrical Sounding # ES-5 Date: April 29, 1981

MN (meters)	AB/2 (meters)	$K = \pi(\frac{a^2}{b} - \frac{b}{4})$	$\Delta U/I$ (milli-ohms)	ρ_a (ohm-m)	ρ_a corrected (ohm-m)
0.40	1.0	7.540	968	7.30	8.35
"	1.5	17.36	418	7.26	8.30
"	2	31.10	251	7.81	8.93
"	3	70.37	126.6	8.91	10.2
"	4	125.3	73.5	9.21	10.5
"	5	196.0	49.3	9.66	11.0
"	6	282.4	36.0	10.2	11.7
"	8	502.3	22.5	11.3	12.9
"	10	785.1	14.81	11.63	13.3
4.0	10	75.40	155.8	11.75	13.3
"	15	173.6	64.5	11.2	12.7
"	20	311.0	31.8	9.89	11.2
"	25	487.7	18.0	8.78	9.94
"	30	703.7	11.62	8.18	9.26
"	40	1,253	6.0	7.52	8.51
"	50	1,960	3.18	6.23	7.05
20.0	50	377.0	18.70	7.05	7.05
"	60	549.8	11.28	6.20	6.20
"	80	989.6	5.05	5.00	5.00
"	100	1,555	2.81	4.37	4.37
"	150	3,519	0.888	3.12	3.12
"	200	6,267	-	-	-
"	250	9,802	-	-	-

Schlumberger Resistivity Sounding Data
by Condrill AB Company

Electrical Sounding # ES-6 Date: April 30, 1981

MN (meters)	AB/2 (meters)	$K = \pi(\frac{a^2}{b} - \frac{b}{4})$	$\Delta U/I$ (milli-ohms)	ρ_a (ohm-m)	ρ_a corrected (ohm-m)
0.40	1.0	7.540	263	1.98	1.65
"	1.5	17.36	145.5	2.53	2.10
"	2	31.10	103.2	3.21	2.67
"	3	70.37	63.7	4.48	3.72
"	4	125.3	46.0	5.76	4.79
"	5	196.0	35.5	6.96	5.79
"	6	282.4	30.5	8.61	7.16
"	8	502.3	17.75	8.92	7.42
"	10	785.1	13.62	10.69	8.89
4.0	10	75.40	106.7	8.05	8.89
"	15	173.6	57.0	9.90	10.9
"	20	311.0	37.8	11.8	13.0
"	25	487.7	27.0	13.2	14.6
"	30	703.7	19.81	13.9	15.3
"	40	1,253	12.18	15.3	16.9
"	50	1,960	7.85	15.4	17.0
20.0	50	377.0	45.2	17.0	17.0
"	60	549.8	31.2	17.2	17.2
"	80	989.6	11.0	10.9	10.9
"	100	1,555	4.59	7.14	7.14
"	150	3,519	0.90	3.17	3.17
"	200	6,267	-	-	-
"	250	9,802	-	-	-

Schlumberger Resistivity Sounding Data
by Condrill AB Company

Electrical Sounding # ES-7 Date: April 30, 1981

MN (meters)	AB/2 (meters)	$K = \pi(\frac{a^2}{b} - \frac{b}{4})$	$\Delta U/I$ (milli-ohms)	ρ_a (ohm-m)	ρ_a corrected (ohm-m)
0.40	1.0	7.540	17,090	129	164
"	1.5	17.36	2,220	38.5	48.9
"	2	31.10	900	28.0	35.6
"	3	70.37	394	27.7	35.2
"	4	125.3	296	37.1	47.1
"	5	196.0	158.1	31.0	39.4
"	6	282.4	90.3	25.5	32.4
"	8	502.3	51.8	26.0	33.0
"	10	785.1	30.0	23.6	30.0
4.0	10	75.40	325.0	24.5	30.0
"	15	173.6	145.6	25.3	31.0
"	20	311.0	63.0	19.6	24.0
"	25	487.7	33.7	16.4	20.1
"	30	703.7	24.7	17.4	21.3
"	40	1,253	13.87	17.4	21.3
"	50	1,960	5.93	11.6	14.2
20.0	50	377.0	37.6	14.2	14.2
"	60	549.8	23.8	13.1	13.1
"	80	989.6	9.42	9.32	9.32
"	100	1,555	5.10	7.93	7.93
"	150	3,519	1.471	5.18	5.18
"	200	6,267	-	-	-
"	250	9,802	-	-	-

Schlumberger Resistivity Sounding Data
by Condrill AB Company

Electrical Sounding # ES-8 Date: April 27, 1981

MN (meters)	AB/2 (meters)	$K = \pi(\frac{a^2}{b} - \frac{b}{4})$	$\Delta U/I$ (milli-ohms)	ρ_a (ohm-m)	ρ_a corrected (ohm-m)
0.40	1.0	7.540	987	7.44	9.31
"	1.5	17.36	651	11.3	14.1
"	2	31.10	425	13.2	16.5
"	3	70.37	176.3	12.4	15.5
"	4	125.3	90.1	11.3	14.1
"	5	196.0	67.8	13.3	16.6
"	6	282.4	50.6	14.3	17.9
"	8	502.3	35.8	18.0	22.5
"	10	785.1	24.3	19.1	23.9
4.0	10	75.40	193.6	14.6	23.9
"	15	173.6	77.3	13.4	21.5
"	20	311.0	48.2	15.0	24.1
"	25	487.7	38.1	18.6	29.9
"	30	703.7	21.3	15.0	24.0
"	40	1,253	10.37	13.0	20.9
"	50	1,960	5.31	10.4	16.7
20.0	50	377.0	44.3	16.7	16.7
"	60	549.8	26.5	14.6	14.6
"	80	989.6	10.22	10.1	10.1
"	100	1,555	4.65	7.23	7.23
"	150	3,519	1.175	4.13	4.13
"	200	6,267	0.498	3.12	3.12
"	250	9,802	-	-	-

Schlumberger Resistivity Sounding Data
by Condrill AB Company

Electrical Sounding # ES-9 Date: April 30, 1981

MN (meters)	AB/2 (meters)	$K = \pi(\frac{a^2}{b} - \frac{b}{4})$	$\Delta U/I$ (milli-ohms)	ρ_a (ohm-m)	ρ_a corrected (ohm-m)
0.40	1.0	7.540	22,900	173	139
"	1.5	17.36	11,750	204	164
"	2	31.10	6,890	214	172
"	3	70.37	3,080	217	175
"	4	125.3	1,550	194	156
"	5	196.0	857	168	135
"	6	282.4	479	135	109
"	8	502.3	197	99	79.7
"	10	785.1	96.6	75.8	61.1
4.0	10	75.40	741	55.9	61.1
"	15	173.6	154.9	26.9	29.4
"	20	311.0	71.6	22.3	24.4
"	25	487.7	38.8	18.9	20.6
"	30	703.7	23.7	16.7	18.2
"	40	1,253	10.43	13.1	14.3
"	50	1,960	4.65	9.11	9.95
20.0	50	377.0	26.4	9.95	9.95
"	60	599.8	15.46	8.50	8.50
"	80	989.6	6.32	6.25	6.25
"	100	1,555	3.32	5.16	5.16
"	150	3,519	1.325	4.66	4.66
"	200	6,267	-	-	-
"	250	9,802	-	-	-

Schlumberger Resistivity Sounding Data
by Condrill AB Company

Electrical Sounding # ES-10/A Date: May 2, 1981

MN (meters)	AB/2 (meters)	$K = \pi(\frac{a^2}{b} - \frac{b}{4})$	$\Delta U/I$ (milli-ohms)	ρ_a (ohm-m)	ρ_a corrected (ohm-m)
0.40	1.0	7.540	1,171	8.83	7.54
"	1.5	17.36	574	9.96	8.50
"	2	31.10	382	11.9	10.2
"	3	70.37	187.1	13.2	11.3
"	4	125.3	117.5	14.7	12.5
"	5	196.0	83.8	16.4	14.0
"	6	282.4	65.3	18.4	15.7
"	8	502.3	44.6	22.4	19.1
"	10	785.1	33.2	26.1	24.8
4.0	10	75.40	386.0	29.1	24.8
"	15	173.6	198.1	34.4	29.4
"	20	311.0	93.0	28.9	24.7
"	25	487.7	52.8	25.8	22.0
"	30	703.7	27.3	19.2	16.4
"	40	1,253	11.5	14.4	12.3
"	50	1,960	6.25	12.3	10.5
20.0	50	377.0	27.9	10.5	10.5
"	60	549.8	16.69	9.18	9.18
"	80	989.6	7.11	7.04	7.04
"	100	1,555	3.58	5.57	5.57
"	150	3,519	1.084	3.81	3.81
"	200	6,267	-	-	-
"	250	9,802	-	-	-

Schlumberger Resistivity Sounding Data
by Condrill AB Company

Electrical Sounding # ES-10/B Date: April 30, 1981

MN (meters)	AB/2 (meters)	$K = \pi(\frac{a^2}{b} - \frac{b}{4})$	$\Delta U/I$ (milli-ohms)	ρ_a (ohm-m)	ρ_a corrected (ohm-m)
0.40	1.0	7.540	3,660	27.6	18.1
"	1.5	17.36	903	15.7	10.3
"	2	31.10	537	16.7	11.0
"	3	70.37	313	22.0	14.5
"	4	125.3	185.5	23.2	15.2
"	5	196.0	129	25.3	16.6
"	6	282.4	90.8	25.6	16.8
"	8	502.3	60.0	30.1	19.8
"	10	785.1	31.8	25.0	16.4
4.0	10	75.40	286	21.6	16.4
"	15	173.6	109.8	19.1	14.5
"	20	311.0	46.5	14.5	11.0
"	25	487.7	26.8	13.1	9.96
"	30	703.7	13.0	9.15	6.96
"	40	1,253	8.62	10.8	8.21
"	50	1,960	5.56	10.9	8.29
20.0	50	377.0	22.0	8.29	8.29
"	60	549.8	14.46	7.95	7.95
"	80	989.6	6.42	6.35	6.35
"	100	1,555	450	7.00	7.00
"	150	3,519	1.576	5.55	5.55
"	200	6,267	-	-	-
"	250	9,802	-	-	-

Schlumberger Resistivity Sounding Data
by Condrill AB Company

Electrical Sounding # ES-11/12 Date: May 11, 1981

MN (meters)	AB/2 (meters)	$K = \pi(\frac{a^2}{b} - \frac{b}{4})$	$\Delta U/I$ (milli-ohms)	ρ_a (ohm-m)	ρ_a corrected (ohm-m)
0.40	1.0	7.540	25,900	195	260
"	1.5	17.36	7,640	133	177
"	2	31.10	3,430	107	143
"	3	70.37	1,362	95.8	127
"	4	125.3	837	105	140
"	5	196.0	614	120	160
"	6	282.4	435	123	164
"	8	502.3	217	109	145
"	10	785.1	133.5	105	140
4.0	10	75.40	1,636	123	140
"	15	173.6	596	103	118
"	20	311.0	254	79	90.5
"	25	487.7	169	82.4	94.4
"	30	703.7	87.7	61.7	70.7
"	40	1,253	25.6	32.1	36.8
"	50	1,960	12.62	24.7	28.3
20.0	50	377.0	75	28.3	28.3
"	60	549.8	41.5	22.8	22.8
"	80	989.6	11.25	11.1	11.1
"	100	1,555	5.40	8.40	8.40
"	150	3,519	1.237	4.35	4.35
"	200	6,267	-	-	-
"	250	9,802	-	-	-

Schlumberger Resistivity Sounding Data
by Condrill AB Company

Electrical Sounding # ES-13 Date: May 6, 1981

MN (meters)	AB/2 (meters)	$K = \pi(\frac{a^2}{b} - \frac{b}{4})$	$\Delta U/I$ (milli-ohms)	ρ_a (ohm-m)	ρ_a corrected (ohm-m)
0.40	1.0	7.540	210,000	1,583	741
"	1.5	17.36	36,600	637	298
"	2	31.10	10,060	313	147
"	3	70.37	2,420	170	79.6
"	4	125.3	475	59.6	27.9
"	5	196.0	120.2	23.6	11.0
"	6	282.4	17.90	5.05	2.36
"	8	502.3	4.15	2.08	0.97
"	10	785.1	3.01	2.36	1.10
4.0	10	75.40	21.1	1.59	1.10
"	15	173.6	9.24	1.61	1.12
"	20	311.0	6.10	1.90	1.32
"	25	487.7	road	-	-
"	30	703.7	3.50	2.46	1.71
"	40	1,253	2.01	2.52	1.75
"	50	1,960	1.505	2.95	2.05
20.0	50	377.0	5.45	2.05	2.05
"	60	549.8	3.78	2.08	2.08
"	80	989.6	2.15	2.13	2.13
"	100	1,555	1.287	2.00	2.00
"	150	3,519	water	-	-
"	200	6,267	-	-	-
"	250	9,802	-	-	-

Schlumberger Resistivity Sounding Data
by Condrill AB Company

Electrical Sounding # ES-14 Date: May 6, 1981

MN (meters)	AB/2 (meters)	$K = \pi(\frac{a^2}{b} - \frac{b}{4})$	$\Delta U/I$ (milli-ohms)	ρ_a (ohm-m)	ρ_a corrected (ohm-m)
0.40	1.0	7.540	44.2	0.333	0.355
"	1.5	17.36	18.43	0.321	0.342
"	2	31.10	9.03	0.281	0.299
"	3	70.37	5.12	0.360	0.383
"	4	125.3	3.46	0.434	0.462
"	5	196.0	2.56	0.502	0.535
"	6	282.4	2.42	0.683	0.728
"	8	502.3	1.77	0.889	0.947
"	10	785.1	1.27	0.997	1.06
4.0	10	75.40	14.09	1.062	1.06
"	15	173.6	8.07	1.404	1.40
"	20	311.0	5.28	1.642	1.64
"	25	487.7	3.64	1.775	1.78
"	30	703.7	2.71	1.91	1.91
"	40	1,253	1.731	2.171	2.17
"	50	1,960	1.145	2.24	2.24
20.0	50	377.0	5.99	2.26	2.26
"	60	549.8	4.24	2.33	2.33
"	80	989.6	2.32	2.30	2.30
"	100	1,555	1.500	2.33	2.33
"	150	3,519	0.594	2.09	2.09
"	200	6,267	-	-	-
"	250	9,802	-	-	-

Schlumberger Resistivity Sounding Data
by Condrill AB Company

Electrical Sounding # ES-15 Date: May 10, 1981

MN (meters)	AB/2 (meters)	$K = \pi(\frac{a^2}{b} - \frac{b}{4})$	$\Delta U/I$ (milli-ohms)	ρ_a (ohm-m)	ρ_a corrected (ohm-m)
0.40	1.0	7.540	45.8	0.345	0.345
"	1.5	17.36	19.6	0.340	0.340
"	2	31.10	12.35	0.384	0.384
"	3	70.37	6.37	0.448	0.448
"	4	125.3	4.56	0.571	0.571
"	5	196.0	3.50	0.686	0.686
"	6	282.4	2.75	0.777	0.777
"	8	502.3	1.93	0.969	0.969
"	10	785.1	1.18	0.926	(0.926)
4.0	10	75.40	15.43	1.16	1.10
"	15	173.6	9.87	1.71	1.63
"	20	311.0	6.43	2.00	1.90
"	25	487.7	4.75	2.32	2.21
"	30	703.7	3.62	2.55	2.43
"	40	1,253	2.55	3.20	3.05
"	50	1,960	1.50	2.94	2.80
20.0	50	377.0	7.42	2.80	2.80
"	60	549.8	5.05	2.78	2.78
"	80	989.6	2.65	2.62	2.62
"	100	1,555	1.652	2.57	2.57
"	150	3,519	0.690	2.43	2.43
"	200	6,267	0.348	2.18	2.18
"	250	9,802	0.226	2.22	2.22

Schlumberger Resistivity Sounding Data
by Condrill AB Company

Electrical Sounding # ES-16 Date: May 11, 1981

MN (meters)	AB/2 (meters)	$K = \pi(\frac{a^2}{b} - \frac{b}{4})$	$\Delta U/I$ (milli-ohms)	ρ_a (ohm-m)	ρ_a corrected (ohm-m)
0.40	1.0	7.540	132.8	1.00	0.96
"	1.5	17.36	74.1	1.29	1.23
"	2	31.10	50.1	1.56	1.49
"	3	70.37	29.3	2.06	1.97
"	4	125.3	21.5	2.69	2.57
"	5	196.0	17.08	3.35	3.20
"	6	282.4	13.56	3.83	3.66
"	8	502.3	8.62	4.33	4.14
"	10	785.1	7.18	5.64	5.39
4.0	10	75.40	71.5	5.39	5.39
"	15	173.6	37.0	6.42	6.42
"	20	311.0	23.8	7.40	7.40
"	25	487.7	17.38	8.48	8.48
"	30	703.7	11.15	7.85	7.85
"	40	1,253	5.37	6.73	6.73
"	50	1,960	3.26	6.39	6.39
20.0	50	377.0	14.85	5.60	(5.60)
"	60	549.8	11.02	6.06	6.06
"	80	989.6	4.69	4.64	4.64
"	100	1,555	2.56	3.98	3.98
"	150	3,519	0.837	2.95	2.95
"	200	6,267	0.451	2.83	2.83
"	250	9,802	-	-	-

Schlumberger Resistivity Sounding Data
by Condrill AB Company

Resistivity Profile # RP-1

Distance (meters)	ΔU/I (milli-ohms)	ρ_a (ohm-m)
0	4.0	
5	3.7	
10	3.8	5.91
15	3.4	5.75
20	4.3	5.78
20	3.9	
25	3.5	5.82
30	3.8	5.80
35	3.9	5.64
40	3.3	5.55
40	3.4	
45	3.6	5.30
50	3.2	5.37
55	3.1	5.40
60	3.5	5.27
60	3.6	
65	3.7	5.21
70	3.4	5.18
75	3.0	5.04
80	2.9	4.91
80	3.1	
85	3.1	4.94
90	3.3	5.21
95	3.5	5.40
100	3.7	5.36
100	4.0	
105	3.6	5.18
110	3.0	5.07
115	2.7	4.80
120	2.8	4.56
120	3.5	
125	3.0	4.68
130	2.8	4.80
135	3.4	4.88
140	3.1	5.05
145	3.4	5.49
150	3.1	5.43

Distance (meters)	ΔU/I (milli-ohms)	ρ_a (ohm-m)
150	4.0	
155	4.2	5.37
160	3.2	5.46
165	2.9	5.57
170	3.7	5.57
170	3.7	
175	3.9	5.72
180	4.2	5.78
185	3.7	5.72
190	3.1	5.41
190	3.1	
195	3.5	5.07
200	2.9	4.48
205	3.1	3.95
210	2.0	3.70
210	1.6	
215	1.4	3.51
220	2.7	3.30
225	2.3	3.86
230	1.2	4.57
230	3.6	
235	3.6	4.51
2.40	3.7	5.13
245	2.5	6.38
250	3.3	5.91
250	5.3	
255	6.4	5.26
260	2.1	5.08
265	1.6	4.46
270	2.3	3.69
270	1.6	
275	2.3	4.15
280	3.9	4.11
285	3.6	4.09
290	1.3	3.90

Schlumberger Resistivity Sounding Data
by Condrill AB Company

Resistivity Profile #RP-1
(Continued)

Distance (meters)	ΔU/I (milli-ohms)	ρ_a (ohm-m)
290	1.6	
295	1.9	3.31
300	1.7	2.80
305	2.0	2.97
310	2.0	3.03
310	1.9	
315	2.0	3.09
320	1.9	3.19
325	2.2	3.31
330	2.4	3.56
330	2.1	
335	2.4	3.93
340	2.7	4.24
345	3.4	4.37
350	3.4	4.49
350	3.1	
355	2.8	4.46
360	3.1	4.57
365	3.3	4.76
370	3.8	4.76
370	3.4	
375	3.4	4.70
380	3.1	4.49
385	3.1	4.31
390	3.3	4.28
390	2.6	
395	3.1	4.28
400	3.1	4.39
405	3.0	4.40
410	3.9	4.34
410	3.0	
415	3.0	4.37
420	2.9	4.45
425	3.2	4.37
430	3.7	4.43
430	2.8	
435	3.2	4.65
440	3.2	4.77
445	3.6	4.85
450	3.8	5.04

Distance (meters)	ΔU/I (milli-ohms)	ρ_a (ohm-m)
450	3.4	
455	3.5	5.38
460	3.8	5.69
465	4.3	6.16
470	5.0	6.62
470	4.2	
475	5.1	7.15
480	5.0	7.28
485	5.5	7.18
490	6.3	7.06
490	4.1	
495	4.3	7.12
500	4.7	7.12
505	5.2	7.25
510	5.7	7.56
510	5.3	
515	5.1	7.84
520	5.3	7.91
525	5.6	7.73
530	6.0	7.67
530	4.9	
535	4.9	7.57
540	4.9	7.37
545	5.0	7.01
550	5.3	6.70
550	4.6	
555	4.3	6.52
560	3.9	6.34
565	4.3	7.14
570	4.4	8.13
570	4.5	
575	7.5	9.31
580	7.5	10.6
585	7.7	10.4
590	9.2	9.35
590	7.5	
595	3.9	8.29
600	4.1	7.34
605	4.1	6.33
610	4.6	6.80

Schlumberger Resistivity Sounding Data
by Condrill AB Company

Resistivity Profile # RP-1
(continued)

Distance (meters)	ΔU/I (milli-ohms)	ρ_a (ohm-m)
610	4.7	
615	5.1	7.29
620	5.4	7.91
625	5.7	8.09
630	5.9	8.05
630	6.3	
635	5.2	8.18
640	5.0	8.30
645	5.8	8.40
650	6.1	8.52
650	6.1	
655	6.4	8.58
660	5.6	8.13
665	5.2	8.23
670	4.3	8.44
670	4.4	
675	6.4	8.94
680	7.1	10.1
685	7.2	10.4
890	7.8	10.1
690	9.8	
695	5.4	9.67
700	5.4	9.30
705	5.8	8.37
710	6.5	8.46
710	5.5	
715	5.8	8.55
720	5.7	8.51
725	5.7	8.26
730	5.7	7.85
730	5.6	
735	5.2	7.73
740	4.5	7.68
745	5.3	7.32
750	5.6	7.23
750	5.5	
755	4.5	7.23
760	4.9	6.90
765	4.5	6.30
770	4.4	5.86
770	4.1	
775	3.6	5.33
780	3.1	5.41
785	3.2	5.86
790	4.2	6.45
790	5.3	
795	5.7	7.26
800	5.5	7.79
805	5.7	
810	4.9	

Schlumberger Resistivity Sounding Data
by Condrill AB Company

Resistivity Profile # RP-2

Distance (meters)	ΔU/I (milli-ohms)	ρ_a (ohm-m)
0	1.50	
5	1.72	
10	1.48	2.61
10	1.66	
15	1.93	2.62
20	1.66	2.56
25	1.54	2.53
30	1.57	2.42
30	1.49	
35	1.55	2.38
40	1.53	2.38
45	1.54	2.36
50	1.56	2.28
50	1.37	
55	1.31	2.27
60	1.49	2.32
65	1.70	2.39
70	1.98	2.55
70	1.44	
75	1.82	2.61
80	1.67	2.63
85	1.78	2.58
90	1.45	2.42
90	1.64	
95	1.31	2.30
100	1.26	2.13
105	1.26	2.12
110	1.34	2.19

Distance (meters)	ΔU/I (milli-ohms)	ρ_a (ohm-m)
110	1.67	
115	1.54	2.31
120	1.63	2.41
125	1.59	2.45
130	1.54	2.51
130	1.76	
135	1.73	2.51
140	1.63	2.56
145	1.75	2.61
150	1.74	2.62
150	1.84	
155	1.76	2.71
160	1.94	2.68
165	' / .	Asph. Rd.
170	1.58	2.59
170	1.70	
175	1.51	2.42
180	1.38	2.23
185	' / .	Asph. Rd.
190	1.32	2.13
190	1.10	
195	1.58	
200	1.18	

Schlumberger Resistivity Sounding Data
by Condrill AB Company

Resistivity Profile # 3

Distance (meters)	ΔU/I (milli-ohms)	ρ_a (ohm-m)
0	5.3	
5	4.2	
10	3.3	6.7
15	4.0	6.6
20	5.0	6.8
20	4.7	
25	4.9	7.1
30	4.9	7.4
35	4.1	7.3
40	5.1	7.6
40	4.9	
45	4.7	7.6
50	5.6	8.0
55	5.0	7.8
60	6.0	7.9
60	5.1	
65	4.3	7.8
70	4.9	7.9
75	5.3	7.7
80	5.8	7.7
80	5.0	
85	4.7	7.6
90	4.4	7.4
95	4.6	7.1
100	4.8	7.2

Distance (meters)	ΔU/I (milli-ohms)	ρ_a (ohm-m)
100	4.6	
105	4.5	7.3
110	4.9	7.8
115	4.9	8.1
120	6.4	8.6
120	5.7	
125	5.8	8.9
130	5.9	9.4
135	6.1	9.2
140	6.9	9.0
140	6.1	
145	5.3	8.8
150	5.0	8.6
155	5.3	
160	5.5	

APPENDIX 2

Digitized Well Log Data and Well Log Record

DIGITIZED WELL LOG DATA

CORE WELL CW 1

DEPTH INT. (m)	S P (mV)	L N R (Ohm-m)	S N R (Ohm-m)	N D (CPS)	G R (CPS)
34-35	+ 4.0	13.0	4.0	86.0	30.0
35-36	+ 4.0	10.0	5.0	81.0	18.0
36-37	+ 4.0	8.0	8.0	94.0	17.5
37-38	+ 5.0	8.0	7.0	187.0	16.5
38-39	+ 4.0	10.0	7.5	170.0	12.5
39-40	+ 3.0	9.0	7.5	175.0	8.5
40-41	+ 1.0	9.0	7.5	205.0	9.5
41-42	0.5	10.5	10.0	163.0	12.5
42-43	+ 2.0	8.5	9.0	193.0	16.0
43-44	+ 2.0	9.0	7.0	200.0	17.5
44-45	+ 2.0	9.0	7.0	145.0	20.0
45-46	+ 2.0	8.0	6.0	163.0	18.5
46-47	+ 2.0	7.5	5.5	231.0	15.0
47-48	+ 2.0	7.5	5.5	165.0	11.5
48-49	+ 2.0	7.5	6.0	175.0	16.0
49-50	+ 1.0	7.0	6.0	170.0	14.0
50-51	+ 1.0	7.0	6.0	170.0	12.5
51-52	+ 1.0	6.5	6.0	190.0	13.5
52-53	0.5	6.5	6.0	175.0	11.5
53-54	- 1.0	7.0	6.0	188.0	12.5
54-55	- 2.0	7.0	5.5	200.0	12.5
55-56	- 2.0	7.0	5.5	180.0	12.5
56-57	- 2.0	7.5	5.5	185.0	11.5
57-58	- 2.0	6.5	5.5	162.0	8.5
58-59	- 3.0	6.5	5.5	162.0	12.5
59-60	- 3.0	6.5	5.5	190.0	9.5
60-61	- 3.0	6.5	5.5	175.0	8.5
61-62	- 4.0	6.5	5.0	170.0	8.5
62-63	- 5.0	6.5	4.5	177.0	6.5
63-64	- 7.0	5.5	4.5	164.0	6.5
64-65	- 7.0	6.0	4.5	165.0	7.5
65-66	- 7.0	6.0	5.0	165.0	8.5
66-67	- 7.5	6.0	5.0	162.0	7.0
67-68	- 8.5	6.0	5.0	177.0	6.5
68-69	- 9.0	6.0	5.5	162.0	6.5
69-70	- 10.0	6.0	5.5	163.0	7.5
70-71	- 12.0	6.0	5.5	170.0	8.5
71-72	- 12.0	6.0	5.5	180.0	12.5
72-73	- 13.0	6.5	5.5	200.0	12.5
73-74	- 14.0	6.5	5.5	218.0	7.5
74-75	- 16.0	6.5	5.5	216.0	5.5
75-76	- 17.0	7.0	7.0	182.0	7.0
76-77	- 19.0	5.5	7.5	200.0	7.0
77-78	- 20.0	6.5	5.0	230.0	8.5
78-79	- 22.0	6.5	4.5	190.0	9.5
79-80	- 23.0	6.5	4.5	175.0	8.0
80-81	- 25.0	6.5	6.0	182.0	7.0
81-82	- 27.0	6.5	7.0	186.0	9.0
82-83	- 27.0	6.5	8.0	211.0	11.5
83-84	- 29.0	7.0	8.0	220.0	12.5
84-85	- 31.0	7.5	8.5	220.0	11.5
85-86	- 33.0	7.0	8.5	221.0	12.5
86-87	- 35.0	7.5	8.0	250.0	11.0

WELL (CW1) (continued)

DEPTH INT. (m)	SP (mV)	L N R (Ohm-m)	S N R (Ohm-m)	ND (CPS)	GR (CPS)
87-88	- 38.0	7.0	6.5	238.0	11.5
88-89	- 41.0	7.0	7.0	200.0	11.0
89-90	- 43.0	6.0	7.5	180.0	9.0
90-91	- 47.0	7.0	7.5	266.0	9.0
91-92	- 48.0	7.0	7.0	207.0	8.0
92-93	- 50.0	6.5	6.0	235.0	6.0
93-94	- 52.5	6.0	5.5	189.0	6.5
94-95	- 54.0	5.5	5.5	208.0	7.0
95-96	- 57.0	5.5	5.5	178.0	7.0
96-97	- 58.0	5.5	5.5	175.0	8.0
97-98	- 60.0	5.0	5.5	199.0	8.5
98-99	- 65.0	5.0	5.5	186.0	6.5
99-100	- 68.0	5.5	5.5	185.0	6.0
100-101	- 72.0	5.5	6.0	192.0	7.0
101-102	- 72.5	6.5	7.0	144.0	10.0
102-103	- 73.0	7.0	7.5	186.0	12.5
103-104	- 75.0	8.0	8.0	188.0	10.0
104-105	- 76.0	8.5	7.0	206.0	12.5
105-106	- 76.0	7.0	5.5	220.0	17.0
106-107	- 76.0	5.0	4.5	187.0	13.5
107-108	- 77.0	4.5	4.0	162.0	10.0
108-109	- 77.5	4.0	4.0	190.0	8.5
109-110	- 77.5	3.5	3.5	181.0	11.0
110-111	- 78.0	3.0	3.5	175.0	14.0
111-112	- 82.0	2.5	3.0	183.0	17.5
112-113	- 82.0	1.5	2.5	183.0	15.0
113-114	- 85.0	1.0	1.5	150.0	7.5
114-115	- 92.0	1.0	1.5	55.0	5.0
115-116	- 95.0	1.0	2.5	75.0	7.0
116-117	- 95.0	1.5	3.0	130.0	6.0
117-118	- 96.0	3.0	3.5	140.0	7.5
118-119	- 96.0	4.0	4.0	205.0	10.0
119-120	- 96.0	4.5	4.5	206.0	18.5
120-121	- 97.0	5.0	5.0	131.0	23.5
121-122	- 97.0	4.5	4.5	260.0	11.0
122-123	- 97.0	4.5	5.0	250.0	6.0
123-124	- 97.0	4.0	4.5	244.0	6.0
124-125	- 97.0	3.5	4.0	257.0	7.5
125-126	- 97.0	2.5	3.0	161.0	7.5
126-127	- 97.0	2.0	2.5	132.0	8.0
127-128	- 97.0	2.0	2.5	150.0	9.0
128-129	- 97.0	2.0	2.5	150.0	6.0
129-130	- 97.0	2.0	2.5	168.0	6.0
130-131	- 97.0	2.0	2.5	150.0	6.5
131-132	- 97.0	2.0	3.0	156.0	7.5
132-133	- 96.0	2.5	3.5	164.0	12.5
133-134	- 96.0	2.5	3.5	244.0	21.5
134-135	- 96.0	2.5	3.5	175.0	15.0
135-136	- 97.0	2.5	3.5	175.0	14.0
136-137	- 97.0	2.5	3.5	175.0	14.0
137-138	- 97.5	2.5	3.5	170.0	11.5
138-139	- 98.0	3.0	3.5	200.0	10.0
139-140	- 100.0	3.0	3.5	168.0	7.5
140-141	- 101.0	2.5	3.0	200.0	7.5
141-142	- 101.0	2.5	3.5	200.0	9.5
142-143	- 102.0	2.0	2.5	145.0	10.0
143-144	- 102.0	2.0	2.5	162.0	14.5
144-145	- 100.0	2.0	2.5	144.0	12.5
145-146	- 99.0	2.5	2.5	162.0	11.5
146-147	- 99.0	2.5	3.0	166.0	12.0

WELL (CW1)
(continued)

DEPTH INT. (m)	SP (mV)	L N R (Ohm-m)	S N R (Ohm-m)	ND (CPS)	GR (CPS)
147-148	- 98.0	2.5	3.5	179.0	8.0
148-149	- 98.0	2.5	3.5	182.0	8.0
149-150	- 97.5	2.7	3.0	225.0	8.0
150-151	- 97.5	2.7	3.0	190.0	8.5
151-152	- 97.0	2.5	3.0	168.0	11.0
152-153	- 97.0	2.5	3.0	139.0	13.5
153-154	- 96.5	3.5	4.0	172.0	18.0
154-155	- 96.5	3.5	5.0	228.0	25.0
155-156	- 96.0	4.0	5.5	252.0	30.0
156-157	- 96.0	4.0	5.5	218.0	32.0
157-158	- 96.0	4.5	5.5	275.0	24.0
158-159	- 96.0	4.5	6.0	232.0	21.5
159-160	- 96.0	5.5	6.5	236.0	20.0
160-161	- 96.0	6.0	7.0	275.0	25.0
161-162	- 96.0	6.0	7.0	237.0	24.0
162-163	- 96.0	6.5	7.5	265.0	18.5
163-164	- 96.0	7.0	8.0	254.0	15.5
164-165	- 97.0	7.5	8.5	258.0	17.0
165-166	- 97.0	8.0	9.0	268.0	17.0
166-167	- 97.0	9.0	12.0	239.0	14.0
167-168	- 97.5	11.0	13.0	266.0	14.5
168-169	- 97.5	13.0	13.5	283.0	13.0
169-170	- 97.5	12.0	12.0	268.0	14.5
170-171	- 97.5	11.0	9.0	245.0	10.0
171-172	- 97.5	12.0	11.0	220.0	9.0
172-173	- 97.5	11.0	12.0	212.0	11.0
173-174	- 98.0	11.0	11.0	263.0	13.0
174-175	- 98.0	11.0	8.0	305.0	15.0
175-176	- 98.0	9.0	7.0	225.0	11.5
176-177	- 98.0	8.5	7.0	208.0	12.5
177-178	- 98.0	7.0	6.0	205.0	15.5
178-179	- 98.0	6.0	5.0	225.0	12.5
179-180	- 98.0	6.0	5.0	212.0	8.5
180-181	- 98.0	6.0	5.5	192.0	10.5
181-182	- 98.0	6.5	7.5	222.0	11.0
182-183	- 98.0	7.0	8.5	225.0	10.0
183-184	- 98.0	7.5	9.5	262.0	13.0
184-185	- 98.0	7.5	7.0	259.0	11.5
185-186	- 99.0	6.5	5.0	260.0	10.5
186-187	- 99.0	5.0	4.5	206.0	13.5
187-188	-100.0	5.0	4.5	215.0	13.0
188-189	-100.0	5.5	5.5	255.0	12.5
189-190	-100.0	6.0	6.5	283.0	10.0
190-191	-102.0	6.5	7.0	238.0	15.0
191-192	-100.0	6.5	7.0	262.0	19.5
192-193	-100.0	6.5	8.0	188.0	18.0
193-194	-100.0	5.5	7.0	253.0	19.5
194-195	-100.0	4.0	5.0	278.0	13.5
195-196	-100.0	4.0	4.5	235.0	9.5
196-197	-120.0	4.0	5.0	185.0	10.0

CORE WELL CW 2

DEPTH INT. (m)	S P (mV)	L N R (Ohm-m)	S N R (Ohm-m)	N D (CPS)	G R (CPS)
30-31	- 37.0	93.0	88.0	215.0	10.5
31-32	- 39.0	88.0	89.0	215.0	11.0
32-33	- 40.0	82.0	100.0	205.0	11.5
33-34	- 43.0	78.0	110.0	200.0	11.0
34-35	- 45.0	82.0	98.0	215.0	11.5
35-36	- 46.0	84.0	100.0	237.0	12.0
36-37	- 48.0	75.0	96.0	247.0	13.0
37-38	- 50.0	72.0	85.0	262.0	12.5
38-39	- 50.0	72.0	84.0	225.0	11.0
39-40	- 52.0	65.0	84.0	210.0	11.5
40-41	- 56.0	62.0	78.0	212.0	13.0
41-42	- 60.0	56.0	65.0	217.0	15.5
42-43	- 67.0	53.0	74.0	212.0	15.0
43-44	- 74.0	48.0	67.0	215.0	12.5
44-45	- 80.0	45.0	55.0	212.0	9.5
45-46	- 88.0	42.0	43.0	215.0	9.5
46-47	- 97.0	40.0	47.0	235.0	10.0
47-48	-108.0	35.0	45.0	200.0	10.5
48-49	-114.0	32.0	27.5	217.0	13.5
49-50	-117.0	30.0	60.0	235.0	15.0
50-51	-118.0	32.0	53.0	200.0	15.5
51-52	-119.0	43.0	48.0	190.0	16.5
52-53	-120.0	40.0	47.0	225.0	15.5
53-54	-120.0	40.0	46.0	200.0	15.0
54-55	-122.0	42.0	43.0	215.0	16.0
55-56	-122.0	43.0	46.0	217.0	14.0
56-57	-120.0	41.0	47.0	200.0	13.5
57-58	-120.0	42.0	46.0	200.0	15.5
58-59	-122.0	38.0	42.0	235.0	17.0
59-60	-120.0	43.0	40.0	207.0	16.5
60-61	-120.0	37.0	42.0	215.0	16.5
61-62	-119.0	32.0	40.0	192.0	19.5
62-63	-116.0	30.0	31.0	187.0	17.0
63-64	-117.0	27.0	28.0	242.0	19.5
64-65	-116.0	23.0	25.0	212.0	17.0
65-66	-116.0	22.0	24.0	200.0	14.5
66-67	-116.0	23.0	23.0	190.0	15.0
67-68	-115.0	24.0	23.0	197.0	15.5
68-69	-115.0	24.0	23.0	192.0	14.5
69-70	-115.0	21.0	24.0	200.0	13.0
70-71	-114.0	22.0	23.0	210.0	13.5
71-72	-114.0	22.0	22.5	187.0	14.5
72-73	-113.0	25.0	24.0	165.0	12.5
73-74	-113.0	23.0	25.0	175.0	12.0
74-75	-113.0	21.0	25.0	162.0	10.5
75-76	-113.0	19.0	23.0	165.0	10.0
76-77	-113.0	19.0	23.0	187.0	11.0
77-78	-112.0	17.0	22.0	170.0	11.5
78-79	-112.0	18.0	19.0	162.0	11.0
79-80	-112.0	18.0	17.5	150.0	10.0
80-81	-112.0	15.0	17.0	162.0	8.5
81-82	-112.0	15.0	17.0	167.0	8.0

WELL (CW2)
(continued)

DEPTH INT. (m)	SP (mV)	LNR (Ohm-m)	SNR (Ohm-m)	ND (CPS)	GR (CPS)
82-83	-110.0	14.0	16.5	162.0	10.0
83-84	-110.0	15.0	17.0	175.0	10.0
84-85	-111.0	16.0	17.5	162.0	8.0
85-86	-111.0	18.0	17.5	169.0	7.0
86-87	-111.0	19.0	18.0	152.0	8.0
87-88	-110.0	20.0	19.0	165.0	10.5
88-89	-110.0	20.0	19.0	167.0	14.0
89-90	-110.0	24.0	20.0	185.0	14.0
90-91	-110.0	21.0	18.0	205.0	14.0
91-92	-110.0	18.0	18.0	210.0	12.5
92-93	-112.0	13.0	17.0	200.0	11.5
93-94	-109.0	13.0	17.0	232.0	8.0
94-95	-109.0	14.0	17.0	212.0	8.0
95-96	-109.0	17.0	17.5	180.0	9.5
96-97	-108.0	22.0	17.5	170.0	9.5
97-98	-107.0	22.0	16.0	175.0	11.0
98-99	-107.0	17.0	18.0	185.0	11.0
99-100	-107.0	18.0	18.0	215.0	13.0
100-101	-107.0	19.0	17.0	232.0	15.0
101-102	-107.0	15.0	15.5	232.0	13.0
102-103	-107.0	13.0	15.0	187.0	13.0
103-104	-107.0	15.0	15.0	207.0	15.0
104-105	-107.0	15.0	14.5	220.0	13.0
105-106	-106.0	14.0	15.0	165.0	11.0
106-107	-106.0	13.0	14.5	185.0	11.0
107-108	-106.0	13.0	14.5	205.0	11.5
108-109	-106.0	12.5	13.0	187.0	10.0
109-110	-106.0	13.0	13.0	190.0	8.0
110-111	-106.0	13.0	13.0	185.0	8.5
111-112	-105.0	13.0	12.0	175.0	7.5
112-113	-105.0	13.0	12.0	160.0	8.0
113-114	-105.0	13.0	12.0	190.0	10.0
114-115	-105.0	13.0	12.5	175.0	11.0
115-116	-105.0	14.0	12.5	165.0	7.0
116-117	-105.0	15.0	16.0	172.0	7.0
117-118	-104.0	17.0	25.0	165.0	8.5
118-119	-104.0	17.5	28.0	160.0	10.0
119-120	-104.0	22.0	25.0	165.0	13.5

WELL (CW2)
(continued)

DEPTH INT. (m)	SP (mV)	LNR (Ohm-m)	SNR (Ohm-m)	ND (CPS)	GR (CPS)
120-121	-104.0	20.0	19.0	250.0	16.0
121-122	-104.0	21.0	17.5	212.0	15.0
122-123	-104.0	17.5	17.5	220.0	13.5
123-124	-103.0	17.5	22.5	185.0	14.5
124-125	-103.0	17.5	18.0	237.0	15.5
125-126	-102.0	17.5	17.5	190.0	11.5
126-127	-102.0	14.0	19.0	200.0	12.0
127-128	-101.0	16.0	18.5	205.0	13.5
128-129	-100.0	16.0	17.5	202.0	15.5
129-130	-100.0	15.0	15.5	195.0	21.0
130-131	-100.0	17.0	15.5	187.0	21.0
131-132	-102.0	17.0	15.0	200.0	13.5
132-133	-101.0	17.5	18.0	195.0	11.5
133-134	-102.0	17.5	22.5	195.0	10.5
134-135	-100.0	18.0	20.0	185.0	9.5
135-136	-102.0	19.0	20.0	190.0	7.5
136-137	-100.0	18.5	19.5	205.0	5.5
137-138	- 99.0	25.0	19.5	200.0	6.5
138-139	- 99.0	22.0	18.5	225.0	6.0
139-140	-100.0	18.0	18.0	200.0	5.0
140-141	-100.0	17.0	18.0	260.0	5.5
141-142	- 99.0	23.0	17.5	237.0	6.0
142-143	- 99.0	18.0	15.5	180.0	6.0
143-144	-100.0	12.5	15.5	210.0	6.5
144-145	-100.0	13.0	13.0	235.0	8.5
145-146	- 99.0	12.5	12.5	195.0	7.0
146-147	- 98.0	11.5	11.5	150.0	5.5

CORE WELL CW 4/1

DEPTH INT. (m)		S P (mV)	L N R (Ohm-m)	S N R (Ohm-m)	N D (CPS)	G R (CPS)
5-6	+	7.5	34.0	42.5	212.0	22.5
6-7	+	7.	38.	42.	235.	32.
7-8	+	7.	33.	27.	275.	32.
8-9	+	7.	27.	17.	242.	38.
9-10	+	7.	24.	17.	195.	35.
10-11	+	7.5	22.	15.	175.	17.5
11-12	+	8.	21.	15.	212.	15.5
12-13	+	8.	21.	20.	265.	17.
13-14	+	8.	19.5	23.	212.	17.
14-15	+	8.	22.	29.	225.	15.5
15-16	+	8.	22.	28.	259.	38.
16-17	+	8.	26.	39.	255.	32.5
17-18	+	8.	24.	22.	225.	26.5
18-19	+	8.	23.	18.	225.	27.5
19-20	+	8.	19.	14.	212.	22.
20-21	+	8.	17.	14.	212.	17.5
21-22	+	8.	15.	12.	200.	16.5
22-23	+	8.	14.	13.	200.	13.5
23-24	+	8.	14.	15.	195.	13.
24-25	+	7.5	13.	9.5	200.	13.
25-26	+	8.	14.	21.	195.	14.
26-27	+	8.	13.	17.	225.	12.5
27-28	+	8.	11.	13.	232.	14.
28-29	+	10.	11.	10.	195.	12.
29-30	+	10.	11.	18.	200.	15.
30-31	+	9.	11.	16.	242.	17.5
31-32	+	9.	11.	13.	275.	17.5
32-33	+	8.	13.	14.	265.	16.
33-34	+	8.	15.	16.	192.	13.
34-35	+	7.	9.	17.	242.	12.
35-36	+	7.5	9.	18.	259.	11.
36-37	+	6.	9.	14.	262.	9.
37-38	+	6.	7.	8.	257.	7.5
38-39	+	6.	6.	5.	235.	7.
39-40	+	6.	6.	5.	215.	7.
40-41	+	6.	5.	5.	215.	10.
41-42	+	6.	5.	5.	210.	10.
42-43	+	6.	5.	5.	225.	9.
43-44	+	6.	5.	5.	225.	7.
44-45	+	6.	5.	5.	175.	8.
45-46	+	6.	5.	5.	170.	7.5
46-47	+	6.	5.	5.	182.	9.
47-48	+	6.	5.	6.	200.	9.
48-49	+	1.	5.	6.	200.	12.

CORE WELL CW 4/2

DEPTH INT. (m)	S P (mV)	L N R (Ohm-m)	S N R (Ohm-m)	N D (CPS)	G R (CPS)
4-5	- 3.0	21.0	23.0	200.0	20.0
5-6	- 2.5	19.0	22.5	200.0	17.5
6-7	- 2.5	21.0	34.0	215.0	25.0
7-8	- 2.5	23.0	25.5	210.0	37.5
8-9	- 2.5	22.0	22.0	270.0	42.5
9-10	- 2.0	19.0	18.0	230.0	30.0
10-11	- 2.0	18.0	15.5	260.0	21.0
11-12	- 2.0	14.0	13.0	235.0	16.0
12-13	- 2.5	14.0	14.0	230.0	15.0
13-14	- 2.0	12.5	17.5	205.0	15.0
14-15	0.0	11.5	15.0	205.0	20.0
15-16	- 2.0	14.5	15.0	260.0	38.0
16-17	- 2.0	12.0	23.0	212.0	25.0
17-18	- 2.0	11.0	15.0	215.0	28.0
18-19	- 1.0	12.5	11.0	300.0	27.0
19-20	- 1.0	11.0	10.5	235.0	24.0
20-21	- 1.0	10.5	12.0	212.0	13.0
21-22	- 2.0	9.5	13.0	195.0	14.5
22-23	- 2.0	10.0	10.5	210.0	14.5
23-24	- 2.0	11.0	12.5	200.0	11.5

CORE WELL CW 4/3

DEPTH INT. (m)	S P (mV)	L N R (Ohm-m)	S N R (Ohm-m)	N D (CPS)	G R (CPS)
3-4	+ 23.0	30.0	22.0	215.0	25.0
4-5	+ 23.0	31.0	21.0	185.0	20.0
5-6	+ 22.0	31.0	24.0	165.0	14.5
6-7	+ 21.0	26.0	28.0	175.0	14.5
7-8	+ 20.0	29.0	32.5	200.0	20.0
8-9	+ 21.0	30.0	27.0	215.0	33.0
9-10	+ 23.0	26.0	18.0	245.0	35.0
10-11	+ 22.0	22.0	18.0	250.0	35.0
11-12	+ 22.0	19.0	16.5	165.0	17.0
12-13	+ 20.0	18.0	13.0	200.0	13.5
13-14	+ 18.0	18.0	17.5	212.0	12.5
14-15	+ 16.0	18.0	21.0	190.0	12.0
15-16	+ 15.0	22.0	24.0	195.0	15.0
16-17	+ 13.0	27.0	33.0	210.0	24.0
17-18	+ 7.0	25.0	38.0	200.0	17.5
18-19	+ 5.0	17.0	20.0	215.0	27.5

CORE WELL CW 4/4

DEPTH INT. (m)	S P (mV)	L N R (Ohm-m)	S N R (Ohm-m)	N D (CPS)	G R (CPS)
2-3	+ 8.0	14.0	11.0	125.0	13.5
3-4	+ 8.0	14.0	12.5	170.0	14.0
4-5	+ 7.5	14.5	11.5	175.0	20.0
5-6	+ 7.0	14.5	12.0	150.0	15.0
6-7	+ 4.0	15.0	14.0	160.0	14.0
7-8	+ 2.5	16.0	15.0	180.0	13.5
8-9	+ 2.0	17.0	22.0	185.0	16.5
9-10	+ 2.0	15.0	19.5	190.0	16.0
10-11	0.0	17.0	17.5	190.0	25.0
11-12	0.0	17.0	18.0	215.0	21.0
12-13	0.6	16.5	20.0	230.0	18.5
13-14	0.0	17.0	16.0	212.0	15.5
14-15	0.0	14.0	10.0	215.0	30.0
15-16	0.0	10.0	7.0	230.0	31.0
16-17	0.0	8.0	5.0	230.0	32.0
17-18	0.0	7.0	4.5	205.0	30.0
18-19	- 1.0	6.0	4.5	185.0	17.5
19-20	0.0	6.0	4.5	175.0	11.5
20-21	0.0	6.0	7.0	175.0	12.5
21-22	- 2.0	6.0	6.5	172.0	16.5

CORE WELL CW 4/5

DEPTH INT. (m)	S P (mV)	L N R (Ohm-m)	S N R (Ohm-m)	N D (CPS)	G R (CPS)
5-6	+ 10.0	30.0	14.0	185.0	28.5
6-7	+ 9.5	26.0	13.0	185.0	12.5
7-8	+ 8.0	23.0	13.0	160.0	10.5
8-9	+ 7.0	22.0	13.0	170.0	10.0
9-10	+ 10.0	21.5	12.0	170.0	14.0
10-11	+ 9.0	21.0	13.5	180.0	15.0
11-12	+ 8.0	18.0	17.0	165.0	18.0
12-13	+ 12.0	16.5	18.0	165.0	35.0
13-14	+ 7.0	16.0	17.0	185.0	31.5
14-15	+ 8.0	14.5	16.0	240.0	37.5
15-16	+ 6.0	13.5	12.0	250.0	27.5
16-17	+ 6.0	11.5	8.5	235.0	29.5
17-18	+ 6.0	11.0	8.0	205.0	22.5
18-19	+ 5.0	10.5	15.5	205.0	14.0
19-20	+ 5.0	10.5	12.0	200.0	12.0
20-21	+ 3.0	11.0	12.5	200.0	11.5
21-22	+ 3.0	10.0	12.0	200.0	10.0
22-23	+ 4.0	11.5	11.5	205.0	11.0
23-24	+ 3.0	10.5	10.5	215.0	11.5
24-25	+ 4.0	10.0	9.5	220.0	12.0
25-26	+ 6.0	12.5	10.5	225.0	10.0

WELL LOG RECORD

Electrical Logs

1) 16-inch Short Normal Resistivity
2) 64-inch Long Normal Resistivity

Gamma Ray - Neutron Log

1) Source: Am, Be-241
2) Spacing: 13-inch

Spontaneous Potential (SP) Log

Caliper Log

Temperature Log

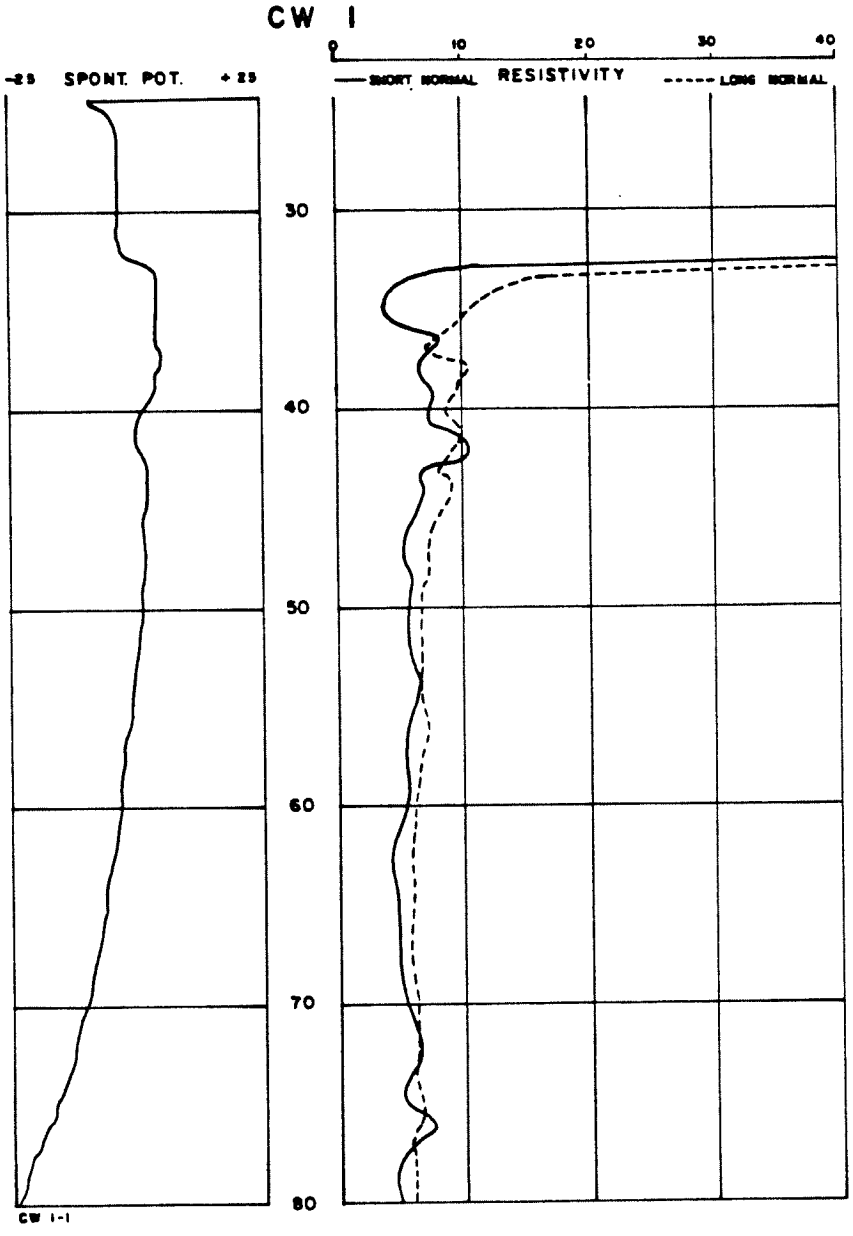
CW I
-25 SPONT. POT. +25
0 10 20 30 40
SHORT NORMAL RESISTIVITY LONG NORMAL
30
40
50
60
70
80
CW I-1

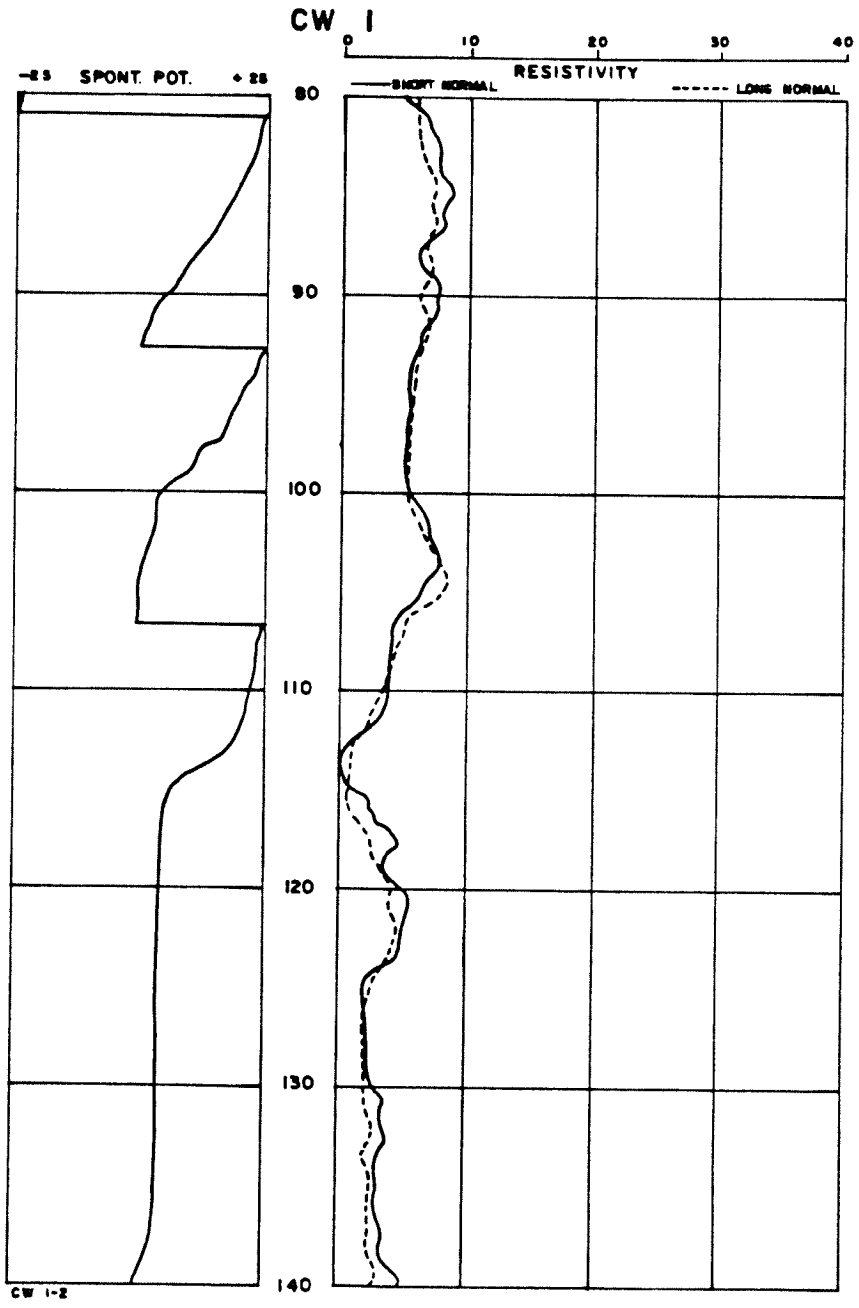
CW 1
0
10
20
30
40
RESISTIVITY
SHORT NORMAL
LONG NORMAL
-25
SPONT. POT.
+25
80
90
100
110
120
130
140
CW 1-2

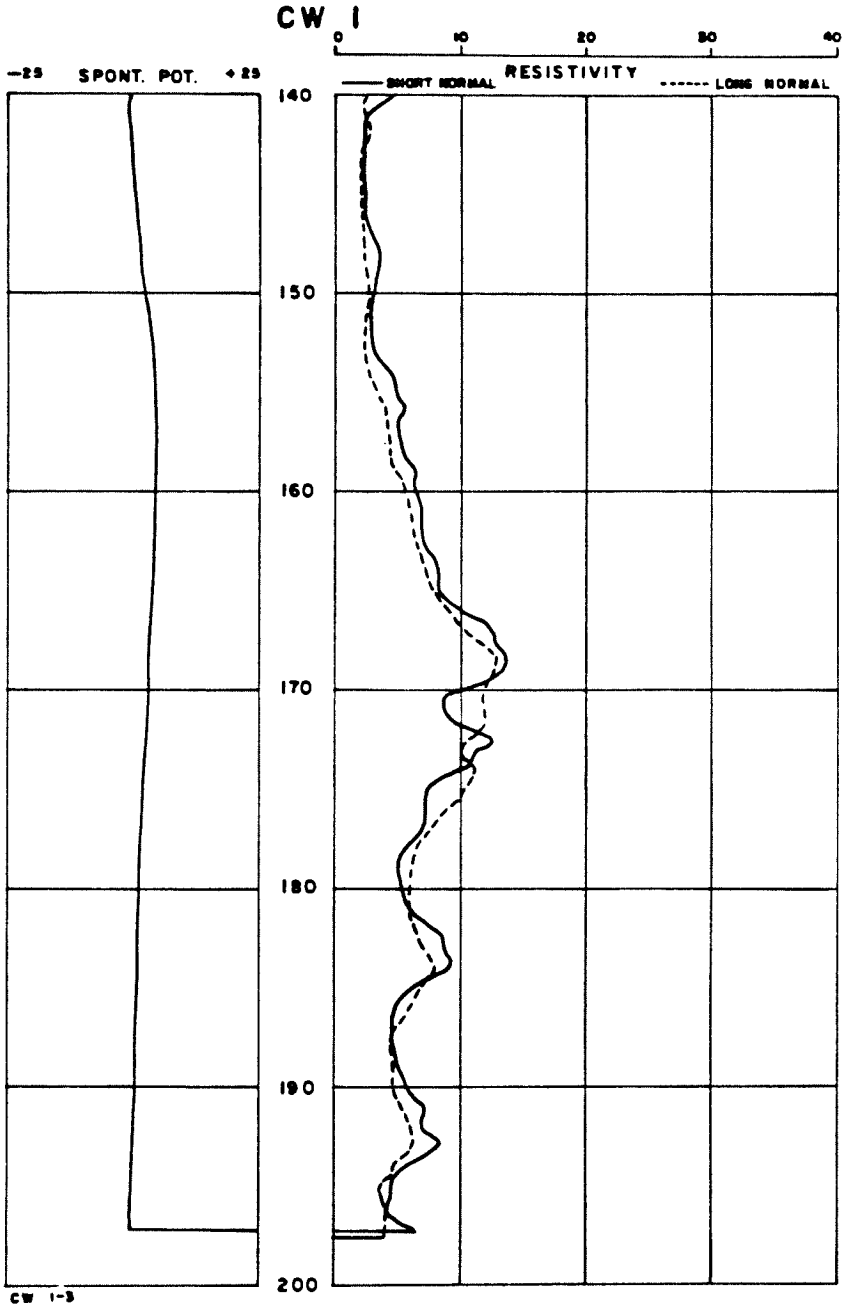
CW 1
0
10
20
30
40
-25
SPONT. POT.
+25
RESISTIVITY
SHORT NORMAL
LONG NORMAL
140
150
160
170
180
190
200
CW 1-3

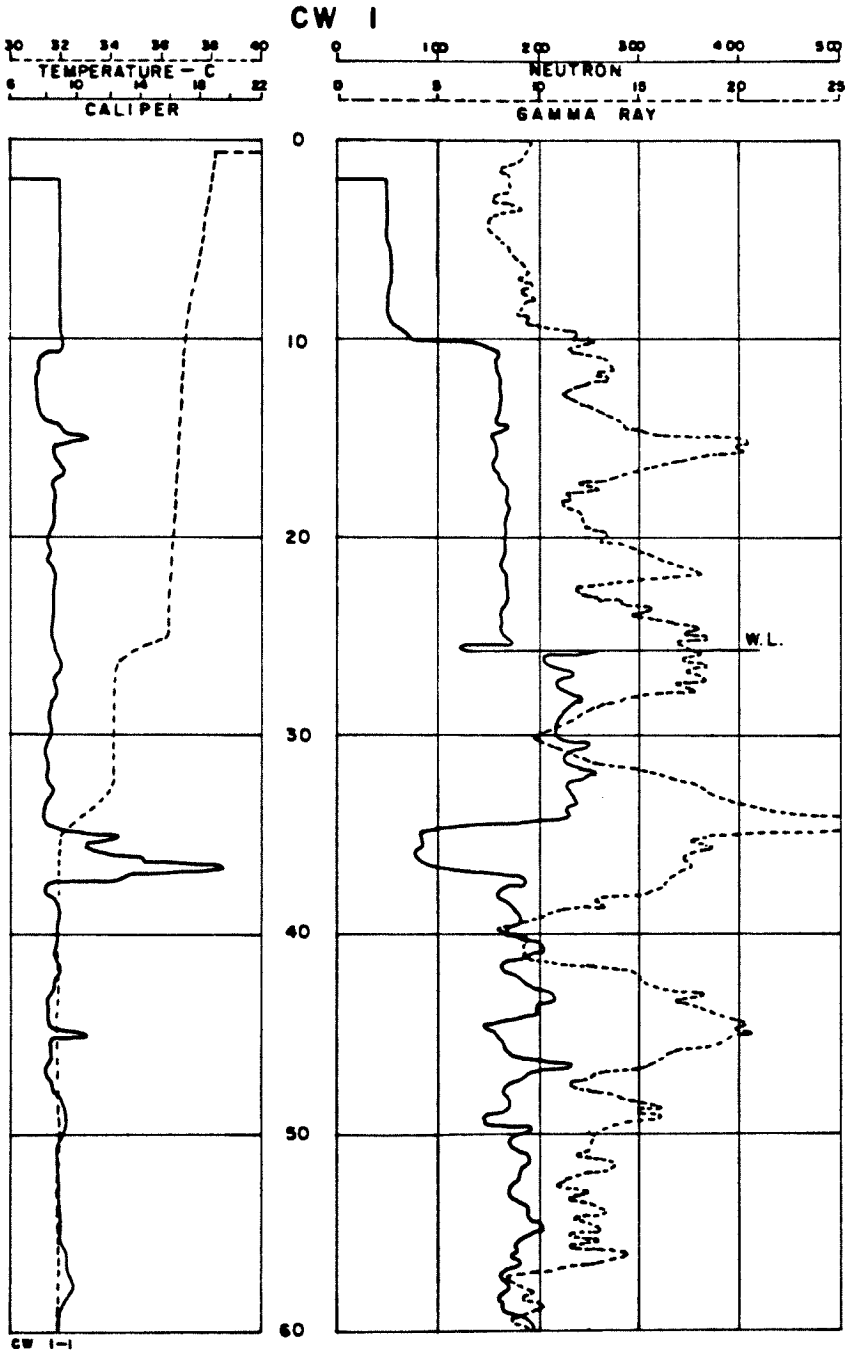
CW 1
30 32 34 36 38 40
TEMPERATURE - C
6 10 14 18 22
CALIPER
0 100 200 300 400 500
NEUTRON
0 5 10 15 20 25
GAMMA RAY
0
10
20
30
40
50
60
W.L.
CW 1-1

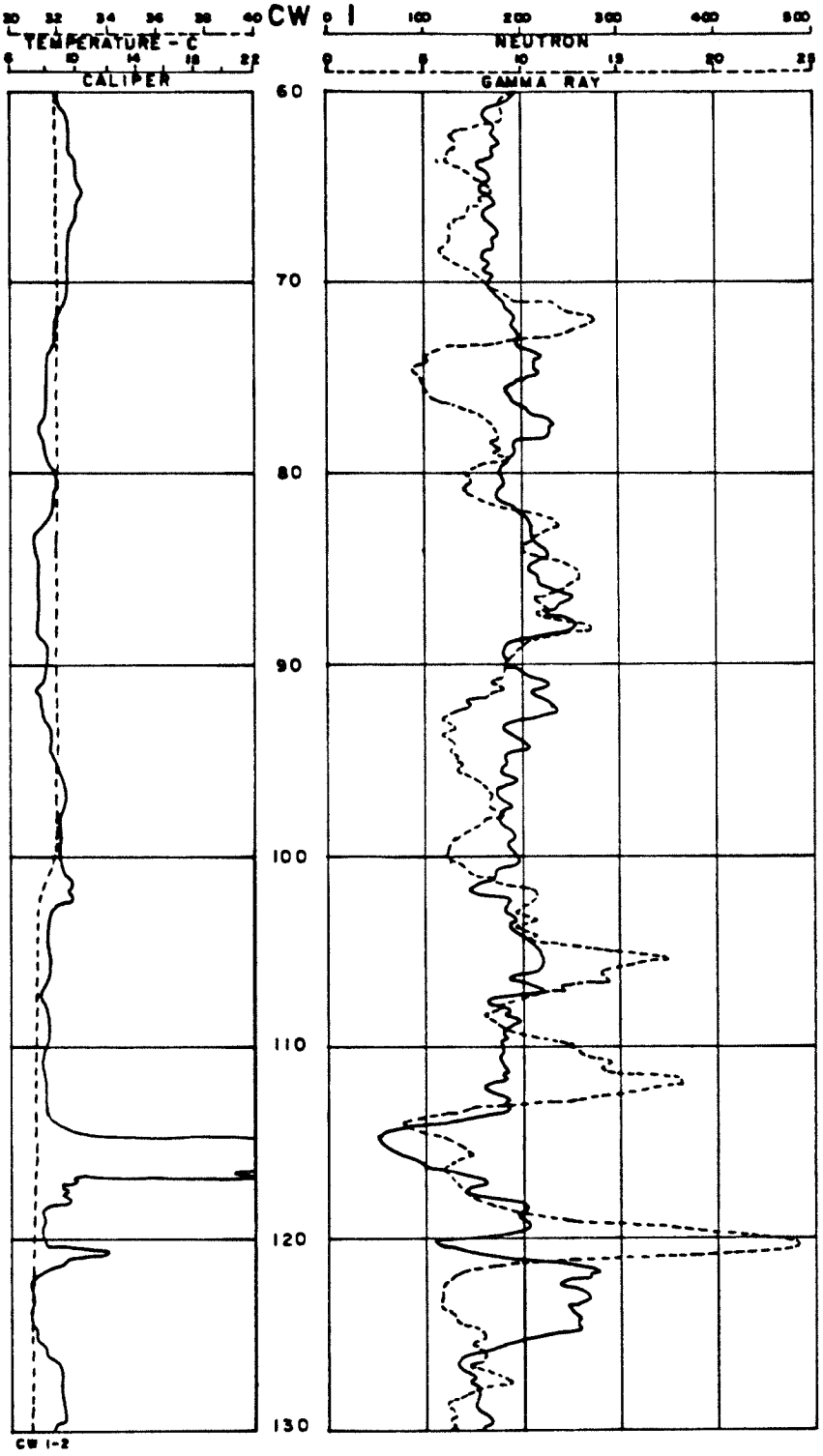
CW 1
TEMPERATURE - C
CALIPER
NEUTRON
GAMMA RAY
60
70
80
90
100
110
120
130
CW 1-2

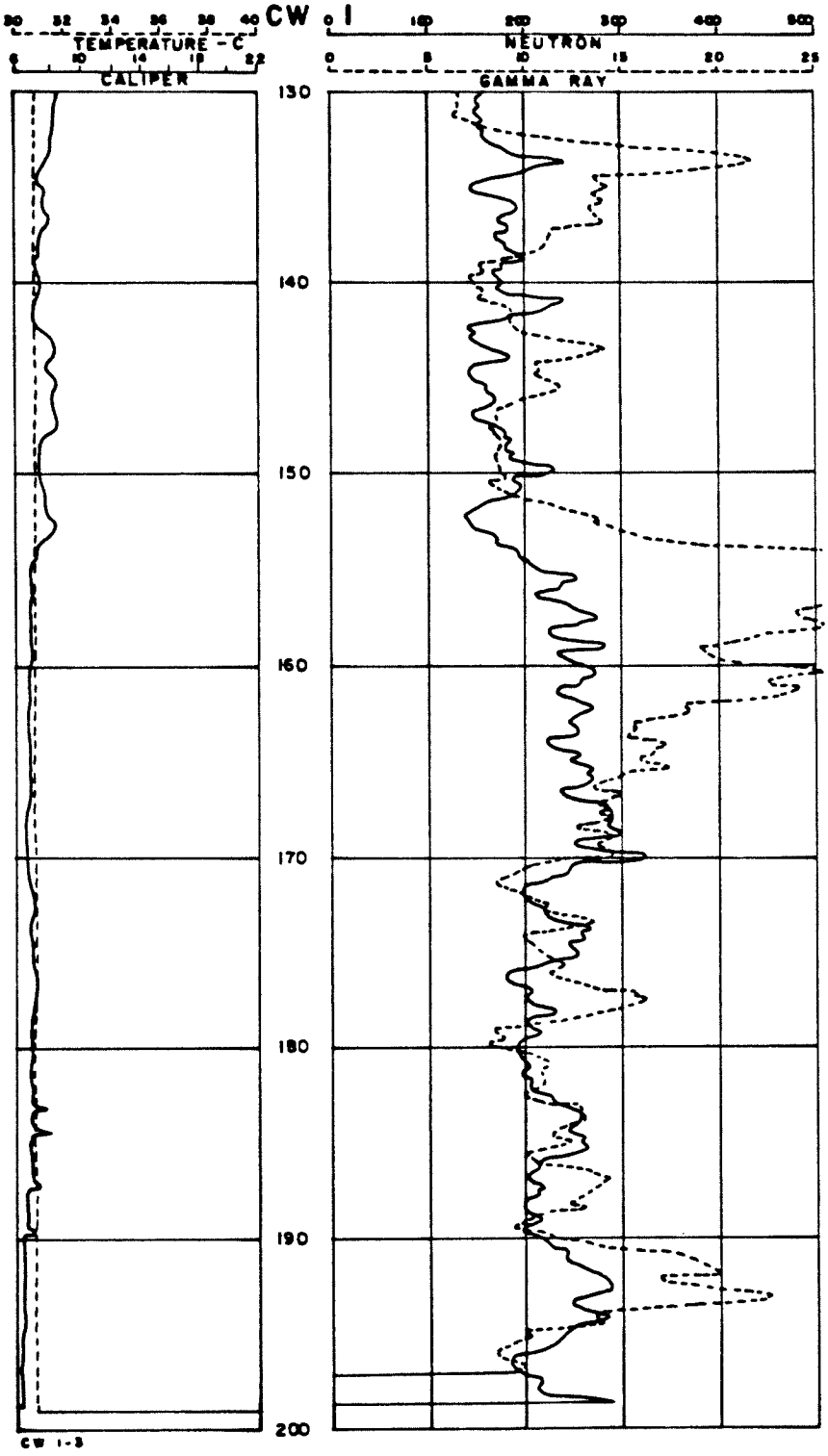
CW
TEMPERATURE - C
CALIPER
NEUTRON
GAMMA RAY
130
140
150
160
170
180
190
200
CW 1-3

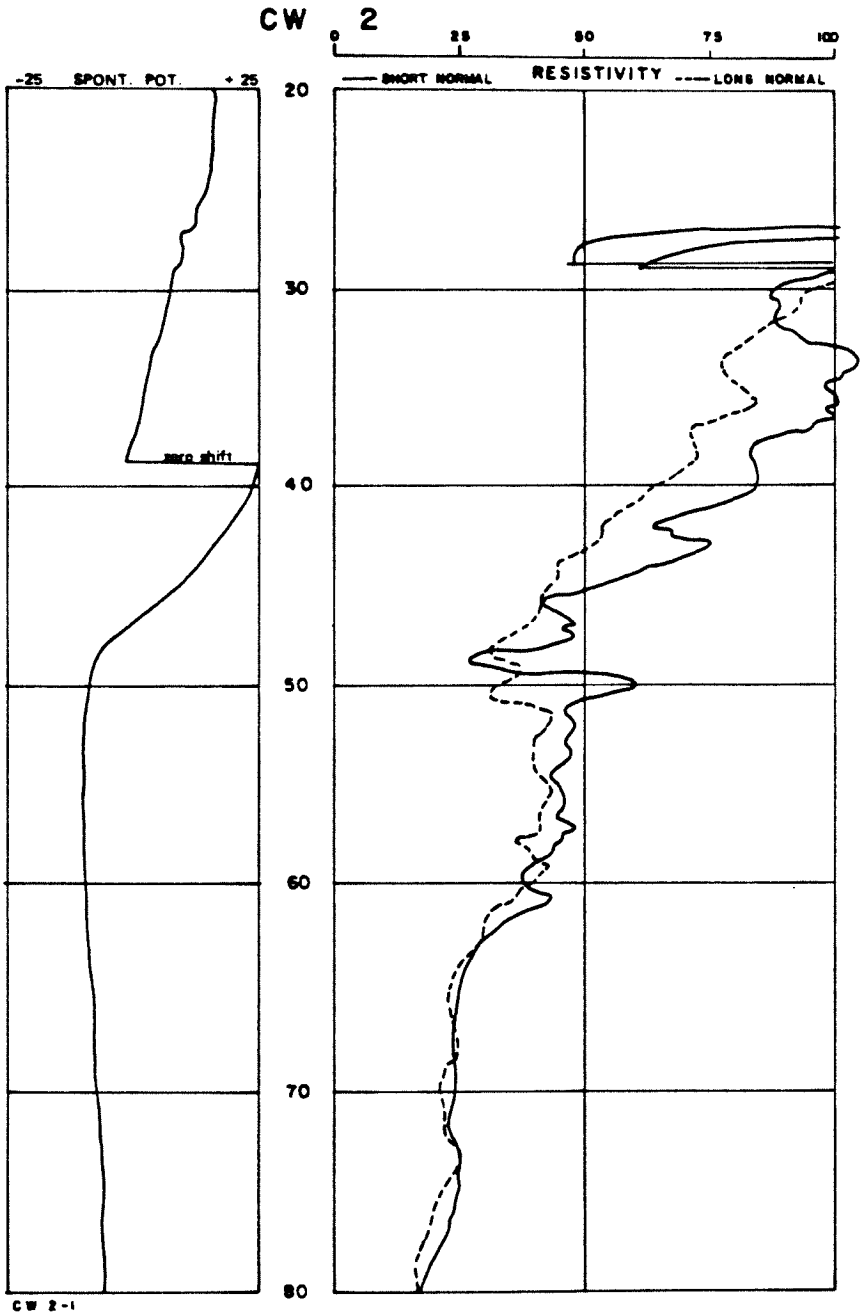
CW 2
0
25
50
75
100
-25 SPONT. POT. +25
SHORT NORMAL
RESISTIVITY
LONG NORMAL
20
30
40
50
60
70
80
zero shift
CW 2-1

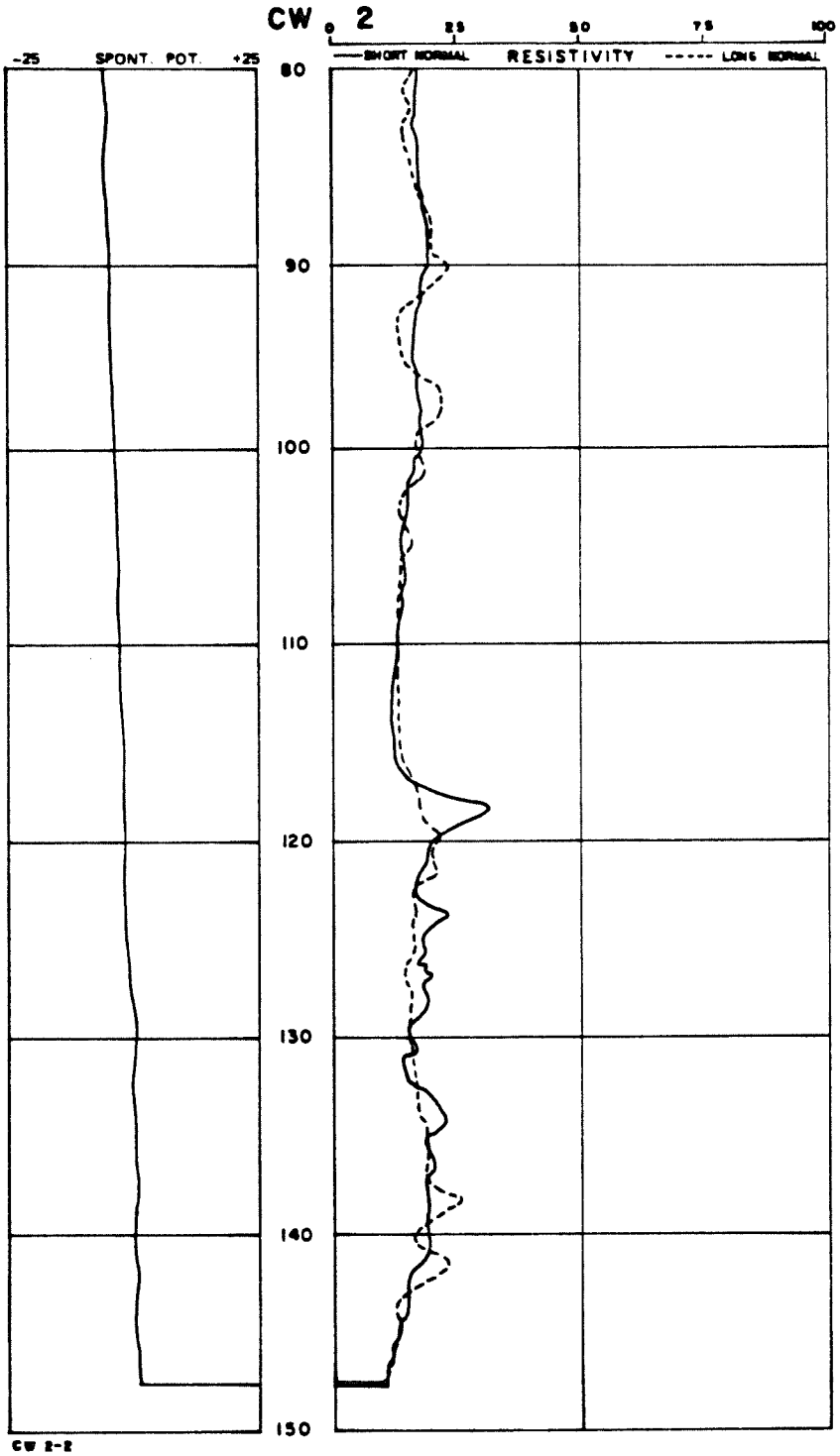
CW 2
0
25
50
75
100
SHORT NORMAL
RESISTIVITY
LONG NORMAL
-25
SPONT. POT.
+25
80
90
100
110
120
130
140
150
CW 2-2

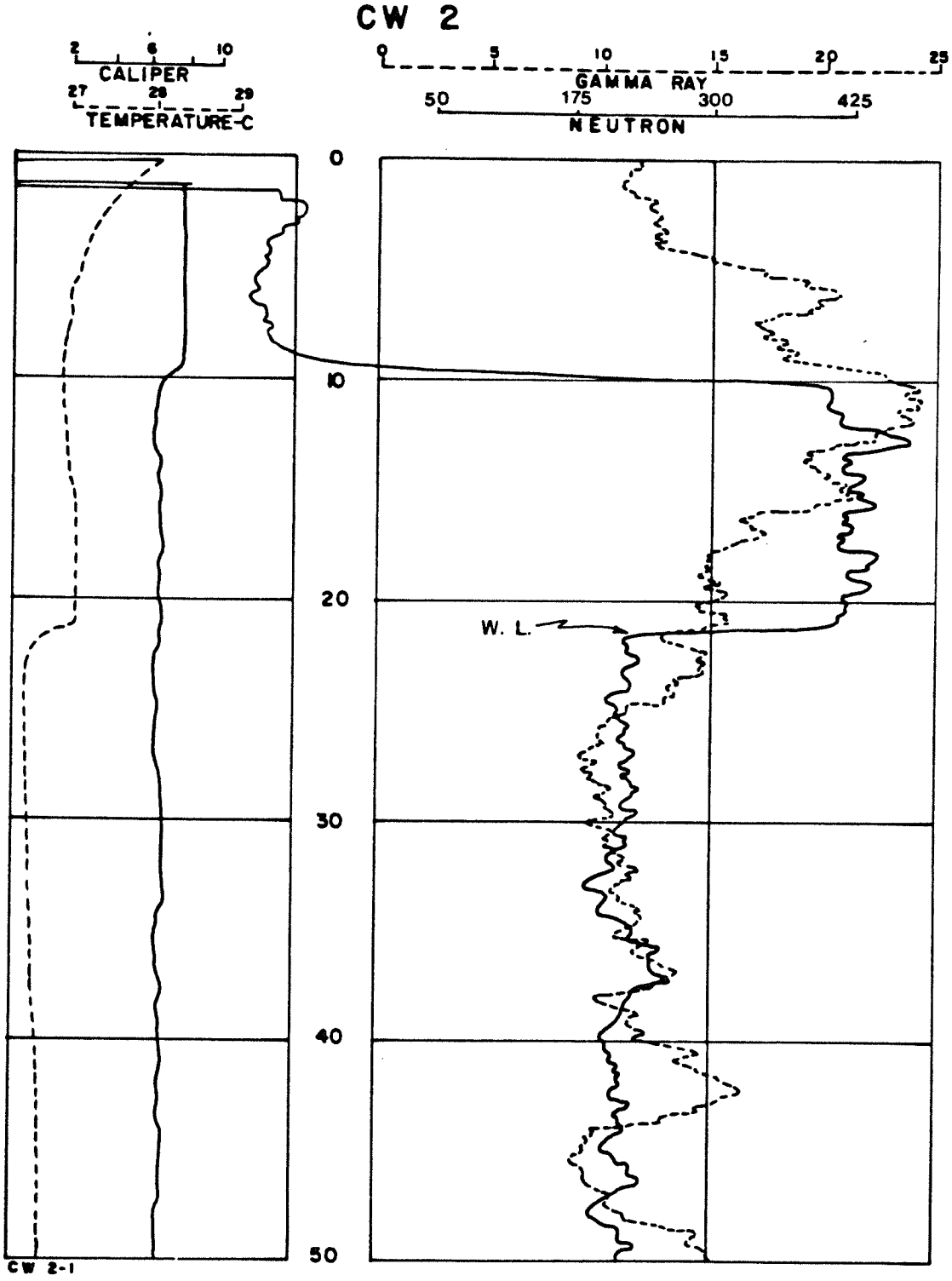
CW 2
2 6 10
CALIPER
27 28 29
TEMPERATURE-C
0 5 10 15 20 25
GAMMA RAY
50 175 300 425
NEUTRON
0
10
20
30
40
50
W. L.
CW 2-1

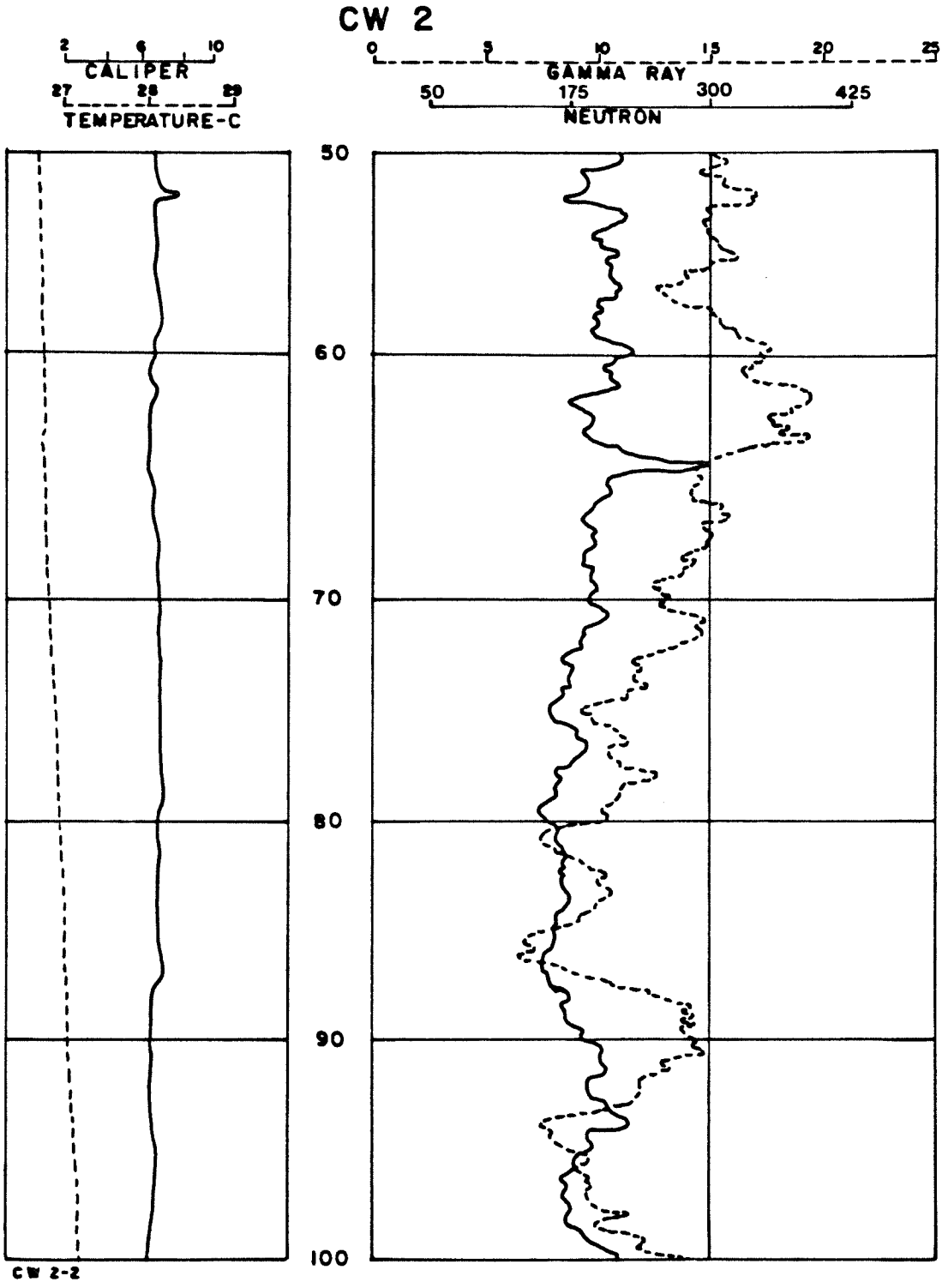
CW 2
2 6 10
CALIPER
27 28 29
TEMPERATURE-C
0 5 10 15 20 25
GAMMA RAY
50 175 300 425
NEUTRON
50
60
70
80
90
100
CW 2-2

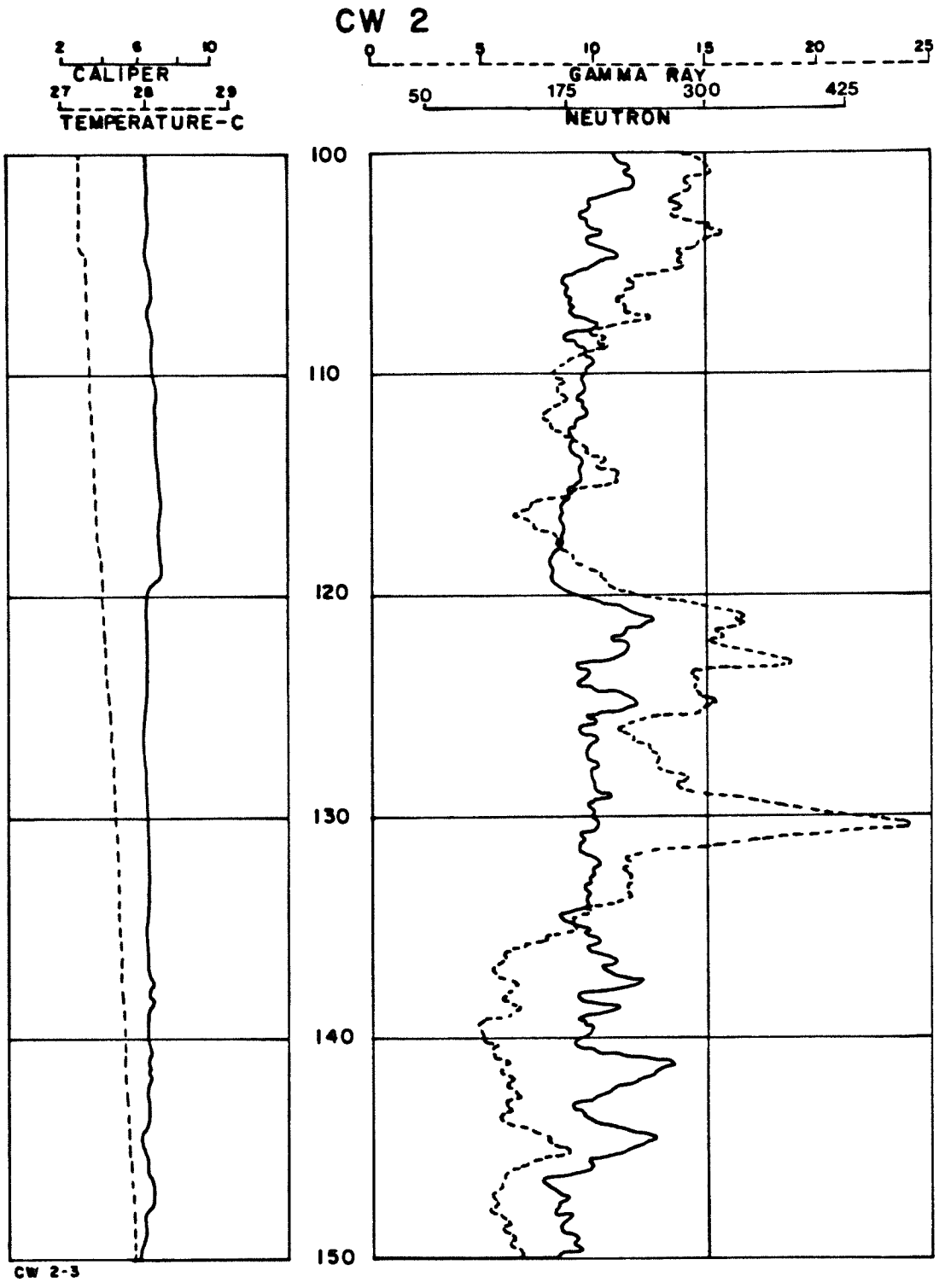
CW 2
2
6
10
CALIPER
27
28
29
TEMPERATURE-C
0
5
10
15
20
25
GAMMA RAY
50
175
300
425
NEUTRON
100
110
120
130
140
150
CW 2-3

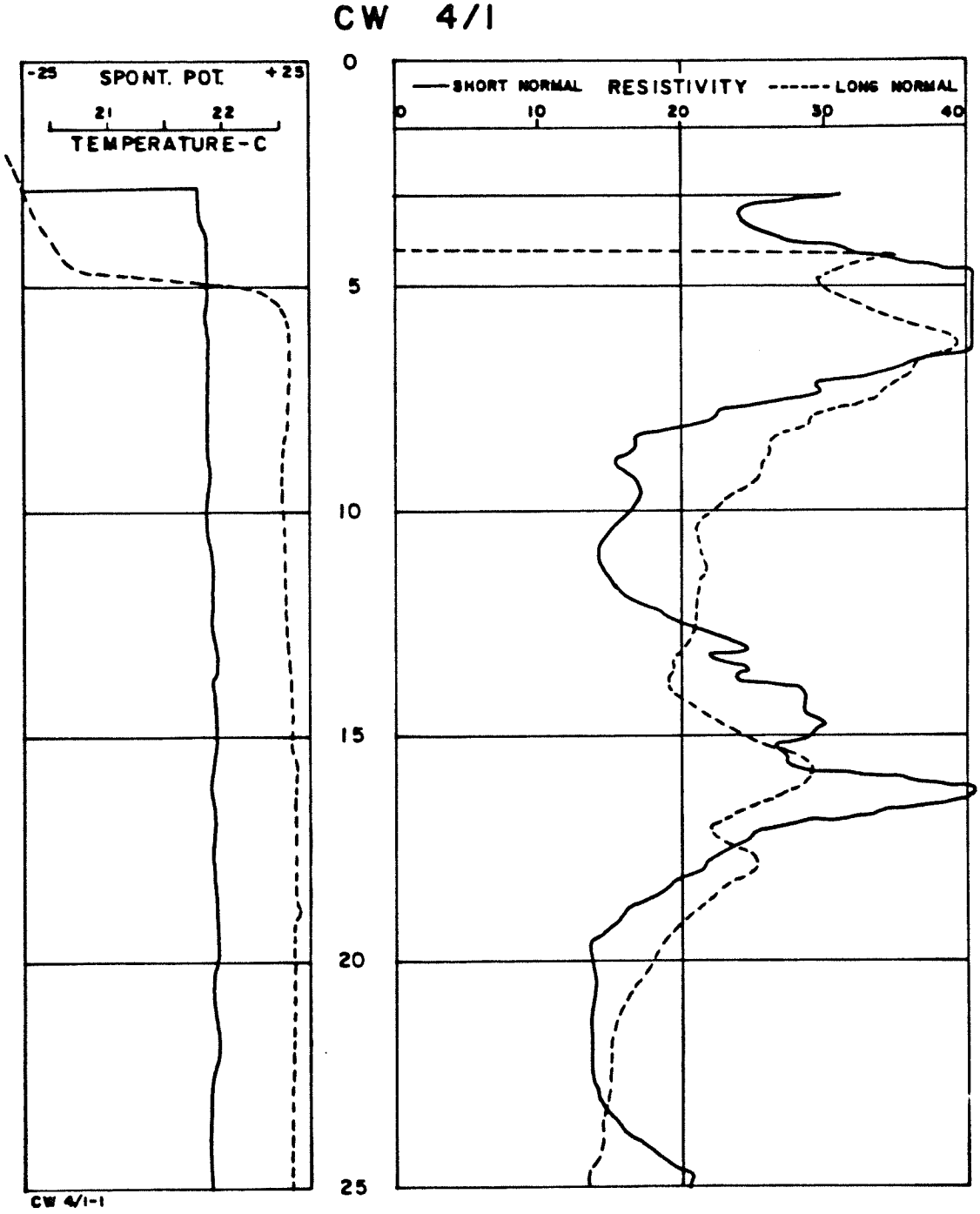
CW 4/1
-25
SPONT. POT.
+25
21
22
TEMPERATURE-C
0
5
10
15
20
25
SHORT NORMAL
RESISTIVITY
LONG NORMAL
0
10
20
30
40
CW 4/1-1

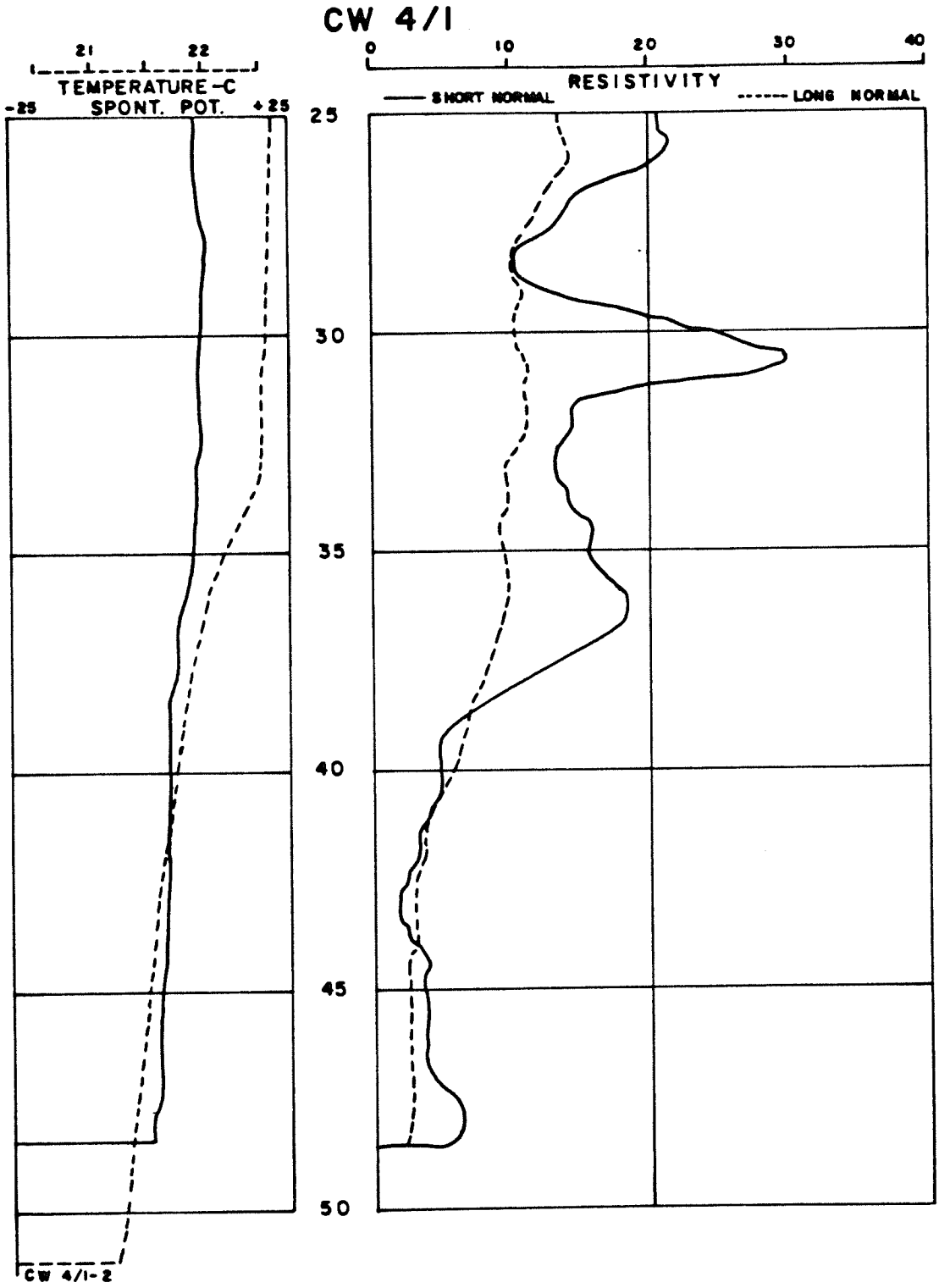
CW 4/1
21
22
TEMPERATURE-C
-25
SPONT. POT.
+25
0
10
20
30
40
RESISTIVITY
SHORT NORMAL
LONG NORMAL
25
30
35
40
45
50
CW 4/1-2

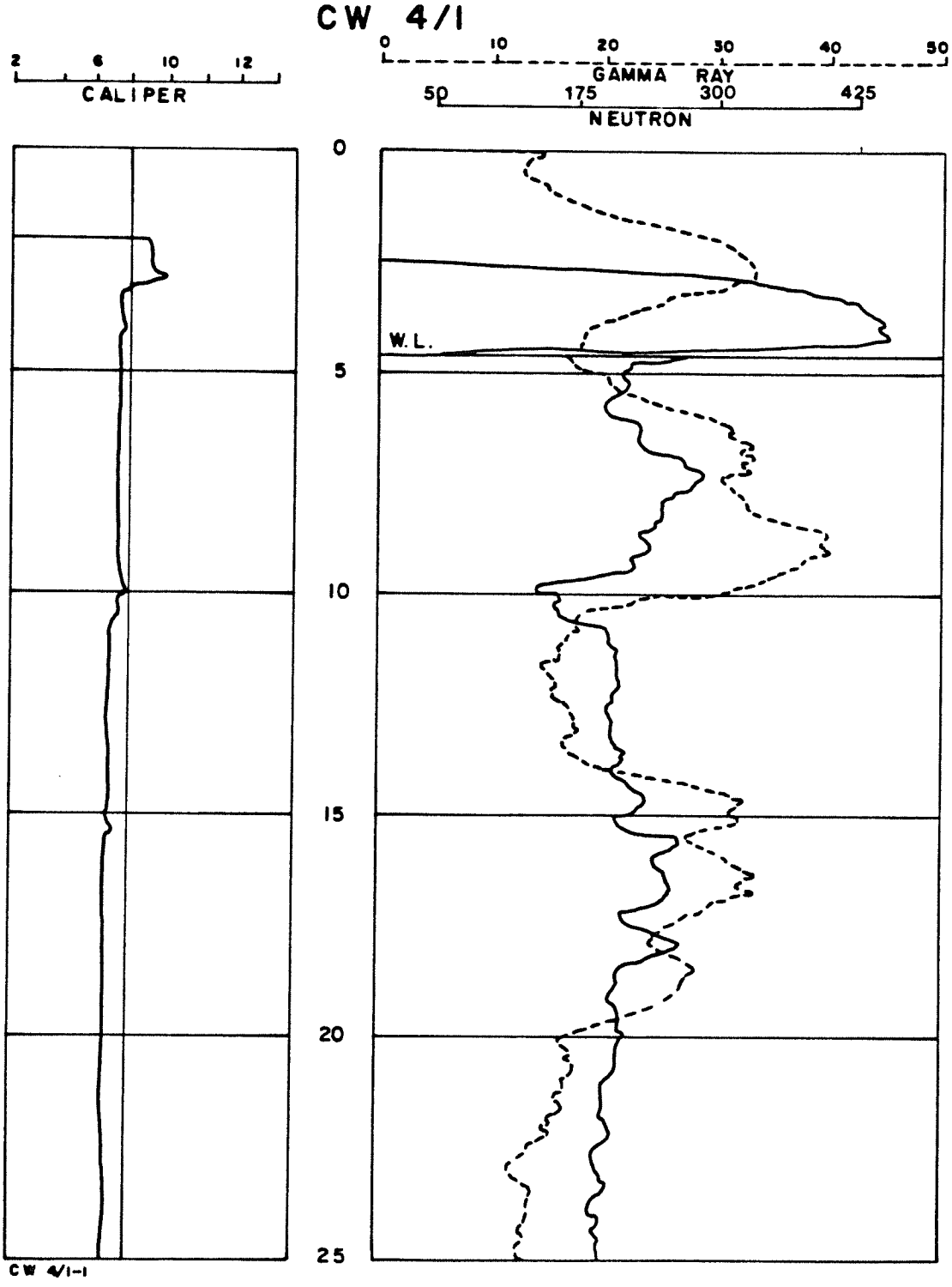
CW 4/1
2 6 10 12
CALIPER
0 10 20 30 40 50
GAMMA RAY
50 175 300 425
NEUTRON
W. L.
0
5
10
15
20
25
CW 4/1-1

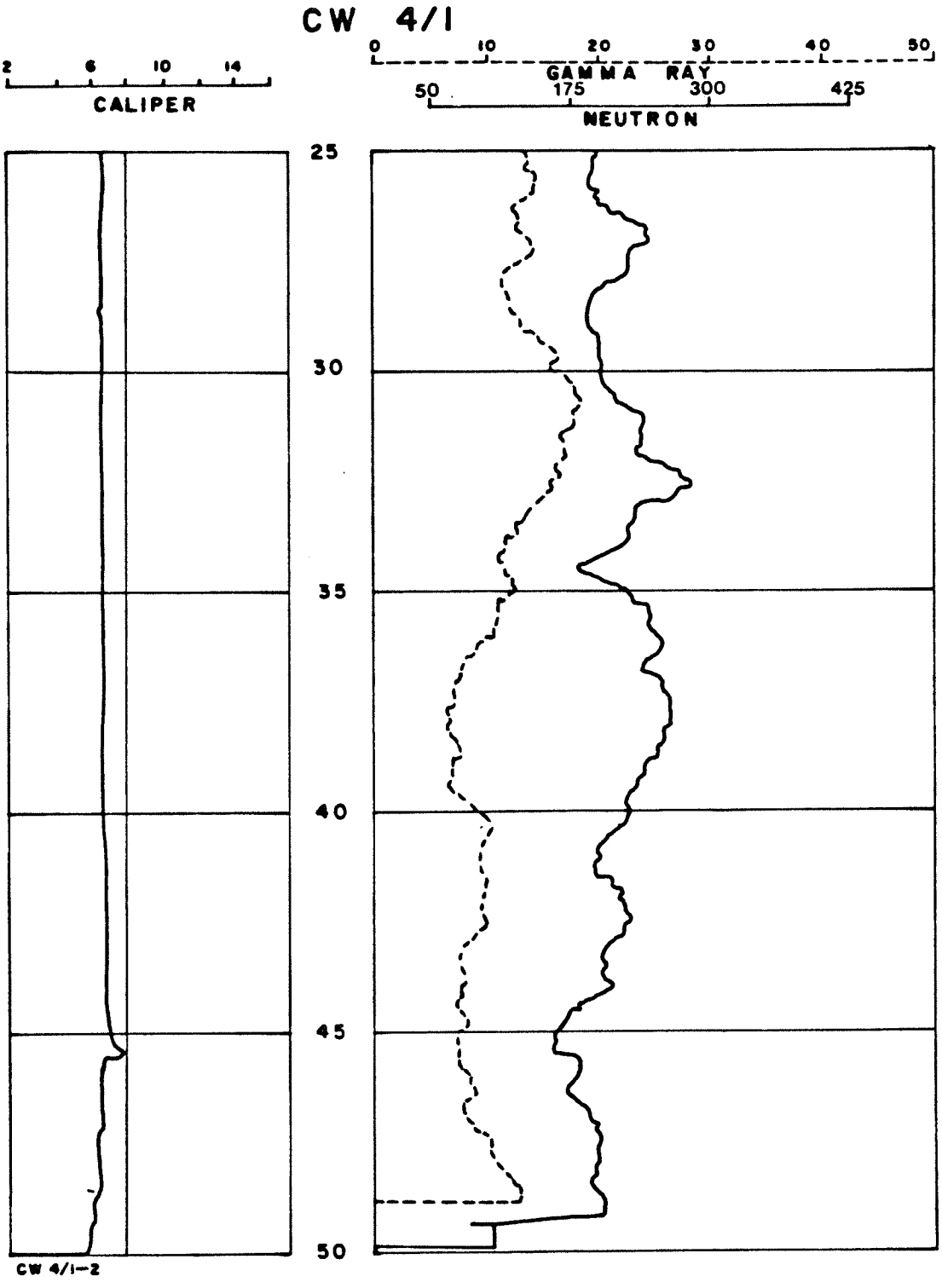
CW 4/1
2 6 10 14
CALIPER
0 10 20 30 40 50
GAMMA RAY
50 175 300 425
NEUTRON
25
30
35
40
45
50
CW 4/1-2

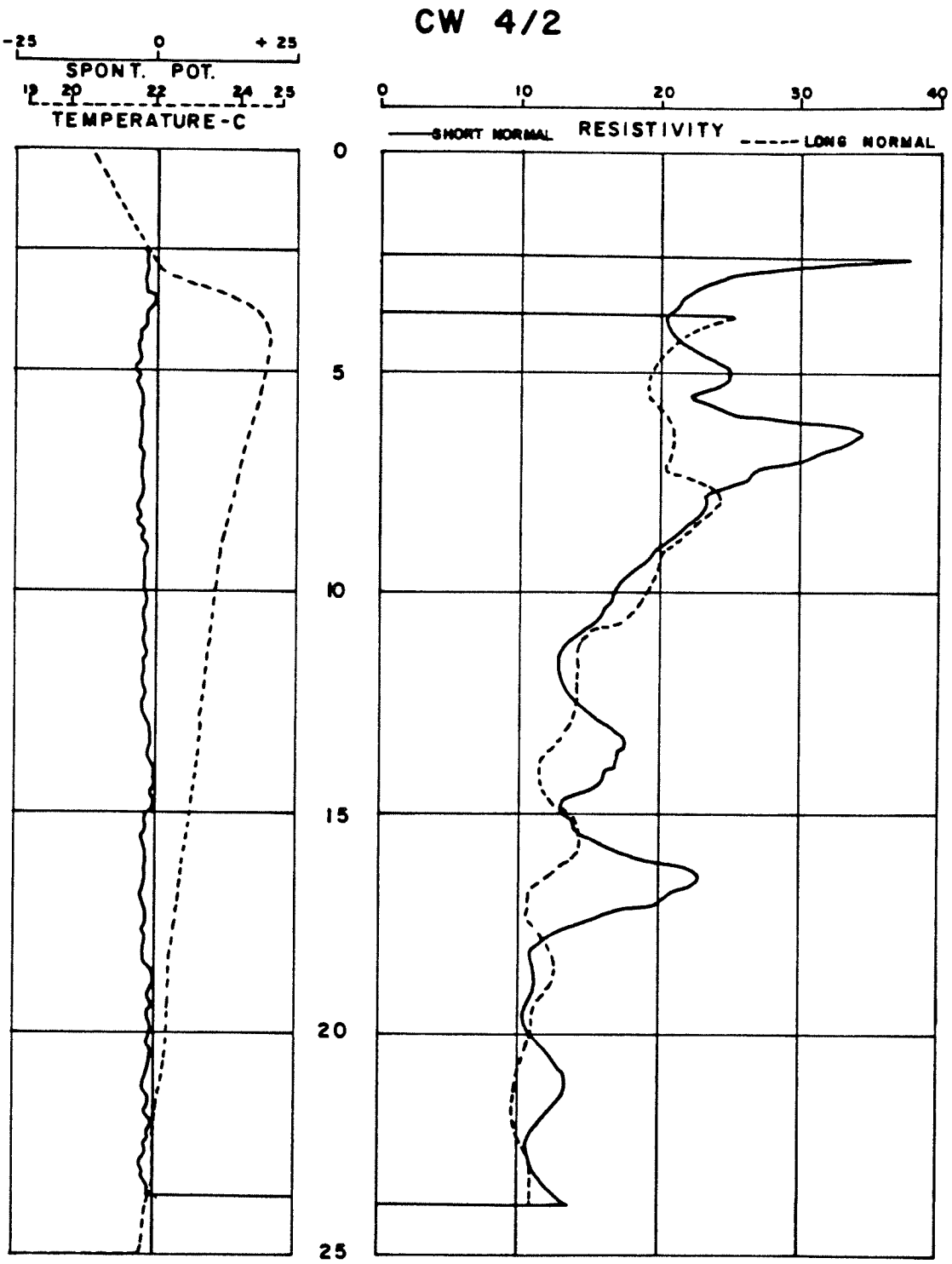
CW 4/2
-25
0
+ 25
SPONT. POT.
18
20
22
24
25
TEMPERATURE-C
0
10
20
30
40
SHORT NORMAL
RESISTIVITY
LONG NORMAL
0
5
10
15
20
25

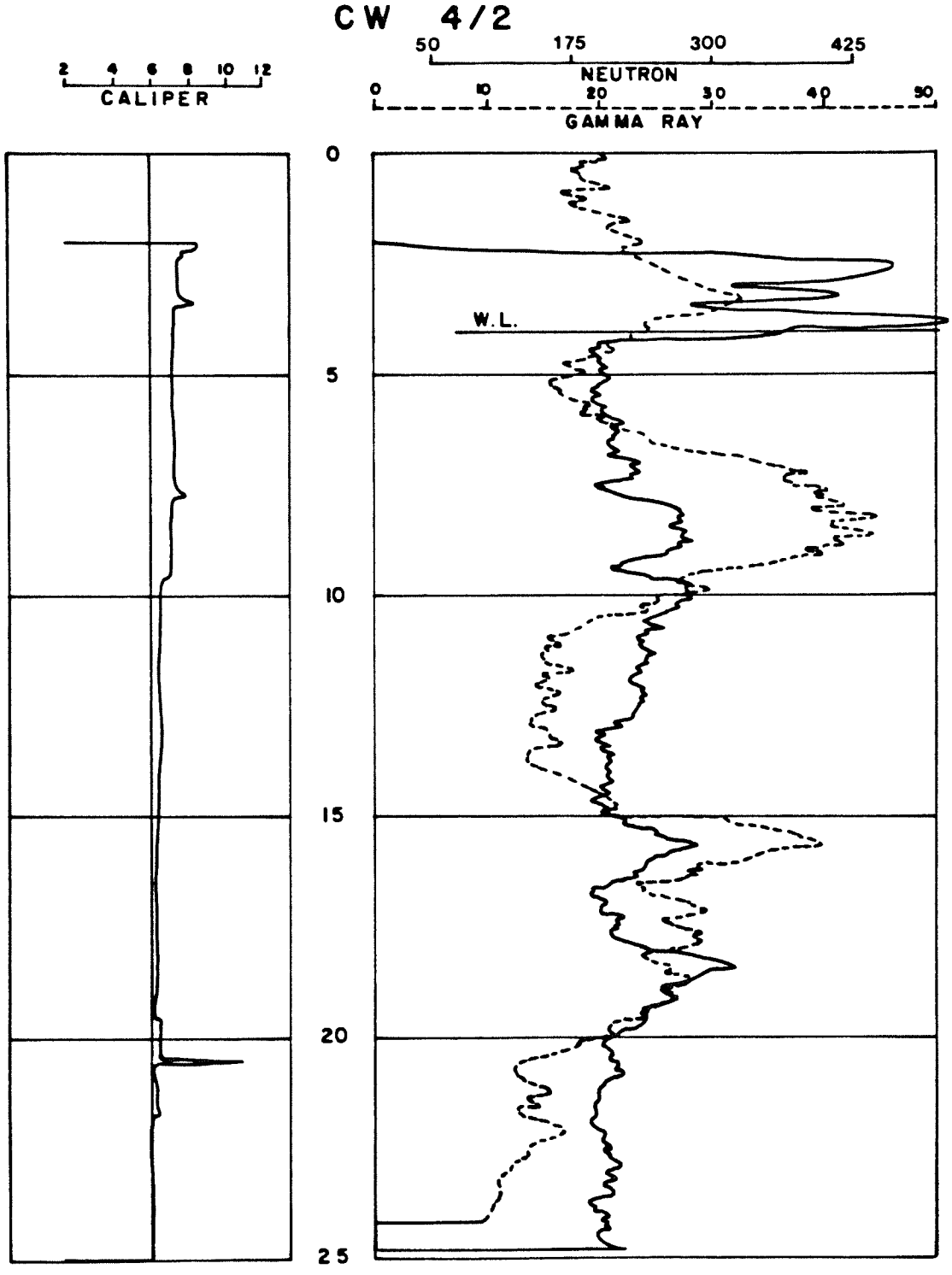
CW 4/2
2 4 6 8 10 12
CALIPER
50 175 300 425
NEUTRON
0 10 20 30 40 50
GAMMA RAY
W.L.
0
5
10
15
20
25

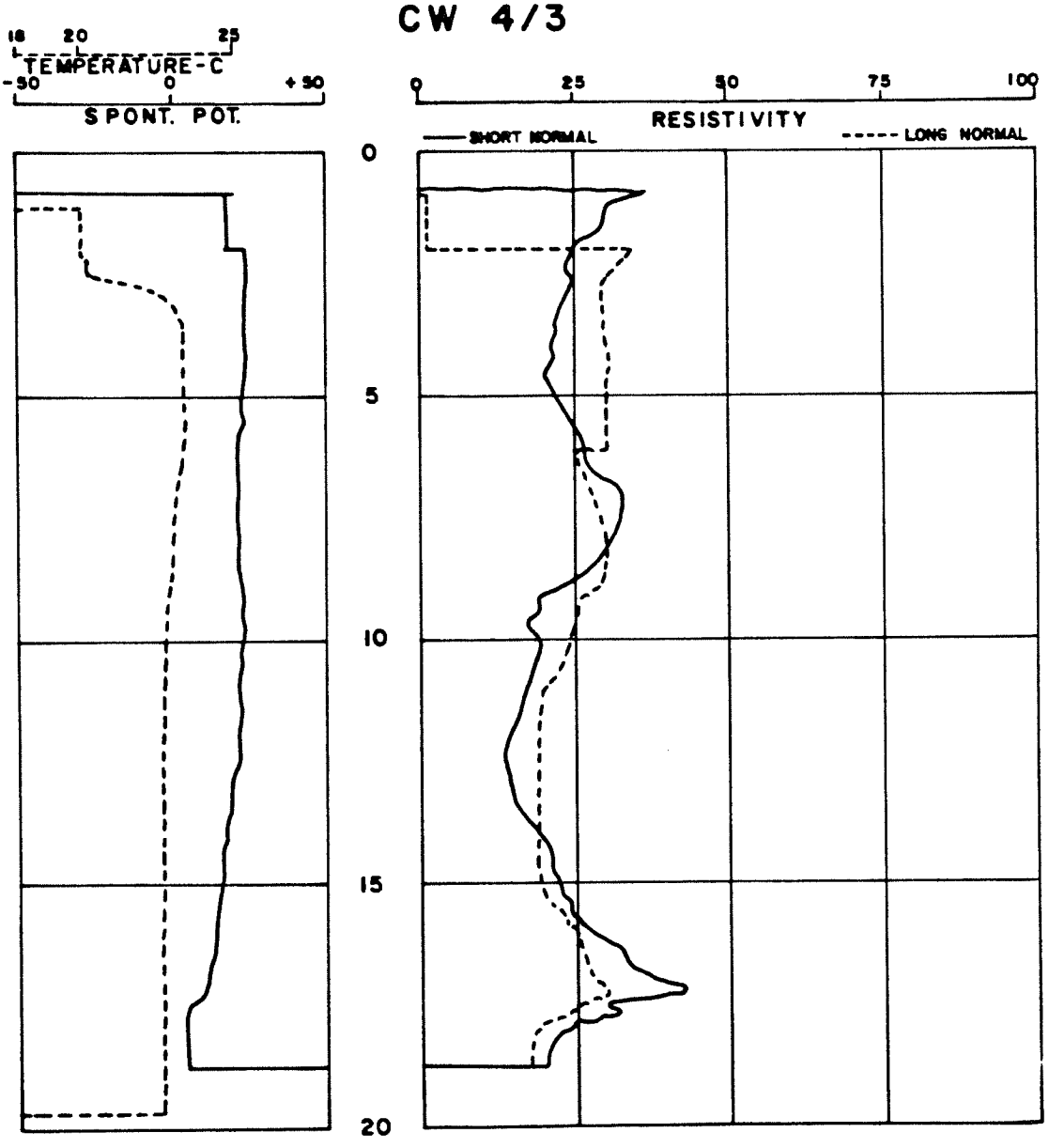
CW 4/3
18 20 25
TEMPERATURE-C
-50 0 +50
SPONT. POT.
0 25 50 75 100
RESISTIVITY
SHORT NORMAL
LONG NORMAL
0
5
10
15
20

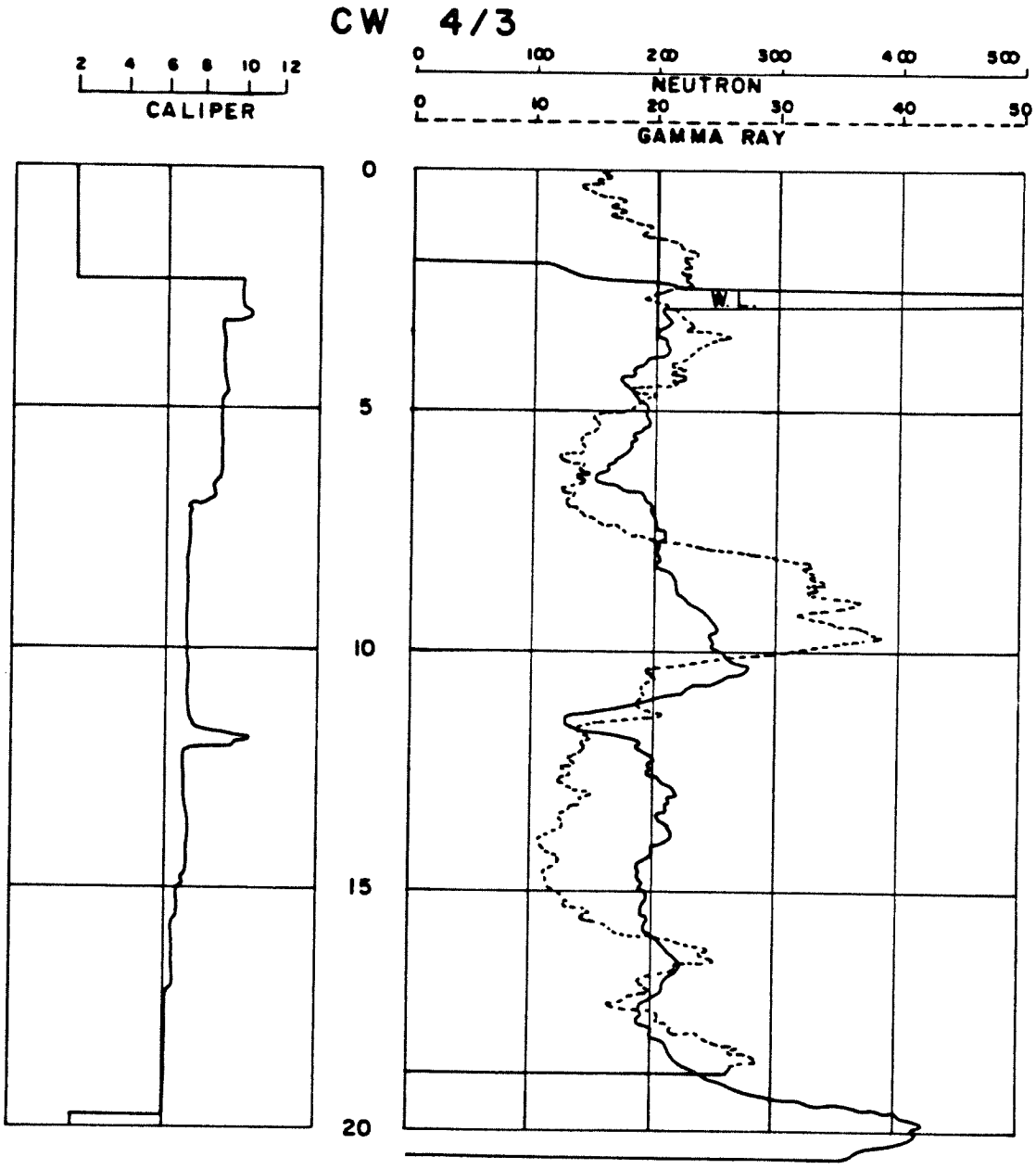
CW 4/3
2 4 6 8 10 12
CALIPER
0 100 200 300 400 500
NEUTRON
0 10 20 30 40 50
GAMMA RAY
W.L.
0
5
10
15
20

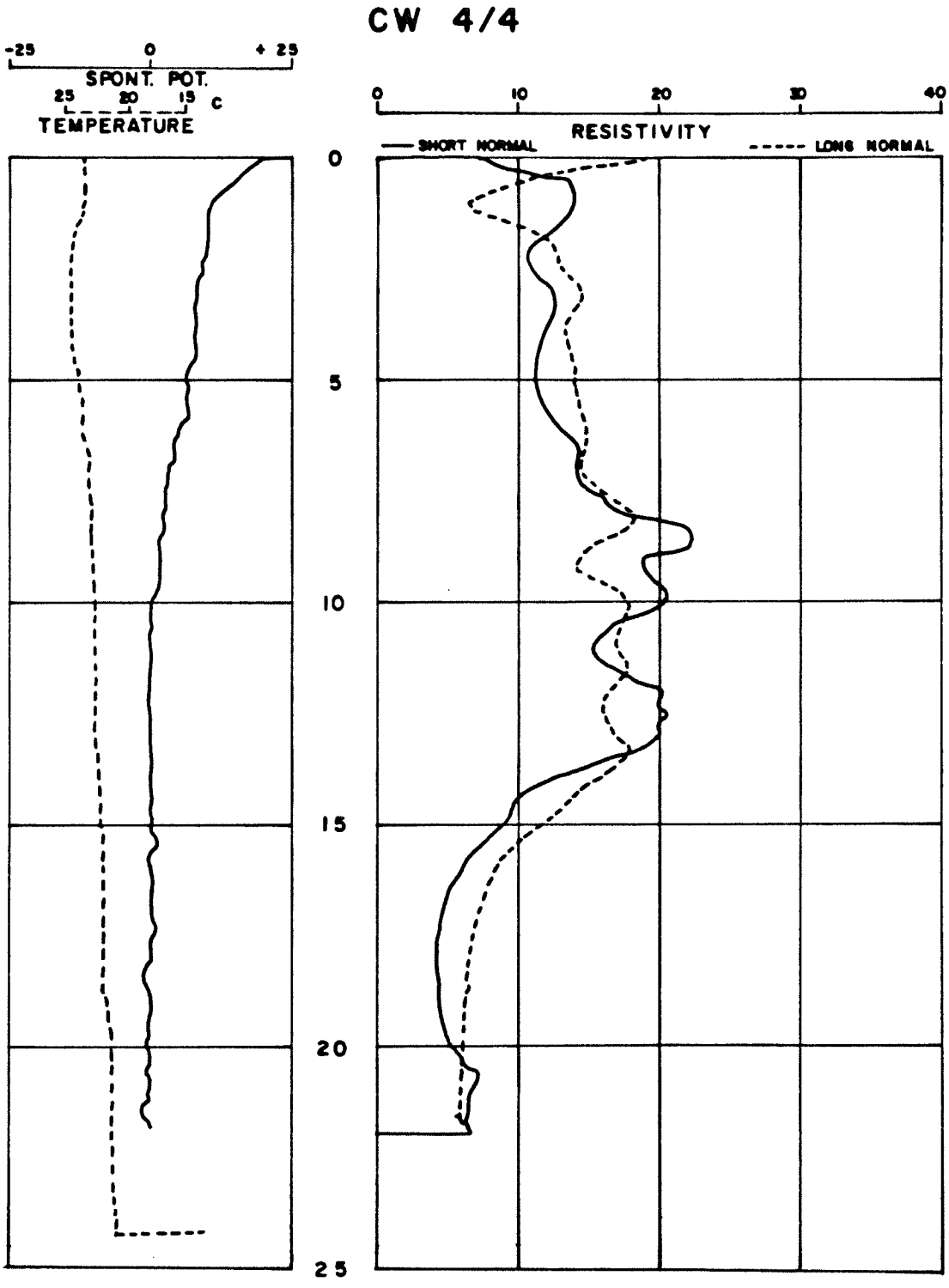
CW 4/4
-25
0
+25
SPONT. POT.
25
20
15
C
TEMPERATURE
0
10
20
30
40
RESISTIVITY
SHORT NORMAL
LONG NORMAL
0
5
10
15
20
25

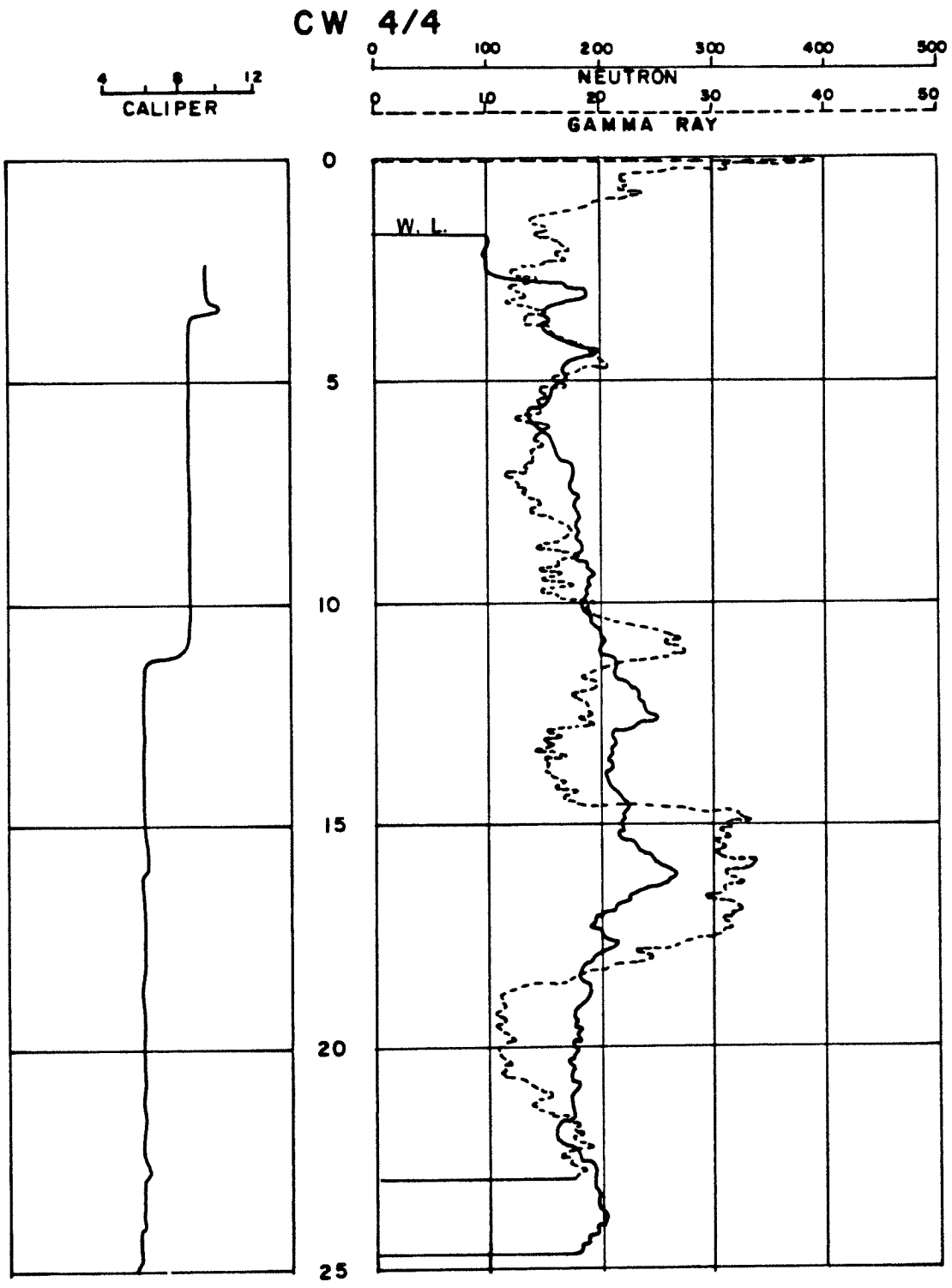
CW 4/4
4
8
12
CALIPER
0
100
200
300
400
500
NEUTRON
0
10
20
30
40
50
GAMMA RAY
W. L.
0
5
10
15
20
25

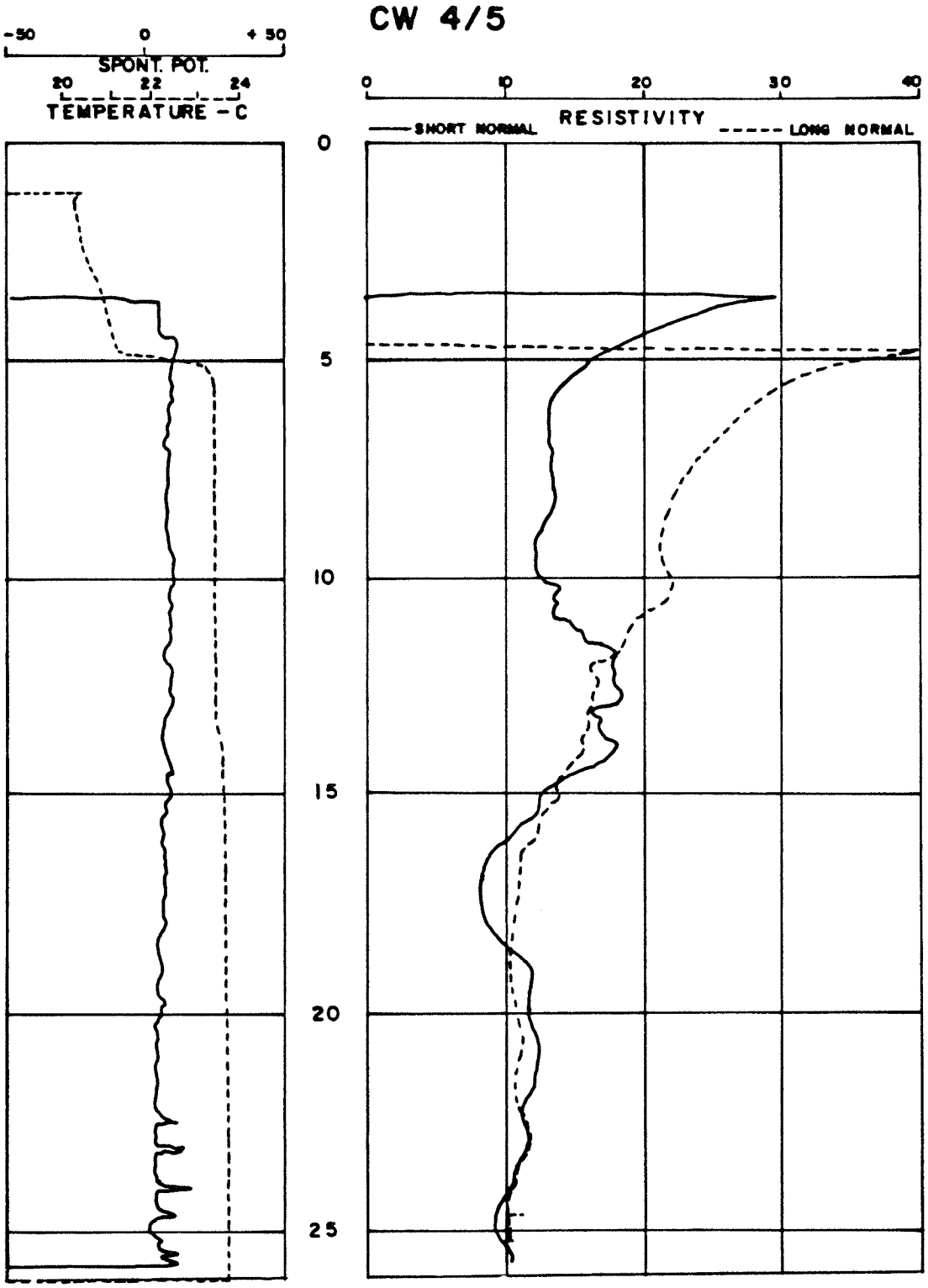
CW 4/5
-50
0
+50
SPONT. POT.
20
22
24
TEMPERATURE - C
0
10
20
30
40
RESISTIVITY
SHORT NORMAL
LONG NORMAL
0
5
10
15
20
25

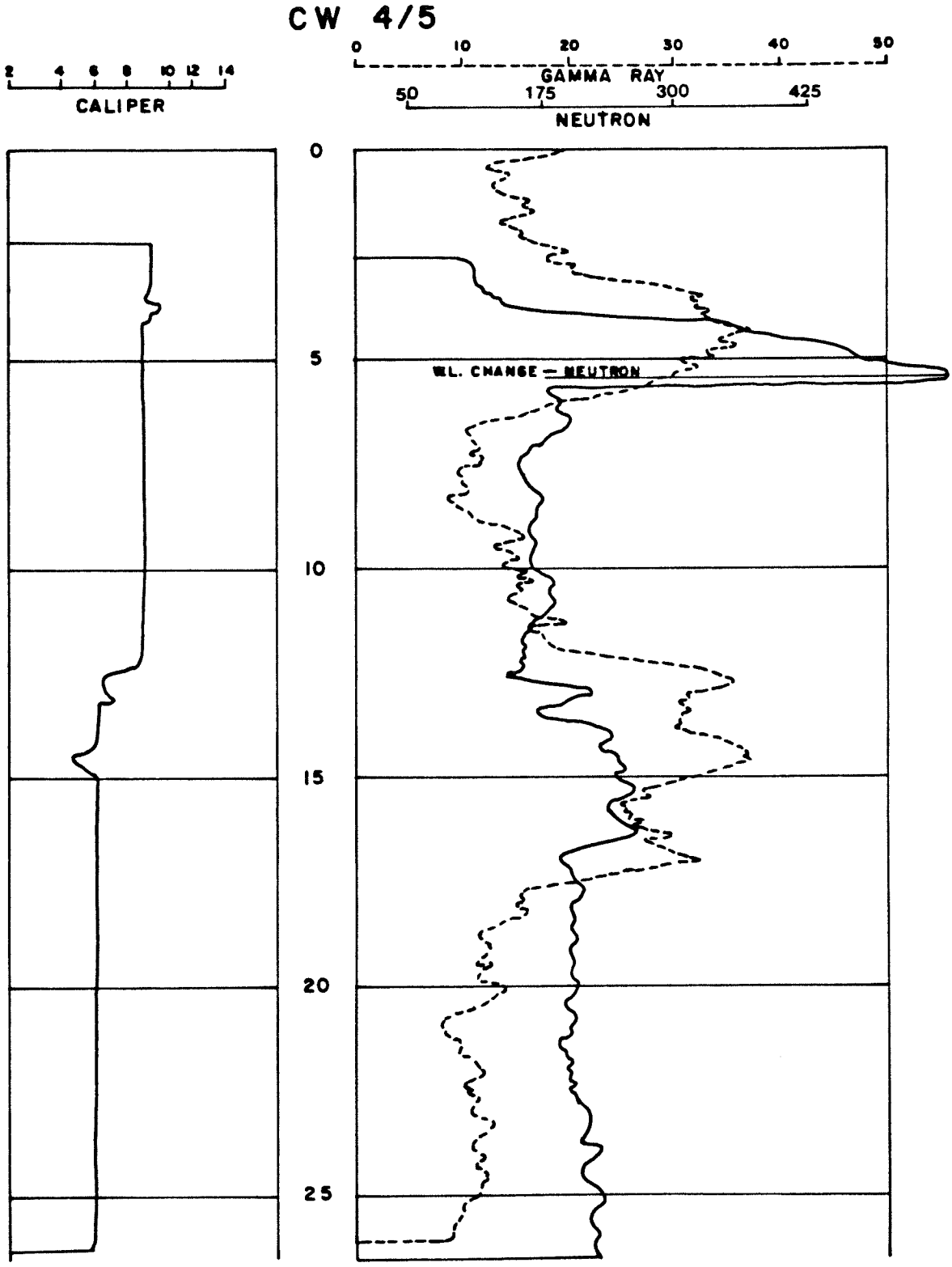
CW 4/5
2 4 6 8 10 12 14
CALIPER
0 10 20 30 40 50
GAMMA RAY
50 175 300 425
NEUTRON
WL. CHANGE — NEUTRON
0
5
10
15
20
25

APPENDIX 3

Core Well Lithology, Permeability Tests, and Drilling Schemes

CW I

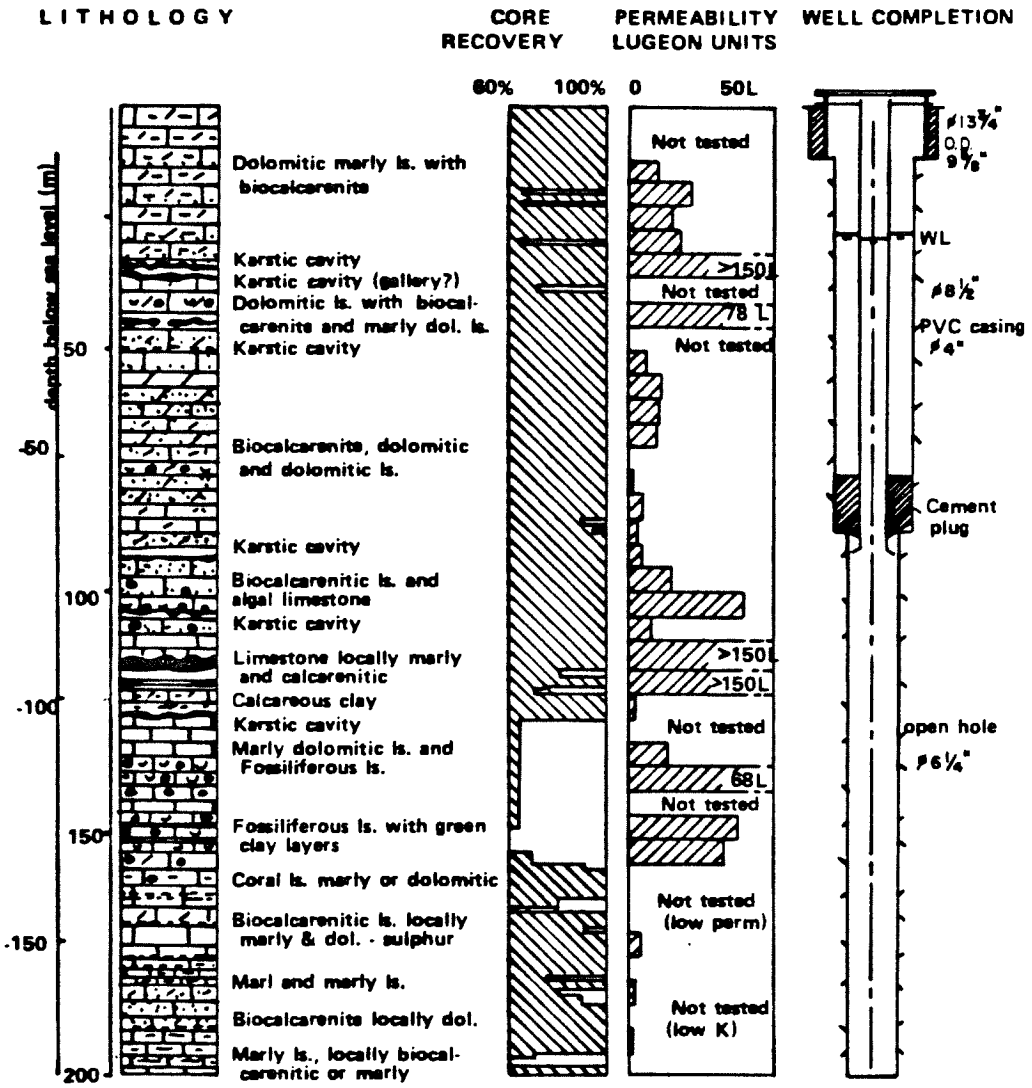
LITHOLOGY
CORE RECOVERY
60% 100%
PERMEABILITY LUGEON UNITS
0 50L
WELL COMPLETION
depth below sea level (m)
50
100
150
200
Dolomitic marly ls. with biocalcarenite
Karstic cavity
Karstic cavity (gallery?)
Dolomitic ls. with biocalcarenite and marly dol. ls.
Karstic cavity
Biocalcarenite, dolomitic and dolomitic ls.
Karstic cavity
Biocalcarenitic ls. and algal limestone
Karstic cavity
Limestone locally marly and calcarenitic
Calcareous clay
Karstic cavity
Marly dolomitic ls. and Fossiliferous ls.
Fossiliferous ls. with green clay layers
Coral ls. marly or dolomitic
Biocalcarenitic ls. locally marly & dol. - sulphur
Marl and marly ls.
Biocalcarenite locally dol.
Marly ls., locally biocalcarenitic or marly
Not tested
>150L
Not tested
78 L
Not tested
>150L
>150L
Not tested
68L
Not tested
Not tested (low perm)
Not tested (low K)
ø13¾" O.D. 9⅞"
WL
ø8½"
PVC casing ø4"
Cement plug
open hole
ø6¼"

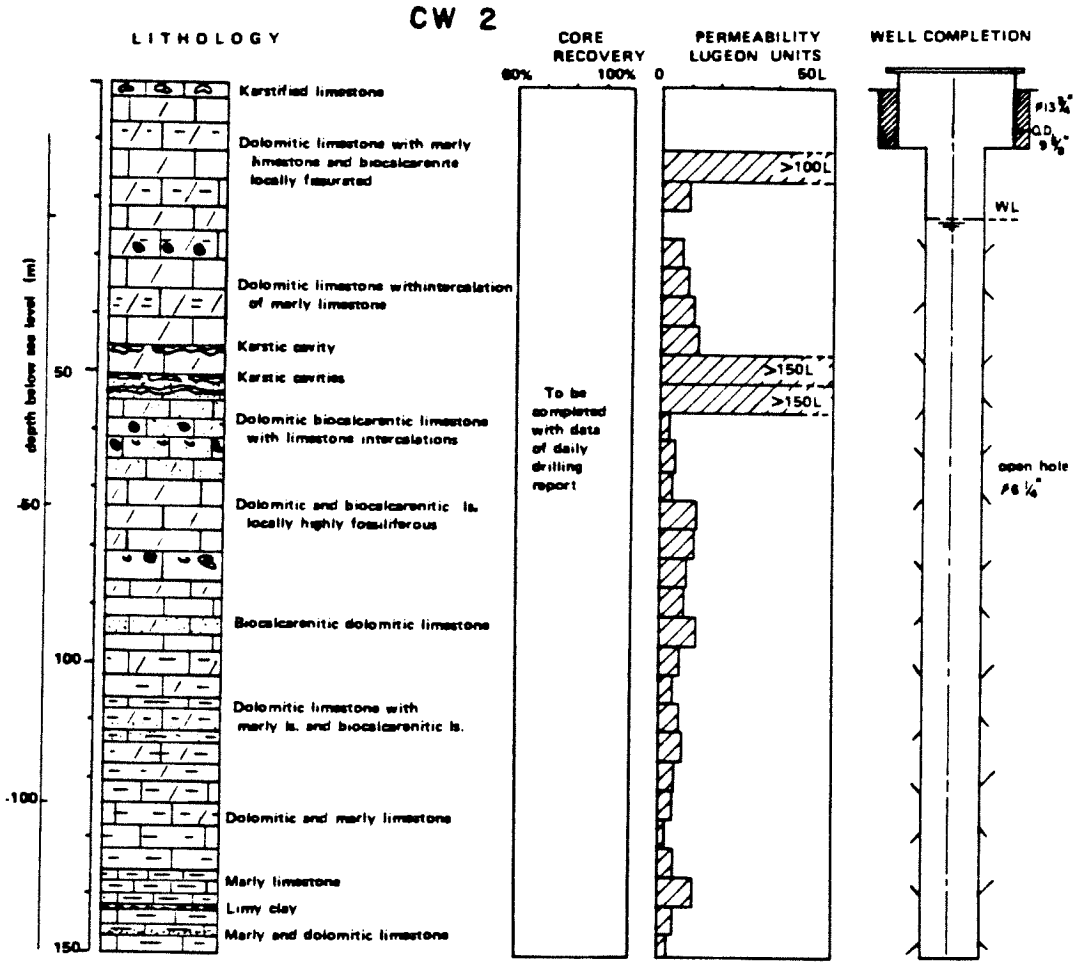
CW 2
LITHOLOGY
CORE RECOVERY
80% 100%
PERMEABILITY LUGEON UNITS
0 50L
WELL COMPLETION
depth below sea level (m)
50
-50
100
-100
150
Karstified limestone
Dolomitic limestone with marly limestone and biocalcarenite locally fissurated
Dolomitic limestone withintercalation of marly limestone
Karstic cavity
Karstic cavities
Dolomitic biocalcarentic limestone with limestone intercalations
Dolomitic and biocalcarenitic ls. locally highly fossiliferous
Biocalcarenitic dolomitic limestone
Dolomitic limestone with marly ls. and biocalcarenitic ls.
Dolomitic and marly limestone
Marly limestone
Limy clay
Marly and dolomitic limestone
To be completed with data of daily drilling report
>100L
>150L
>150L
WL
open hole

CW 3

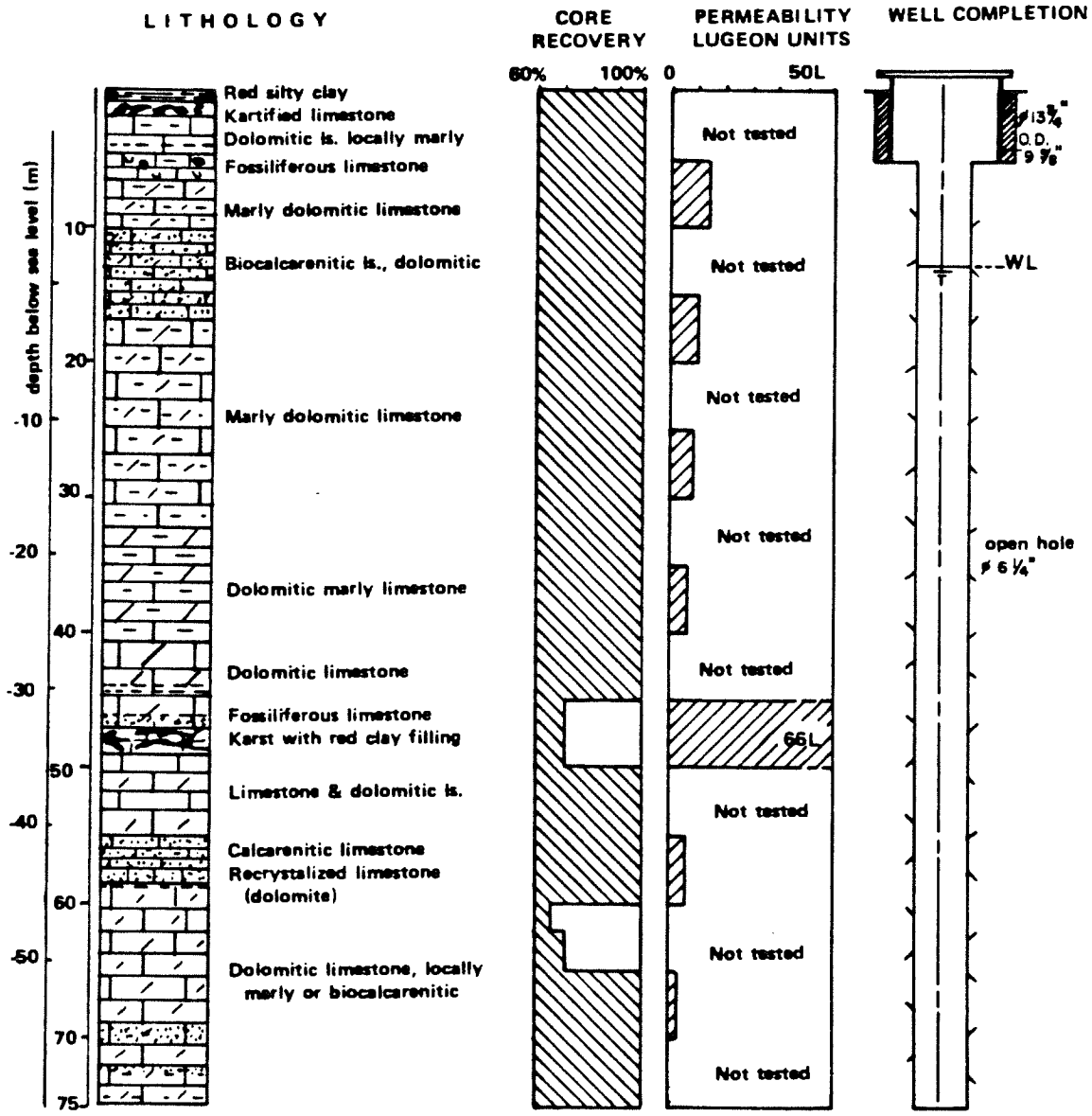
LITHOLOGY
CORE RECOVERY
60% 100%
PERMEABILITY LUGEON UNITS
0 50L
WELL COMPLETION
depth below sea level (m)
10
20
30
40
50
60
70
75
-10
-20
-30
-40
-50
Red silty clay
Kartified limestone
Dolomitic ls. locally marly
Fossiliferous limestone
Marly dolomitic limestone
Biocalcarenitic ls., dolomitic
Marly dolomitic limestone
Dolomitic marly limestone
Dolomitic limestone
Fossiliferous limestone
Karst with red clay filling
Limestone & dolomitic ls.
Calcarenitic limestone
Recrystalized limestone (dolomite)
Dolomitic limestone, locally marly or biocalcarenitic
Not tested
Not tested
Not tested
Not tested
66L
Not tested
Not tested
Not tested
ϕ 13¾" O.D. 9⅝"
WL
open hole ϕ 6¼"

CW 4/1

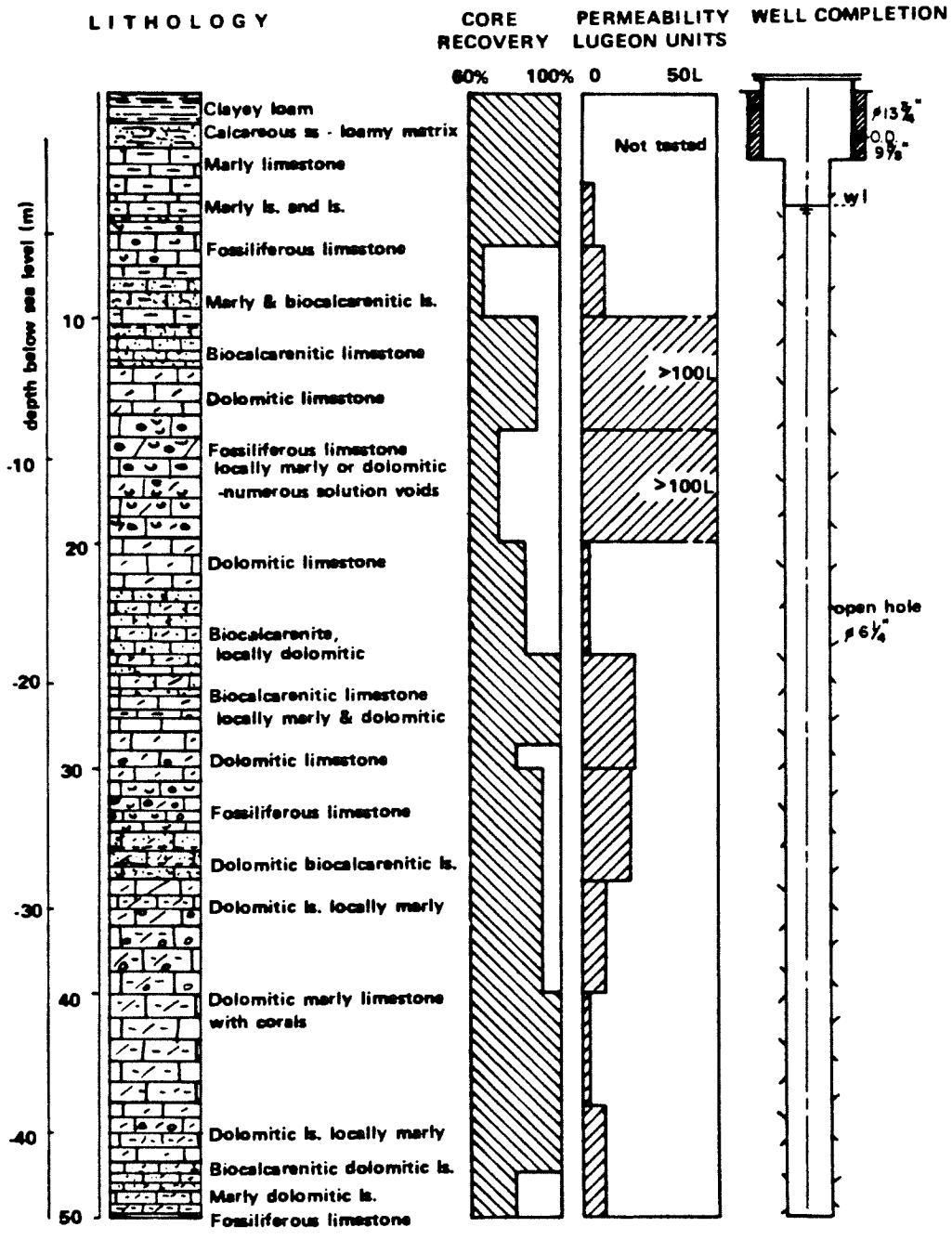
LITHOLOGY
CORE RECOVERY
60% 100%
PERMEABILITY LUGEON UNITS
0 50L
WELL COMPLETION
depth below sea level (m)
Clayey loam
Calcareous ss - loamy matrix
Marly limestone
Marly ls. and ls.
Fossiliferous limestone
Marly & biocalcarenitic ls.
Biocalcarenitic limestone
Dolomitic limestone
Fossiliferous limestone locally marly or dolomitic -numerous solution voids
Dolomitic limestone
Biocalcarenite, locally dolomitic
Biocalcarenitic limestone locally marly & dolomitic
Dolomitic limestone
Fossiliferous limestone
Dolomitic biocalcarenitic ls.
Dolomitic ls. locally marly
Dolomitic marly limestone with corals
Dolomitic ls. locally marly
Biocalcarenitic dolomitic ls.
Marly dolomitic ls.
Fossiliferous limestone
Not tested
>100L
>100L
10
20
30
40
50
-10
-20
-30
-40
wl
open hole

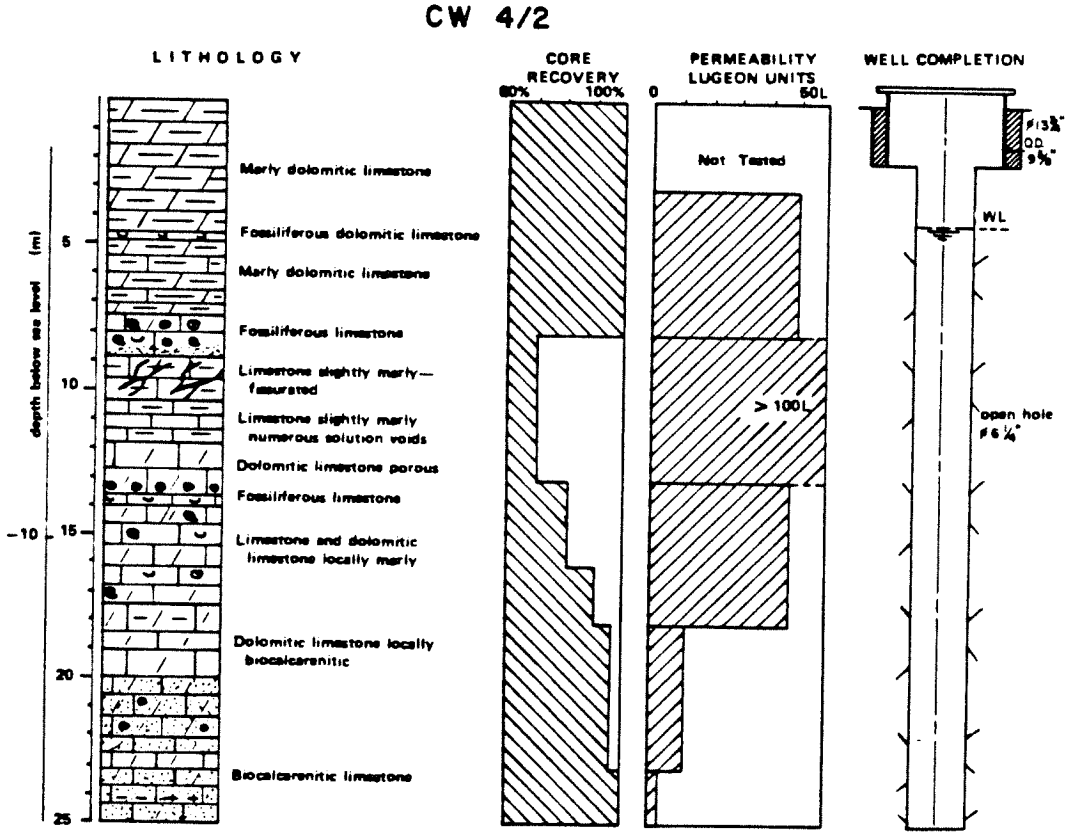
CW 4/2
LITHOLOGY
CORE RECOVERY
80%
100%
PERMEABILITY LUGEON UNITS
0
50L
WELL COMPLETION
depth below sea level (m)
5
10
-10
15
20
25
Marly dolomitic limestone
Fossiliferous dolomitic limestone
Marly dolomitic limestone
Fossiliferous limestone
Limestone slightly marly—fissurated
Limestone slightly marly numerous solution voids
Dolomitic limestone porous
Fossiliferous limestone
Limestone and dolomitic limestone locally marly
Dolomitic limestone locally biocalcarenitic
Biocalcarenitic limestone
Not Tested
> 100L
WL
open hole

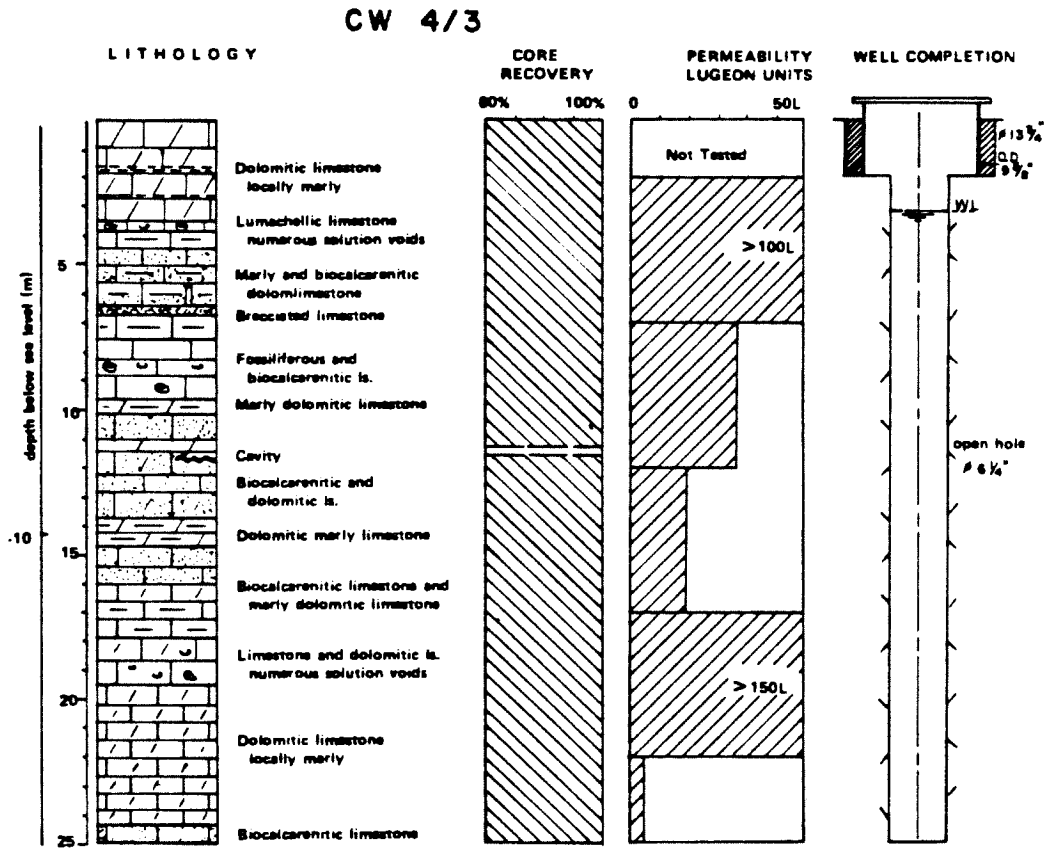
CW 4/3
LITHOLOGY
CORE RECOVERY
80%
100%
PERMEABILITY LUGEON UNITS
0
50L
WELL COMPLETION
depth below sea level (m)
-5
-10
-15
-20
-25
Dolomitic limestone locally marly
Lumachellic limestone numerous solution voids
Marly and biocalcarenitic dolomlimestone
Brecciated limestone
Fossiliferous and biocalcarenitic ls.
Marly dolomitic limestone
Cavity
Biocalcarenitic and dolomitic ls.
Dolomitic marly limestone
Biocalcarenitic limestone and marly dolomitic limestone
Limestone and dolomitic ls. numerous solution voids
Dolomitic limestone locally marly
Biocalcarenitic limestone
Not Tested
>100L
>150L
WL
open hole
ø 6 1/4"

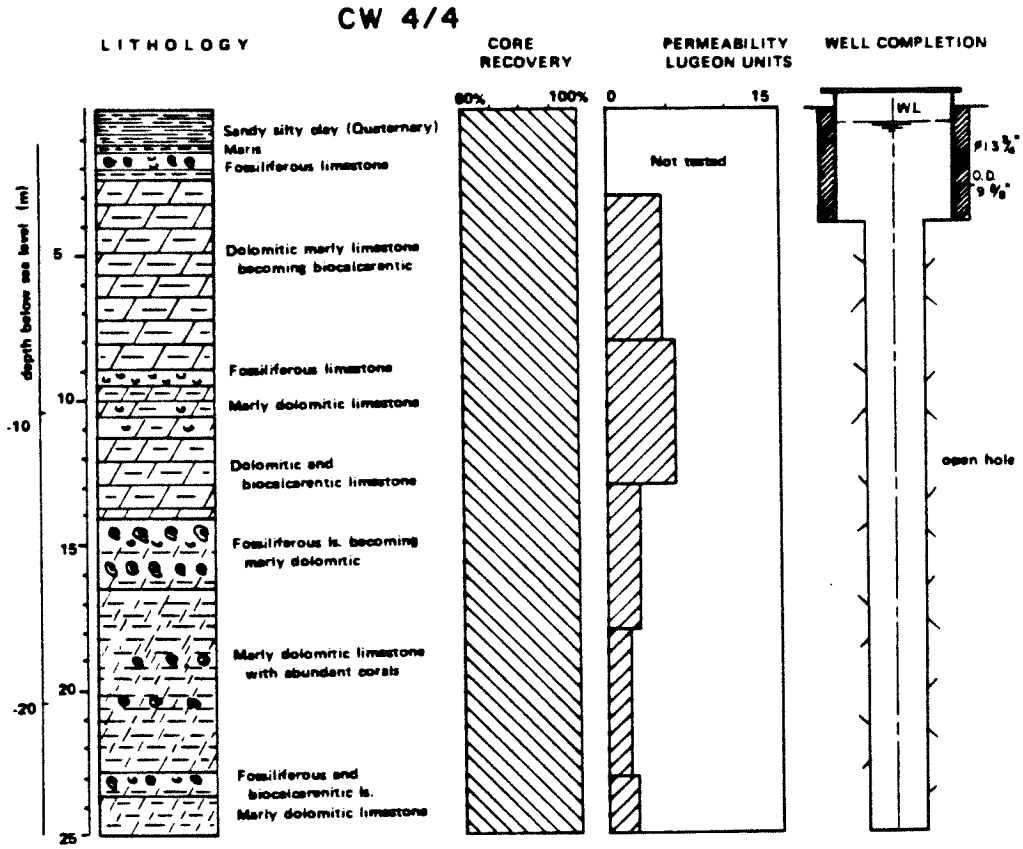
CW 4/4
LITHOLOGY
CORE RECOVERY
PERMEABILITY LUGEON UNITS
WELL COMPLETION
80%
100%
0
15
Not tested
WL
O.D. 9⅝"
open hole
depth below sea level (m)
5
10
-10
15
20
-20
25
Sandy silty clay (Quaternary)
Marls
Fossiliferous limestone
Dolomitic marly limestone becoming biocalcarentic
Fossiliferous limestone
Marly dolomitic limestone
Dolomitic and biocalcarentic limestone
Fossiliferous ls. becoming marly dolomitic
Marly dolomitic limestone with abundant corals
Fossiliferous and biocalcarenitic ls.
Marly dolomitic limestone

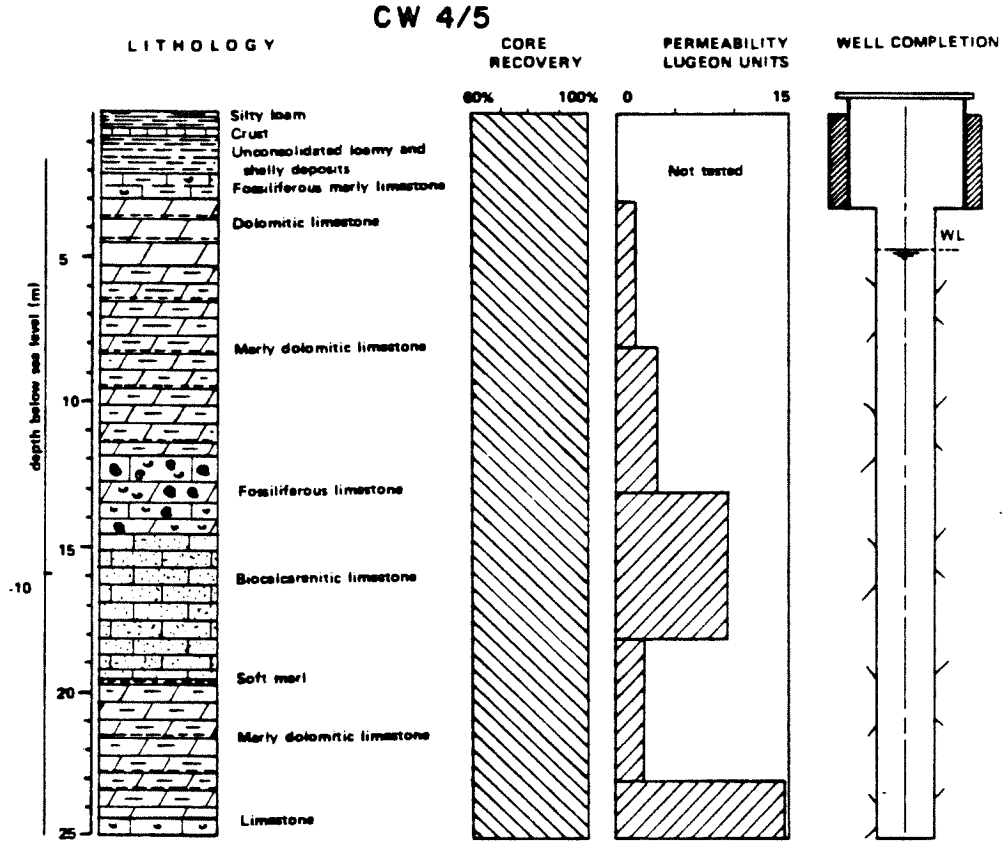
CW 4/5
LITHOLOGY
CORE RECOVERY
PERMEABILITY LUGEON UNITS
WELL COMPLETION
60%
100%
0
15
Not tested
WL
depth below sea level (m)
-10
5
10
15
20
25
Silty loam
Crust
Unconsolidated loamy and shelly deposits
Fossiliferous marly limestone
Dolomitic limestone
Marly dolomitic limestone
Fossiliferous limestone
Biocalcarenitic limestone
Soft marl
Marly dolomitic limestone
Limestone

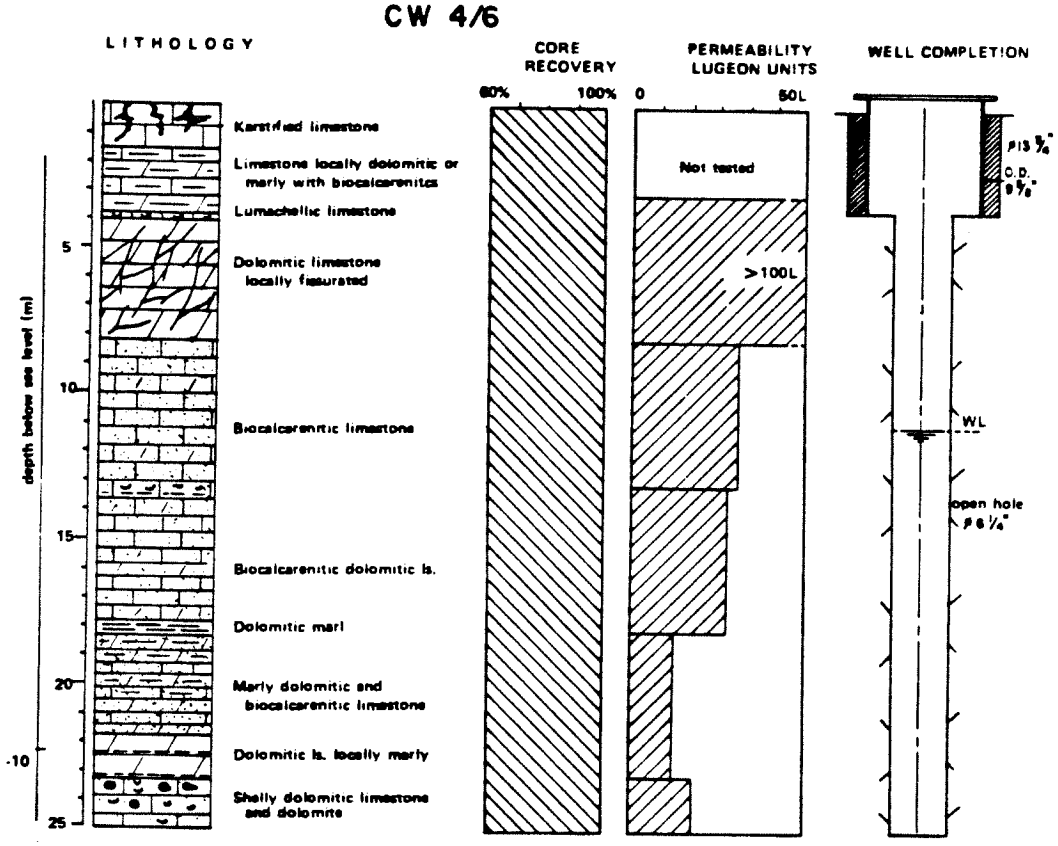
CW 4/6
LITHOLOGY
CORE RECOVERY
60%
100%
PERMEABILITY LUGEON UNITS
0
50L
WELL COMPLETION
depth below sea level (m)
5
10
15
20
-10
25
Karstified limestone
Limestone locally dolomitic or marly with biocalcarenites
Lumachellic limestone
Dolomitic limestone locally fissurated
Biocalcarenitic limestone
Biocalcarenitic dolomitic ls.
Dolomitic marl
Marly dolomitic and biocalcarenitic limestone
Dolomitic ls. locally marly
Shelly dolomitic limestone and dolomite
Not tested
>100L
WL
open hole

T-2733

LEGEND

LITHOLOGY:

QUATERNARY

Post-Miocene

- Terra Rossa
- Clay and Sand, Sebkha Deposits (Terra Rossa)
- Fine-grained Carbonate Sand
- Fine-grained Carbonate Sandstone
- Sandy and Dolomitic Limestone

MIOCENE

- Marly Limestone with Chert Concretions
- Fine Crystalline and Dolomitic Limestone
- Limestone and Marly Limestone
- Marly and Sandy Limestone with Marl Intercalations

GEOLOGICAL FEATURES:

- Established Lithological Boundary
- Established Fault
- Supposed Fault

GEOMORPHOLOGICAL FEATURES:

- Doline (Sinkhole) with Water
- Dry Doline (Sinkhole)
- Cave

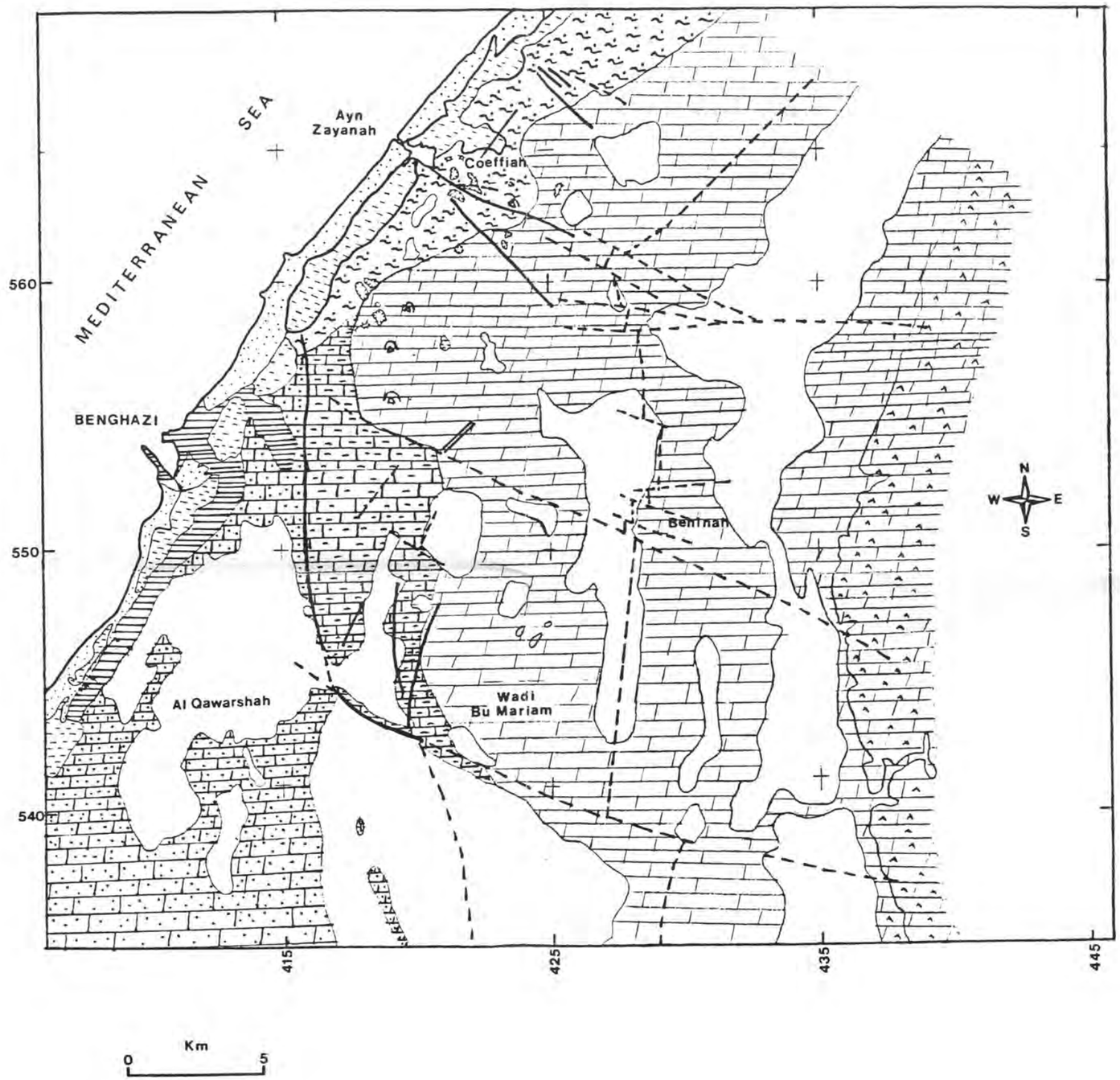

Map 1. Geological map of Ayn Zayanah-Benghazi area (after Geozavod, 1972).

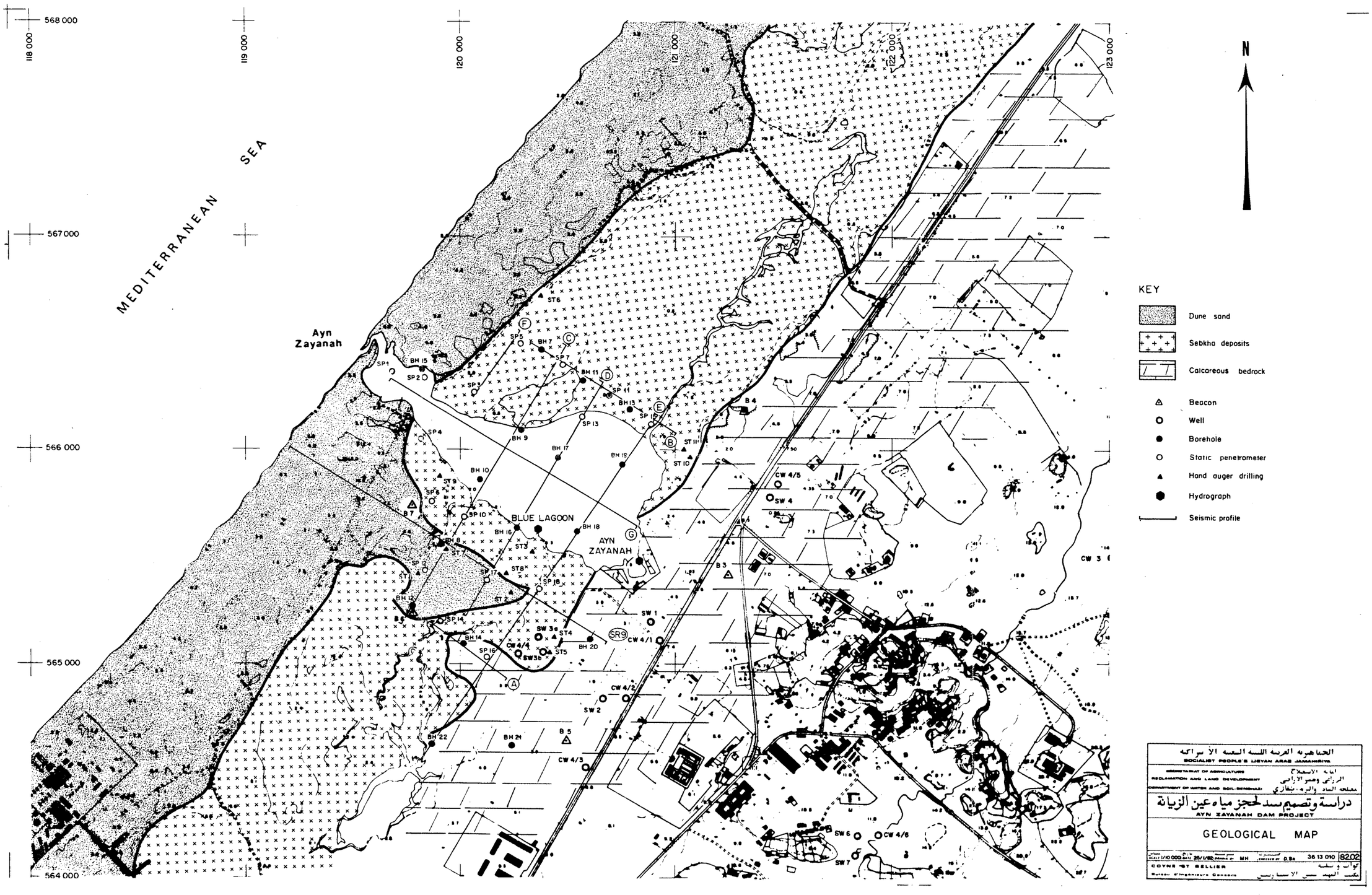

Map 2. Geological map of Ayn Zayanah area (after Coyne and Bellier, 1982).